Nano Research

Open Access

Review Article

Application of quantum dots in cancer diagnosis and treatment: Advances and perspectives

Mei Li[1,§], Yan Huang[2,§], Chen Shen[1,§], Yiqing Wang[1], Yue'ai Lin[1], Zejun Wang[3] ✉, Nan Chen[2] ✉, and Yao Luo[1] ✉

[1] *Department of Laboratory Medicine, and Innovation Institute for Integration of Medicine and Engineering, West China Hospital, Sichuan University, Chengdu 610041, China*
[2] *College of Chemistry and Materials Science, The Education Ministry Key Lab of Resource Chemistry, Joint International Research Laboratory of Resource Chemistry of Ministry of Education, Shanghai Key Laboratory of Rare Earth Functional Materials, and Shanghai Frontiers Science Center of Biomimetic Catalysis, Shanghai Engineering Research Center of Green Energy Chemical Engineering, Shanghai Normal University, Shanghai 200234, China*
[3] *Department of Chemistry, College of Sciences, Northeastern University, Shenyang 110819, China*
§ *Mei Li, Yan Huang and Chen Shen contributed equally to this work.*

Cite this article: *Nano Research*, **2025**, *18*, 94907163. https://doi.org/10.26599/NR.2025.94907163

ABSTRACT: Quantum dots (QDs) are semiconductor nanocrystals with diameters ranging from 2 to 10 nanometers. The development of QDs has greatly advanced nanotechnology, and this achievement was recognized with the awarding of the 2023 Nobel Prize in Chemistry. They have gained significant attention in the field of biomedical applications due to their high adjustability, stability, sensitivity, and selectivity. QDs have proven to be suitable for *in vivo* bioimaging and tracking, medical diagnostics, and drug delivery systems. Their exceptional attributes, like high brightness, resistance to photobleaching, and multiplexing capability, combined with a high surface-to-volume ratio, make them ideal for these applications. Their unique optical and electronic properties can be precisely controlled by adjusting the size and material composition. By modifying their surface or encapsulating them, QDs can be conjugated with specific biomolecules, enabling the visualization and quantitative analysis of target entities. The ability to externally manipulate QDs through magnetic fields, electric fields, acoustic waves, or temperature changes enhances their utility in targeted drug delivery and therapy. In the context of cancer, a leading cause of global mortality with increasing incidence rates, QDs offer innovative approaches to diagnosis, treatment, and prevention strategies. This review summarizes the cutting-edge applications of QDs in cancer, providing insights into the mechanisms and strategies used. It also critically evaluates the advantages and limitations of QDs, including their toxicity profile. The discussion concludes with a perspective on the technical advancements needed to enhance the clinical applicability of QDs and identifies upcoming challenges in their journey towards widespread biomedical use.

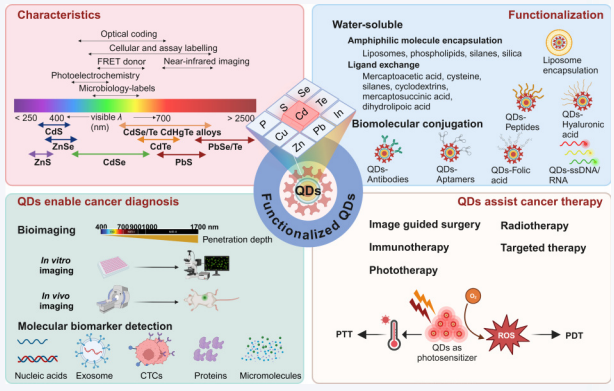

1 Introduction

Nanotechnology has been expanding its application in clinical medicine, especially for the early diagnosis of diseases and real-time monitoring of treatments [1]. In particular, quantum dots (QDs) represent an attractive new class of photoluminescent tags and optical contrast agents for biomedical applications [2]. As one of the most exciting research tools in chemistry, physics, and biology, QDs have gained significant interest in the last few decades [3]. In contrast to conventional organic fluorescent molecules, QDs exhibit superior optical properties including broad excitation spectra, intense photoluminescence with high quantum yields, long luminescence lifetimes, high resistance against photobleaching, narrow and sharp intense emission spectra with large Stokes shifts, size-tunable photoluminescence, and large surface area for functionalization. These properties of QDs facilitate long-term

Received: September 16, 2024; **Revised:** November 13, 2024
Accepted: November 29, 2024

✉Address correspondence to Zejun Wang, wangzejun@mail.neu.edu.cn; Nan Chen, nchen@shnu.edu.cn; Yao Luo, luoyao@scu.edu.cn

monitoring of intermolecular and intramolecular interactions in living cells and tissues [4]. Consequently, much interest has been focused on the exploration of QDs for bioanalytical and biomedical applications such as bioimaging, diagnosis, and drug delivery [5–7]. To achieve optimal stability, monodispersity, solubility, biocompatibility, and targeting in diagnostic and therapeutic research, QDs are typically conjugated with biological molecules, such as aptamers, antibodies, oligonucleotides, and peptides [8, 9]. In addition, the size of QDs affects their fluorescence emission, and the colors emitted by QDs are determined by their band gap. Thus, QDs of different sizes emit light of different colors [1]. This means that the optical performance of QDs depends more on their size than on their material, allowing for manipulation of their electromagnetic radiation across a wide range, from the ultraviolet (UV) region to the far infrared region, by controlling the particle size [10]. The ability to tune the emission wavelength of QDs by controlling their size and/or composition is highly relevant to multiplexed bioanalytical applications [2, 11].

The exceptional optical properties of QDs render them highly versatile in molecular diagnostics, biological imaging, and disease treatment. Standing out from various nanotechnologies, QDs have emerged as a promising multifunctional platform for cancer diagnosis and therapy. QDs prepared using functionalization strategies, such as biomolecular conjugation, exhibit excellent biocompatibility. They can identify tumor biomarkers including cancer cells, enabling precise tumor biomarker detection, tumor tissue imaging, and even facilitating cancer cell apoptosis. In recent years, QDs have demonstrated increasing potential in multimodal imaging and combination therapy approaches. Focusing on the latest advancements of QDs in cancer research and providing a comprehensive summary of application strategies will offer valuable insights for the future QDs and cancer research.

In the current review, we have summarized the biological properties of QDs and provided an overview of the latest advancements in their application in the diagnosis, treatment, and prevention of cancer. We have also highlighted the mechanisms and strategies employed by QDs in cancer research, taking into account the detailed introduction of current cancer diagnosis and treatment methods. Furthermore, we have discussed the merits, drawbacks, and toxicity of QDs. Lastly, we have made an outlook on the technical improvements needed to enhance the biomedical fate of QDs, as well as the future challenges in achieving their clinical applications.

2 Development and categories of quantum dots

QDs are semiconductor nanocrystals (typically 2–10 nm) with remarkable optical properties, which were first reported in the 1980s [3]. The discovery and subsequent development of QDs have opened up new avenues for nanotechnology, earning them recognition as a major breakthrough in the scientific community. The 2023 Nobel Prize in Chemistry was awarded to Moungi G. Bawendi, Louis E. Brus, and Alexei I. Ekimov for their groundbreaking work in the discovery and synthesis of QDs. These tiny nanoparticles, whose properties are defined by their size, have revolutionized nanotechnology and have a wide range of applications in consumer electronics, biochemistry, and medicine. The award recognizes the significant impact of their work on our

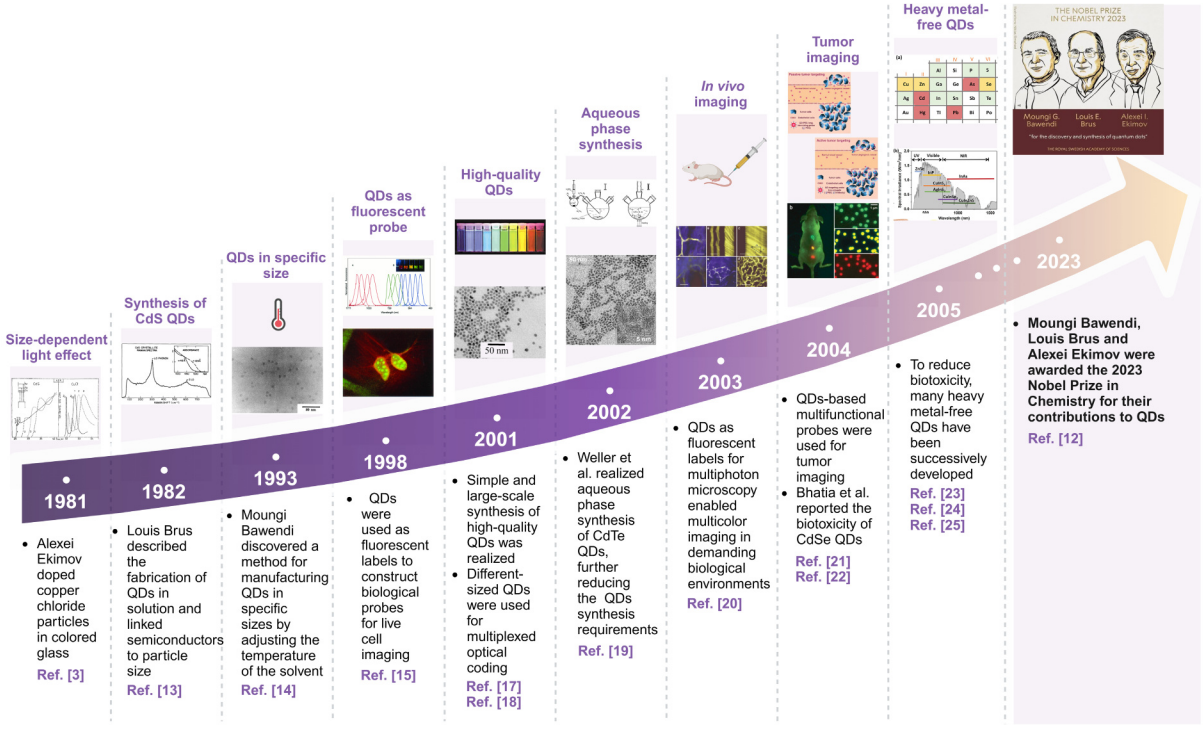

Figure 1 The origins and progression of QDs in biomedical applications. Created using BioRender. Reproduced with permission from Ref. [1], © Published by Elsevier Ltd. 1985. Ref. [13], © American Institute of Physics 1983. Ref. [14], © American Chemical Society 1993. Ref. [15], © American Association for the Advancement of Science 1998. Ref. [17], © American Chemical Society 2001. Ref. [18], © Springer Nature America, Inc. 1969. Ref. [19], © American Chemical Society 2002. Ref. [20], © American Association for the Advancement of Science 2003. Ref. [21], © Springer Nature America, Inc. 2004. Ref. [22], © American Chemical Society 2004. Ref. [23], © H. Utzat, et al. some rights reserved; exclusive licensee American Association for the Advancement of Science 2019. Ref. [24], © Springer Nature Limited 2005. Ref. [25], © American Association for the Advancement of Science 2005. Ref. [12], © Springer Nature Limited 2023.

understanding of nanomaterials and the development of new technologies that leverage the unique properties of QDs [12]. In order to better understand the origins and advancements of QDs in biomedical applications, the processes involved in their development are briefly outlined (Fig. 1).

Alexei I. Ekimov first reported the observation of size-dependent light effects in 1981 by doping copper chloride particles in colored glass [3]. The following year, Louis E. Brus described the fabrication of QDs in solution, making the connection between semiconductors and particle size [13]. However, it wasn't until Moungi G. Bawendi combined inorganic and organometallic techniques and developed a method for manufacturing QDs of specific sizes that the materials system became more accessible [14]. Bawendi's group also improved the efficiency of QDs generation by adjusting the solvent temperature, allowing more researchers to explore the characteristics and potential applications of QDs. As preparation technology continued to improve, QDs gradually found applications in optoelectronic conversion and biomedical research. In 1998, Alivisatos' group [15] and Nie' group [16] simultaneously reported in *Science* that QDs could be used as biological probes, making the first time they were applied as fluorescent markers in living cell systems. This discovery provided new tools for cell imaging and biomedical research. Furthermore, the successful preparation of water-soluble QDs and the strategy of coupling QDs with biological macromolecules through surface active groups have driven a research boom in biomedical applications of QDs. In the 2000s, research on QDs continued to thrive. The synthesis methods of QDs were consistently improved, resulting in enhanced quantum efficiency and stability. Notably, in 2001, Peng et al. achieved the simple and large-scale synthesis of high-quality QDs, laying the foundation for their rapid development [17]. In the same year, Nie et al. successfully embedded QDs of different sizes into polymeric micro-beads at controlled ratios, enabling multi-color optical coding for biological assays [18]. Properties such as size-tunable emission and simultaneous excitation make these highly luminescent QDs ideal fluorophores for wavelength-and-intensity multiplexing. The tunable optical properties of QDs enable precise targeting and multiplexed imaging of cancer cells and tissues. This versatility is crucial for non-invasive cancer detection and monitoring. In 2002, Weller et al. reported a novel method to synthesize photo-stable thiol-capped CdTe nanocrystals, marking a significant achievement in the aqueous phase synthesis of CdTe QDs. This method also reduced the synthesis requirements compared to conventional organometallic syntheses [19]. The following year, Webb's group characterized water-soluble CdSe-ZnS QDs for multiphoton imaging in live animals. This study demonstrated that QDs can be used as fluorescent labels for multiphoton microscopy, enabling multicolor imaging in challenging biological environments [20]. That second year, Nie et al. developed QDs-based multifunctional probes for cancer targeting and imaging in living animals. *In vivo* targeting studies indicated that these probes accumulate in tumors through enhanced permeability and retention at tumor sites, as well as antibody binding to cancer-specific cell surface biomarkers [21]. These studies open up new possibilities for ultra-sensitive and multiplexed imaging of molecular targets *in vivo*. The high photostability of QDs allows for long-term imaging studies, which is essential for tracking cancer progression and evaluating therapeutic responses over extended periods. However, the potential cytotoxicity of QDs remained unclear until Bhatia et al. reported on the biological toxicity of CdSe QDs. They proved that the toxicity is linked to the release of free Cd^{2+} ions resulting from the deterioration of the CdSe lattice. Specifically, their *in vitro* study indicated that CdSe QDs can be rendered non-toxic through proper coating. In addition to surface coatings, they further proposed that the cytotoxicity of QDs can be modulated by synthesis parameters and ultraviolet light, providing design guidelines for both *in vitro* and *in vivo* applications of QDs [22]. In subsequent years, biological toxicity has become a prominent area of research in the development of QDs. As a result, heavy metal-free QDs such as copper indium sulfide (CuInS), indium phosphide/zinc selenide (InP/ZnSe), manganese selenide/zinc selenide (MnSe/ZnSe), silicon (Si) and carbon (C) have been successfully developed [23–25]. This indicates that biological compatibility is gaining increasing attention and is being leveraged to further advance the application of QDs. Moreover, the future direction of QDs research will focus on the development of greener, less toxic, more compatible, and higher luminescence efficiency QDs materials.

Currently, there are various types of QDs that encompass a wide range of materials, structures, and properties. These include:

(i) Semiconductor QDs: group II-VI (CdS, CdSe, CdTe, ZnO, ZnS, ZnSe, ZnTe, HgTe), group III-V (InN, InP, InAs, InSb, GaN, GaP, GaAs, GaSb, AlN, AlP, AlAs, AlSb), group IV-VI (PbS, PbSe, PbTe), and group IV (Si, Ge); (ii) 2D QDs: transition metal dichalcogenide (TMD) QDs, graphene QDs (GQDs), graphitic carbon nitride (g-C_3N_4) QDs (g-CNQDs), hexagonal boron nitride (h-BN) QDs, and black phosphorus QDs (BP QDs); (iii) carbon QDs (CQDs); (iv) perovskite QDs [23, 26–40] (Table 1). These different types of QDs possess unique properties and hold great potential for applications in various fields and industries.

3 QDs functionalization for biomedical applications

The investigation of preparation methodologies and performance optimization for QDs remains a prominent area of research focus. Researchers are continuously exploring novel approaches to cater to the diverse needs of various applications. These approaches aim to precisely manipulate the size, shape, and optical and electrical properties of QDs. The synthesis strategies for QDs include top-down synthesis, bottom-up synthesis, and biological synthesis. Various synthesis routes demonstrate the potential applications of QDs in numerous fields. However, for the use of QDs in biomedicine, proper functionalization is necessary to suit the unique internal environment of the body. This involves enhancing their water solubility and biocompatibility, as well as conducting biomolecular modifications.

3.1 Preparation of water-soluble QDs

QDs synthesized in organic solvents cannot be directly applied in biological systems due to their hydrophobic ligands on the surface. In order to obtain water-soluble QDs that are suitable for biological applications, common strategies include amphiphilic molecule encapsulation and ligand exchange.

Amphiphilic molecule encapsulation involves using amphiphilic molecules containing both hydrophobic and hydrophilic parts to encapsulate hydrophobic QDs. The outward-facing hydrophilic part provides water solubility and subsequent functionalization. Liposomes, phospholipids, silanes, and silica are commonly used encapsulating molecules [41]. Liposomes, for example, are double-layered vesicles that can encapsulate nanoparticles in water. When

Table 1 Classification of QDs

Types of QDs			Characteristics	References
Semiconductor QDs	Group II-VI	CdS, CdSe, CdTe, ZnO, ZnS, ZnSe, ZnTe and HgTe	One of the most widely used and mature QDs with excellent luminescent; however, the heavy metal element cadmium limits their application in nanomedicine	[26]
	Group III-V	InN, InP, InAs, InSb, GaN, GaP, GaAs, GaSb, AlN, AlP, AlAs and AlSb	Some of them have low toxicity and excellent fluorescence properties, which are suitable for application in biological systems	[27, 28]
	Group IV-VI	PbS, PbSe, and PbTe	The lead salt QDs provide chance for studying the effects of strong confinement owing to approach the limit of strong quantum confinement and they are suitable for studying dimensional quantization systems	[32, 33]
	Group IV	Si and Ge	Nano-silicon can produce strong photoluminescence owing to the quantum confinement effect	[39]
	Transition metal dichalcogenide (TMD) QDs	MoS_2, WS_2, ReS_2, TaS_2, $MoSe_2$ and WSe_2	TMD means transition metal atoms covalently sandwiched by two hexagonal planes of chalcogen atoms	[40]
2D QDs	Graphene QDs (GQDs)		Compared with traditional semiconductor QDs, GQDs have higher chemical inertness, smaller size, better solubility and wider emission wavelength coverage	[38]
	Graphitic carbon nitride ($g\text{-}C_3N_4$) QDs (g-CNQDs)		CNQDs have strong blue emission and up-conversion characteristics and can be used as a universal energy transfer element	[37]
	Hexagonal boron nitride (h-BN) QDs		h-BN QDs has excellent chemical stability and thermal stability	[36]
	Black phosphorus QDs (BP QDs)		The independent monolayer phosphene is a semiconductor with an inherent direct band gap theoretically estimated at 0.8–1.5 eV, which fills the gap between GQDs and TMD QDs	[35]
Carbon QDs (CQDs)			In addition to similar fluorescence characteristics, CQDs have the advantages of low toxicity, low cost and good biocompatibility	[34]
Perovskite QDs			Ease of synthesis; high luminescence yield; however, their chemical stability is severely limited by external environmental factors	[29–31]

QDs are encapsulated within liposomes, the resulting hybrids possess the properties of both liposomes and QDs. Moreover, these hybrids can be internalized by tumor cells, and targeting ligands can be attached to the liposome surface to achieve tumor cell targeting. Phospholipid micelles, composed of amphiphilic polyethylene glycol-phosphatidylethanolamine (PEG-PE) and phosphatidylcholine (PC), have been successfully used to encapsulate ZnS/CdSe core-shell QDs. These micelles retain the optical properties of QDs and have been applied for real-time monitoring of embryonic development. Silane-encapsulated QDs not only improve the water solubility of QDs but also allow for easy modification, enabling further coupling with biomolecules. Additionally, dual-layer encapsulation using different encapsulating molecules, such as silica and polymers, can greatly enhance the stability of QDs. Polymer encapsulation, in particular, provides better biocompatibility and reduces the toxicity of QDs. However, the impact of large molecule encapsulation on the final size of encapsulated QDs should be considered.

Ligand exchange involves replacing surface-active agents such as trioctylphosphine oxide (TOPO), HAD, and octadecylamine (ODA) with end-capped ligands to increase the water solubility of QDs. This process disperses hydrophobic QDs in a solution that contains an excess of hydrophilic ligands. Over time, ligand exchange occurs, resulting in QDs with suitable size, excellent optical properties, and good stability. Hydrophilic ligands that contain amino, carboxyl, polyethylene glycol (PEG), and metal-binding groups are ideal for this purpose. Mercaptoacetic acid, cysteine, silanes, cyclodextrins, and mercaptosuccinic acid are commonly used to prepare biocompatible QDs [42]. The use of multidentate ligands can enhance the stability of QDs in biological applications and reduce their toxicity. These ligands, which have multiple coordinating groups, exhibit improved binding stability through cooperative chelation effects, thus making QDs more environmentally tolerant. One commonly used multidentate ligand is dihydrolipoic acid (DHLA), which binds to QDs through two thiol groups [43].

3.2 Biomolecular conjugation

In addition to being used as templates for preparing biocompatible QDs, biomolecules can also serve as functional ligands for QDs modification. Further conjugating water-soluble QDs with biomolecules is crucial for achieving selective recognition and binding of biomarkers. Physical adsorption, covalent conjugation strategy, metal-affinity coordination, ligand-receptor interaction, click chemistry, and virus encapsulation are common strategies for the conjugation of QDs with biomolecules.

Physical adsorption involves attaching biomolecules to the surface of QDs by utilizing their polarity or electrostatic interactions. However, this method is limited by its lack of specificity and the inability to control the orientation of the biomolecules.

The core of the covalent conjugation strategy involves forming new chemical bonds between the functional groups of QDs surface ligands and biomolecules. This approach provides stability advantages. Common covalent conjugation strategies for attaching biomolecules to QDs surfaces include carbodiimide chemistry, amine-reactive chemistry, and sulfhydryl-reactive chemistry [42]. Among these, carbodiimide chemistry is widely used because proteins and peptides contain abundant amino and carboxyl groups. Carbodiimide reagents such as dicyclohexylcarbodiimide (DCC) and 1-ethyl-3-(3-dimethylaminopropyl) carbodiimide (EDC) can coordinate with N-hydroxysuccinimide (NHS) to

catalyze the reaction between carboxylic acid groups and amino groups, resulting in the formation of stable amide bonds. Bharali et al. utilized DCC/NHS-activated thiolated lipoic acid-modified InP-ZnS QDs to obtain NHS-carboxylated intermediates, which were further conjugated with folate amino groups to create folate-QDs [44]. These folate-QDs exhibited good photostability and could specifically enter folate receptor-positive cells through folate receptors. Additionally, amine-reactive chemistry and sulfhydryl-reactive chemistry are universal strategies for preparing QDs-protein conjugates. Amine-reactive chemistry involves using heterobifunctional N-hydroxysuccinimidyl ester 6-hydrazinonicotinamide (NHSHyNic) as a crosslinking agent to achieve covalent conjugation between antibodies and QDs. Sulfhydryl-reactive chemistry, on the other hand, relies on the formation of covalent thioether bonds between antibody sulfhydryl groups and maleimide-modified QDs.

Metal-affinity coordination occurs when biomolecules utilize functional groups to self-assemble on the surface of QDs' inorganic shells. Biomolecular conjugation based on metal-affinity coordination typically adopts two strategies. First, thiol or imidazole functional groups are utilized due to their affinity for the ZnS shell. Multiple thiol-modified biomolecules are often used to enhance stability. Second, multiple histidine tags interact with metals, promoting the spontaneous assembly of histidine-tagged biomolecules onto the surface of QDs. This strategy offers several advantages, including rapid and stable binding. It is widely employed in the development of fluorescence resonance energy transfer (FRET)-based nanosensors and allows for easy preparation of protein/peptide-conjugated QDs, thanks to the fusion histidine tags found in proteins/peptides [45].

Ligand-receptor interaction involves the affinity between ligands and receptors, such as antigen-antibody binding and biotin-streptavidin binding. Taking the preparation of QDs-antibody conjugates as an example, DHLA and its derivatives are commonly used to enhance the stability and solubility of QDs. Electrostatic interactions cause positively charged streptavidin to aggregate onto DHLA-passivated CdSe/ZnS QDs, creating QDs-streptavidin conjugates. These conjugates then employ streptavidin to bind with biotinylated antibodies, resulting in the formation of QDs-antibody conjugates [46]. Similarly, the interaction between biotin and streptavidin is a widely employed approach for conjugating QDs with various biomolecules.

The click reaction is a chemical reaction that is efficient, selective, rapid, and reversible. It is used to construct stable covalent bonds between compounds to connect different molecules. There are several types of click reactions, including the tetrazine-alkene (trans-cyclooctene) click reaction, the Cu(I)-catalyzed azide-alkyne click reaction, and the triazoles-alkyne click reaction. It is worth noting that Cu(I) can permanently reduce the fluorescence of QDs. Therefore, when using Cu(I)-catalyzed click reactions to attach biomolecules to QDs, it is necessary to take steps to prevent the interference of Cu(I) by encapsulating the QDs with polymers and silica, thus avoiding direct contact with Cu(I) [47]. Research has shown that QDs can be successfully utilized in cell membrane imaging by employing the strain-promoted click reaction between cyclooctyne-functionalized quantum dots and azide-modified biomolecules under Cu-free conditions [48].

In addition to the conjugation strategies mentioned above, viral capsid proteins have the ability to self-assemble and form virus-like nanocages. These nanocages can encapsulate QDs, resulting in QDs that possess exceptional biocompatibility. This process is known as virus encapsulation. Virus-encapsulated QDs, with their active infectivity, can be employed for tracking viral infections. The size and function of the virus-like nanocages are controlled by various types of viral proteins, their corresponding modifications, and the surface status of the QDs [49].

4 Current status of cancer diagnosis and treatment

Cancer is a major and widespread disease that poses a significant threat to human health, being one of the leading causes of death worldwide [50]. It has become a global concern, affecting both the economy and society. Early screening and management of cancer are crucial in improving patient outcomes, increasing survival rates, and enhancing quality of life. Early detection of cancer can have significant health benefits. For instance, established screening methods have greatly improved early diagnosis rates for breast cancer, cervical cancer, and colorectal cancer, enabling patients to receive timely treatment [51].

Currently, technologies for early detection of cancer can be classified into three main groups: medical imaging examinations, tissue biopsy, and liquid biopsy (Fig. 2). Imaging methods offer the advantage of being non-invasive and easily repeatable for identifying developing tumors [52]. Commonly used imaging techniques include ultrasound (US), computed tomography (CT), and magnetic resonance imaging (MRI), which analyze tumor morphology, density, and size. Low-dose CT scans are increasingly being used to detect cancer early in high-risk populations [53]. Visual imaging with endoscopy is the primary approach for early detection of colonic lesions. Fluorescence endoscopy, combined with fluorescent molecular imaging probes, has been employed to enhance detection of colorectal neoplastic polyps [54]. Photoacoustic imaging provides high resolution and non-ionizing radiation, but faces challenges in terms of penetration depth and miniaturization for clinical application. Tissue biopsy is a valuable procedure in certain situations, particularly when lesions cannot be conclusively identified using CT or MRI. It can also be used to distinguish histological subtypes with prognostic significance [55, 56]. Due to potential sampling bias and tumor heterogeneity, the collected tissue may not accurately represent the entire lesion. This can lead to potential false-negative results when using tissue biopsy. Furthermore, tissue biopsy carries risks such as invasiveness, pain, and bleeding. However, with the advancements in non-invasive medical techniques, liquid biopsy has emerged as a complementary method to imaging examinations. It is transforming the field of cancer treatment by facilitating non-intrusive, real-time monitoring of tumors and early identification of circulating tumor cells (CTCs), cell-free DNA (cfDNA), non-coding RNAs, and extracellular vesicles (EVs), among others [57]. Liquid biopsy has the potential to improve early detection strategies for cancer, identify minimal residual disease, and monitor the progression of the disease. In addition, it can provide detailed genomic and transcriptomic information without the need for invasive tissue biopsy [58]. This allows for a better understanding of the heterogeneity within the tumor and surrounding tissue, in addition to providing sequential samples.

Upon diagnosis, there are various therapeutic approaches for cancer, such as surgical resection, chemotherapy, radiotherapy, immunotherapy, targeted therapy, and phototherapy (Fig. 2) [59]. Surgery, radiotherapy, and chemotherapy are collectively known as the three major treatment methods for cancer. Surgery is suitable

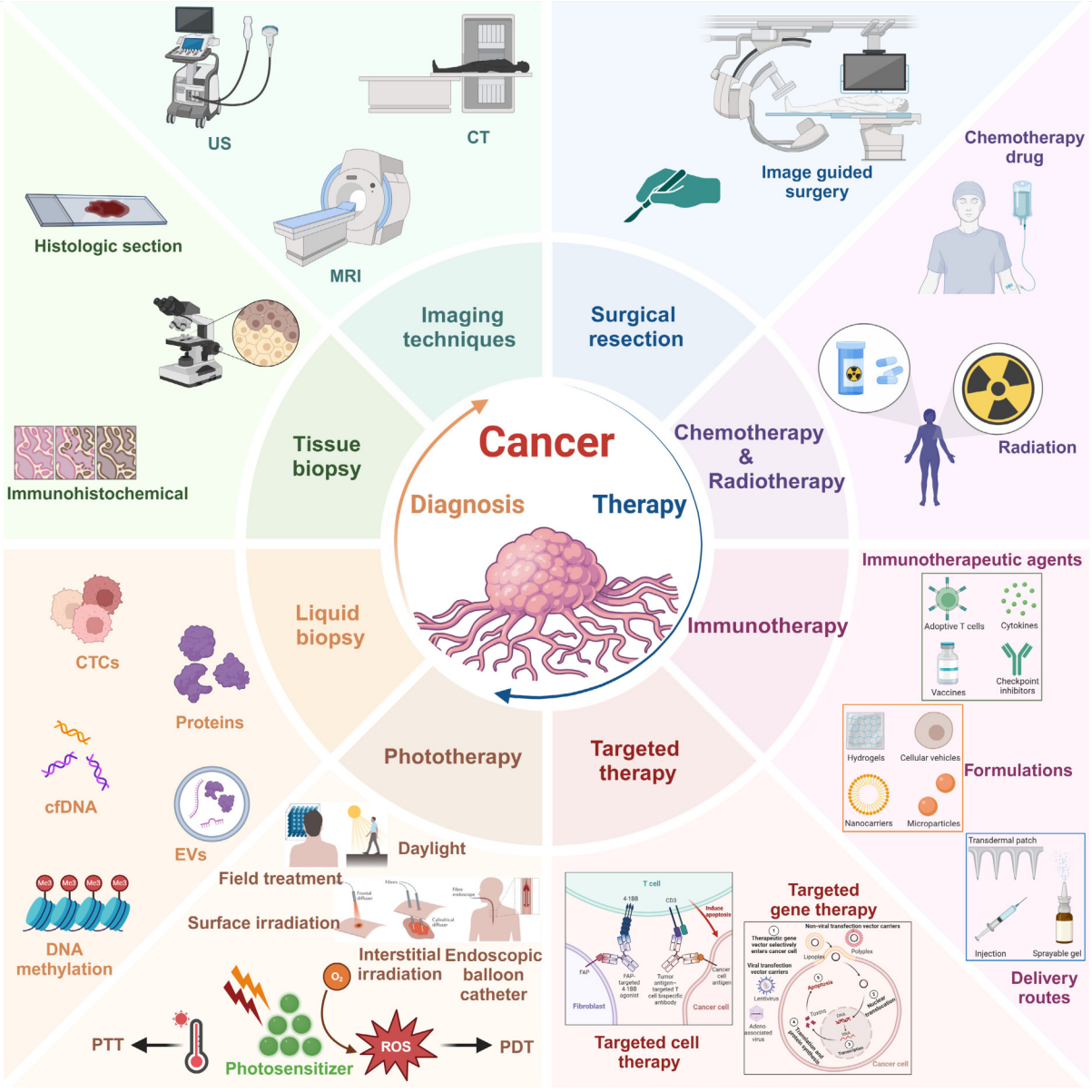

Figure 2 Available approaches for cancer diagnosis and treatment. Created using BioRender.

for early-stage cancer patients, with strict requirements regarding tumor location, size, etc. Radiotherapy utilizes various isotopes, high-energy X-rays, or high-energy electron beams to kill tumor cells and reduce tumor volume. However, the sensitivity to radiation is influenced by factors such as the duration of illness and infection. Chemotherapy uses chemical drugs to kill cancer cells and is a systemic treatment method. Compared to surgery and radiotherapy, which are effective for localized treatment, chemotherapy is more effective for mid-to-late-stage tumors with a tendency for systemic dissemination or metastasis. However, chemotherapy drugs are mostly cytotoxic, and there are various limitations in their application, such as age-related issues, poor physical condition, drug resistance, and insensitivity to chemotherapy drugs, which require alternative treatment options, such as immunotherapy. Traditional treatment methods for cancer, including surgery, radiotherapy, and chemotherapy, often cause excessive damage to the body or inevitable side effects. Under normal circumstances, immune cells recognize and clear abnormal cells, but cancer cells can escape immune recognition. Unlike traditional treatment methods, immunotherapy does not directly target tumors but rather activates the patient's own immune system to kill or inhibit cancer cells. Its side effects are minimal, making it a valuable adjunctive treatment strategy. Additionally, research has found that the occurrence and development of most tumors are driven by "driver genes". Finding and blocking specific "driver genes" is the core principle of molecular targeted therapy. This type of therapy aims to bind specifically to oncogenic sites within tumor cells at the molecular level, using therapeutic drugs. By interfering with specific biological processes of cancer cells, targeted therapy selectively kills or inhibits them. Compared to other treatments, targeted therapy causes less damage to normal cells and has fewer toxic side effects. However, it usually requires genetic testing or immunohistochemical testing to select the appropriate targeted drug. Additionally, phototherapy is a safe and effective mode of cancer treatment, with minimal side effects. The treatment process involves administering a photosensitizer for a certain period of

time, followed by irradiating the target lesion with light of a fixed wavelength. This selective excitation of the photosensitizer induces chemical damage (photodynamic therapy, PDT) or heat damage (photothermal therapy, PTT) to the target lesion, resulting in tumor ablation [60]. The selectivity of PDT and PTT is achieved through the preferential localization of light irradiation and light absorption of the photosensitizer in the target tissue. PTT enhances tissue heating using photothermal agents, causing cells to die when the local tissue temperature exceeds 60 ℃ due to protein denaturation and cell membrane damage. In contrast, PDT utilizes light-activated photosensitizers to generate cytotoxic reactive oxygen species (ROS), leading to cell apoptosis. Photosensitizers can also induce tumor vascular damage and blood stasis, thereby blocking the nutrient supply to tumor cells. When a single therapeutic approach may not completely eradicate tumors, combination therapy is commonly used in clinical practice. This approach offers the advantages of increased efficacy and fewer side effects. There are numerous combination therapy regimens, including the concurrent use of multiple chemotherapy drugs, chemoradiotherapy (CRT), and chemophototherapy (CPT). CRT and CPT integrate the advantages of local and systemic treatments. CRT is typically used as adjuvant therapy before surgical resection to improve organ preservation and survival rates. Chemotherapy drugs such as 5-fluorouracil and cisplatin can act as radiosensitizers and exert systemic effects, which are advantageous in controlling distant micrometastases. Clinical trials have demonstrated that CPT is more effective in producing anti-tumor effects compared to single chemotherapy/PDT [61].

To improve cancer diagnosis and treatment effectiveness, extensive research has been dedicated to developing sensitive and specific techniques for early tumor detection. Additionally, efforts have been made to create more selective anti-cancer drugs and improve drug delivery systems. Nanomedicine has demonstrated great potential in improving cancer diagnosis and treatment through the utilization of nanomaterial-based biosensors, diagnostic probes, contrast agents, and nanodrug carriers. Targeted nanoparticles contrast agents significantly enhance the sensitivity of CT imaging, making it easier to detect suspected tumors at an early stage [62]. Nanofluorescent probes enable the labeling and imaging of specific cancer cells, overcoming the limitations of traditional organic dyes and fluorescent proteins, which are susceptible to photobleaching and degradation [63]. Nanodrugs exhibit a preference for accumulating in tumor tissues through the enhanced permeability and retention (EPR) effect [64]. QDs have been extensively researched for their applications in cancer diagnosis and treatment. They are commonly used as luminescent probes and labels, and are widely applied in bioimaging, molecular sensing, and drug delivery strategies [65]. QDs probes for tumor-targeted imaging possess excellent photostability, a prolonged circulation time, and tumor-specific homing properties. Compared to conventional imaging dyes, QDs allow for a broad excitation wavelength range, a narrow emission spectrum, and spectral tunability, providing a solution for multi-analyte analysis using fluorescent probe labeling for different biomolecules. Moreover, near-infrared QDs offer minimal background interference and strong penetration, making them ideal imaging tools. Due to their size-dependent optical properties, QDs are suitable for constructing fluorescence sensors, which are widely used in the analysis of different types of biomarkers, including small molecules, ions, proteins, and nucleic acids. The high sensitivity, stability, rapidity, and cost-effectiveness of QDs make them superior to organic dyes, fluorescent proteins, and other fluorophores. Additionally, QDs can be surface-modified to obtain water solubility, biocompatibility, and target specificity. Conjugating modified QDs with targeted drugs, photosensitizers, etc., enables the achievement of traceable drug delivery patterns. The use of QDs as carriers enhances blood circulation time and improves drug delivery efficiency [66]. Different types of QDs, such as CdTe, CdSe/ZnS, and ZnO@polymer, have been employed in drug delivery systems. Here, we summarize the applications of QDs in cancer diagnosis and treatment to provide references for future QDs- and cancer-related research.

5 QDs enable cancer visualization and highly sensitive diagnosis

QDs have gained significant attention in the field of disease diagnosis owing to their unique properties, such as small size, surface functionalization, quantum confinement effects, high surface-to-volume ratio, and increased adsorption capacity. Recent studies have focused on the development of functionalized QDs to create diagnostic tools that can detect of disease-related biomolecules with greater precision and sensitivity [42, 67, 68]. By linking QDs with DNAzyme, antibodies, aptamers, ligands, or functional groups, various biomarkers such as nucleic acids, amino acids, peptides, proteins, enzymes, neurotransmitters, vitamins, ions, drugs, toxins, and pathogens can be detected [69–75]. In this regard, classic strategies for using QDs in cancer diagnosis have been introduced. QDs-based biomedical imaging and molecular detection technologies are enhancing the ability to accurately identify early tumors. The following sections will discuss the applications of QDs in cancer diagnosis from the perspectives of fluorescence bioimaging and molecular biomarker detection (Fig. 3).

5.1 QDs based fluorescence bioimaging

Tumor tissue imaging plays a crucial role in cancer research and clinical diagnosis, holding significant biological and clinical importance. Modern biomedical imaging techniques encompass a wide range of methods, including CT, positron emission tomography (PET), single-photon emission computed tomography (SPECT), MRI, ultrasound imaging, photoacoustic imaging, chemiluminescence/fluorescence bioluminescence imaging, radiolabeling, confocal microscopy, scanning electron microscopy (SEM), transmission electron microscopy (TEM), and cryo-electron microscopy. In fluorescence biomedical imaging, QDs are primarily used as image contrast agents for optical imaging modalities. Fluorescence imaging of cancer cells *in vitro* and *in vivo* involves the use of fluorescent agents that specifically bind to cancer cells. In the past, fluorophores such as fluorescein isothiocyanate (FITC), rhodamine B, and R-phycoerythrin have been widely used for targeted cell imaging when conjugated with antibodies [76]. In recent years, QDs such as CdSe, CdS, ZnSe, and ZnS have emerged as promising tools for fluorescence biomedical imaging and labeling strategies (Fig. 4). Compared to traditional fluorophores, QDs exhibit remarkable optical and electronic properties, including high fluorescence intensity, tunable light emission, restricted emission spectra, broad excitation wavelength range, long fluorescence lifetime, and resistance to photobleaching. Functionalized QDs, prepared using biomolecules like glucosamine precursors, can impart water solubility to QDs, thereby reducing cytotoxicity [77]. Moreover, doping QDs can enhance their potential applications in

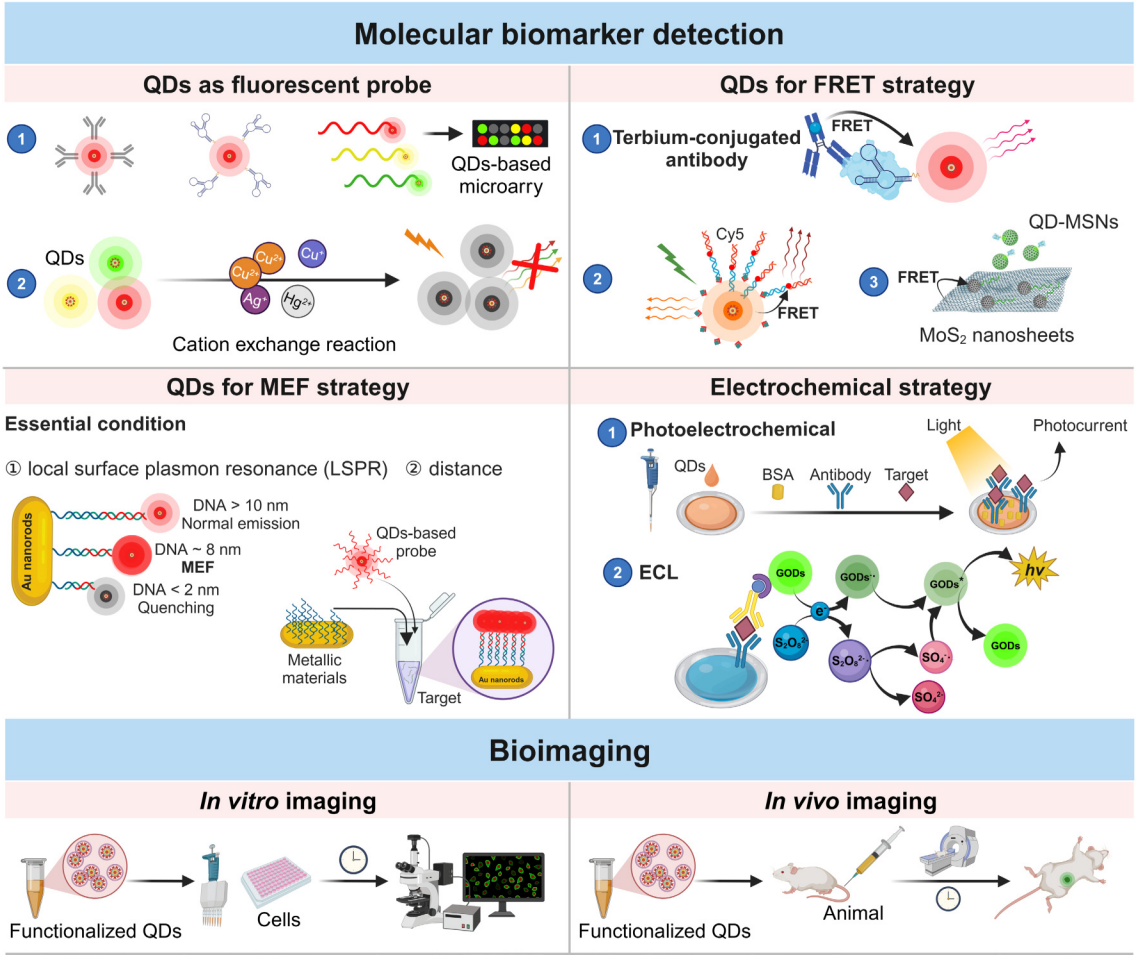

Figure 3 Various strategies of QDs for cancer diagnosis. Created using BioRender.

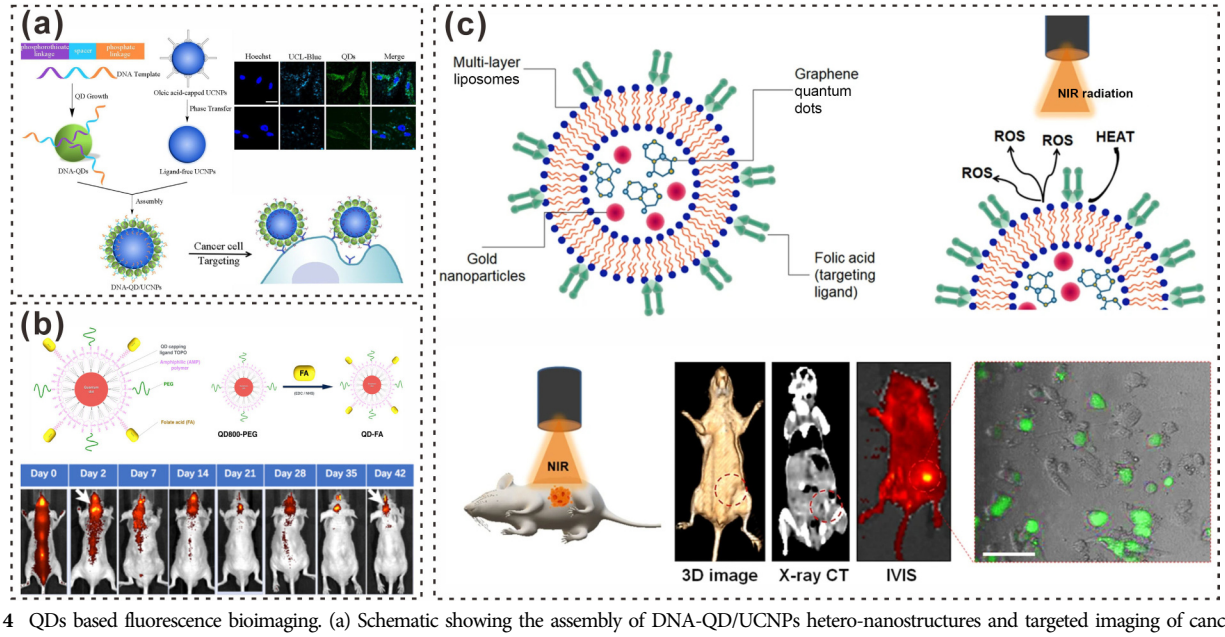

Figure 4 QDs based fluorescence bioimaging. (a) Schematic showing the assembly of DNA-QD/UCNPs hetero-nanostructures and targeted imaging of cancer cells. Reproduced with permission from Ref. [83], © Published by Elsevier B.V. on behalf of Chinese Chemical Society and Institute of Materia Medica, Chinese Academy of Medical Sciences 2019. (b) Structure of QD-FA, synthesis process of QD-FA and *in vivo* tumor-targeted imaging in tumor-bearing mice injected with QD800-FA. Reproduced with permission from Ref. [91], © American Chemical Society 2019. (c) Schematic representation of liposomal nanotheranostics for multimode-targeted bioimaging and photo-triggered cancer therapy. Reproduced with permission from Ref. [97], © Prasad, R. et al. 2020.

cancer imaging. For example, nitrogen (N) and sulfur (S) doping methods can further increase the quantum yield and fluorescence lifetime of QDs, enabling pH-dependent fluorescence characteristics that allow for direct differentiation between cancer cells and healthy cells [78]. Indomethacin, when conjugated with N-GQDs through amino groups, allows for the accumulation of N-GQDs within breast cancer cells, exhibiting enhanced fluorescence [79]. Additionally, the surface of QDs can be modified with specific biomolecules, such as antibodies, aptamers, small molecules, and other suitable targeting ligands, to serve as targeted probes. This modification enables precise localization of tumor lesions, improving initial cancer diagnosis/prognosis and allowing for *in vivo* observation of cancer tissues [80, 81]. One widely used method for targeting tumor cells is the use of antibody-conjugated QDs. By targeting cancer cell surface antigens with antibody-specificity, efficient uptake of QDs is facilitated, providing a stable and universal platform for cancer cell fluorescence imaging. For instance, Wu et al. prepared immunoglobulin G (IgG) and streptavidin-conjugated QDs to specifically label human epidermal growth factor receptor 2 (HER2) breast cancer biomarkers located on the cell surface. These QDs exhibited stronger and more photostable fluorescence compared to organic dye fluorescence. Moreover, by conjugating QDs emitting different spectra using this method, a multi-target imaging system could be constructed [82]. Another technique for tracking and imaging cancer cells is fluorescent labeling based on aptamers. Aptamers are single-stranded oligonucleotides selected from *in vitro* screening techniques from a random single-stranded oligonucleotide library. They have the ability to bind target ligands, including inorganic ions, small molecules, peptides, proteins, drugs, and even entire cells, with high specificity and affinity. Aptamers binding to target ligands generally have a stronger affinity than antigen-antibody interactions. Aptamers also offer advantages such as easy synthesis, modification, rapid reaction speed, and good stability. Xue et al. [83] developed a simple and universal DNA-mediated assembly strategy for creating heterostructures of DNA-QDs/upconversion nanoparticles (QD800-FA). These structures consist of CdTe QDs, lanthanide-doped UCNPs, and DNA. The strategy is based on the coordination interaction between DNA and the surface of QDs, as well as the strong coordination interaction between DNA and lanthanide metal ions on the surface of UCNPs. The resulting DNA-QDs/UCNPs not only retain the fluorescence properties of QDs and the upconversion luminescence characteristics of UCNPs, but also provide a multivalent DNA surface. When combined with aptamer design, this enables dual-mode imaging of cancer cells with targeted specificity. Prior research has shown that functionalizing QDs with dendritic polymers enhances their biocompatibility and cellular uptake. Li et al. [84] used EDC/NHS chemical reactions to couple dendritic polymer-modified CdSe QDs with aptamers specific for glioblastoma cells (GBI-10), preparing Apt-dQDs nanoprobes. *In vitro* imaging demonstrated that these nanoprobes effectively targeted U251 glioblastoma cells. Apart from specific antibody and aptamer recognition, folic acid and its receptor have a high-affinity binding ability. Folate receptors are overexpressed in various tumors, and studies have shown that folate-conjugated core-shell CdSe/CdS/ZnS QDs have fluorescence intensities hundreds of times higher than bare QDs. These QDs can selectively target folate receptor-positive cancer cells. By combining folic acid-modified QDs with biodegradable polymers, the *in vitro* cellular uptake rate of folate-overexpressing MCF-7 breast cancer cells can be further increased [85]. As an example, silica nanoparticles grafted with poly (methyl methacrylate-co-glyceryl methacrylate) can target cancer cells by attaching to glycans on the cell surface. This increases the uptake of nanoparticles specifically by cancer cells [86]. Another example is L-glutathione (LGSH)-terminated core-shell CdSeS/ZnS QDs, which can effectively locate in the cytoplasm of MCF-7 breast cancer cells without harming normal cells [87]. QDs modified with hyaluronic acid ligands can achieve targeted delivery of intracellular proteins by using hyaluronic acid-mediated QDs. This method effectively targets CD44-overexpressing MCF-7 cells and enables real-time fluorescence imaging [88]. In summary, using QDs labeled with specific targeting molecules provides important opportunities for targeted imaging of cancer cells.

Fluorescence imaging offers advantages over PET and MRI in terms of ease of use, cost-effectiveness, and the potential to detect individual isolated cells. However, *in vivo* fluorescence imaging is limited in sensitivity due to factors such as light scattering and absorption, which restrict the detection of optical signals as imaging depth increases. Additionally, autofluorescence from endogenous fluorophores can lead to uneven background signals and reduced signal-to-noise ratio in imaging [89]. As a result, visible fluorescence-based optical imaging cannot be applied to deep tissues, greatly limiting its clinical utility. On the other hand, NIR fluorescence offers greater penetration, facilitating the collection of fluorescence signals from deep tissue layers. This makes it promising for visualizing, resecting, and treating of tumor tissues within organs. NIR fluorescence imaging is also valuable in cancer diagnosis and treatment due to its portability, high spatial resolution, and comprehensive molecular analysis capabilities. Functionalized NIR QDs, which have good biocompatibility and can bioconjugate with various cancer-targeting ligands, can prolong circulation time in the blood, enhance accumulation within tumors, and increase fluorescence signals. Duman et al. [90] developed PEGylated Ag2S QDs functionalized with cetuximab (Cet) and loaded with the anticancer drug 5-fluorouracil (5FU). These Cet-functionalized QDs selectively targeted cell lines that overexpressed the epidermal growth factor receptor (EGFR), facilitating effective NIR imaging. Simultaneously, 5FU was selectively delivered to the EGFR-overexpressing cells, leading to significantly enhanced cell death through apoptosis and reduced drug resistance. Another study reported folate-modified NIR QDs (QD800-FA) with superior tumor-targeting capabilities, with the maximum emission at 800 nm. *In vivo* studies using a xenograft mouse model with folate-rich U87MG cells demonstrated that the tumor uptake of QD800-FA was significantly higher than that of QD800 (approximately 3.7-fold higher), and fluorescence signals could still be observed in the mouse brain 6 weeks after injection [91].

Although current imaging technologies enable the depiction of biological structures and functions at different scales, such as *in vivo*, tissue, and molecular levels, single-modal imaging has its limitations. For example, optical imaging is sensitive to optical background, prone to unstable signals, lacks accurate quantification, and does not allow for the use of different optical methods. These limitations can affect the precision of tissue pathological detection. To overcome these challenges, the field of biomedical imaging is trending towards multimodal imaging, which combines and integrates the strengths of multiple imaging techniques. Electron microscopy, for instance, addresses the low-resolution limitation of optical microscopy and enables detailed observation of the ultrastructure of tumor tissues. It can also help identify differentiation markers of tissue cells and diagnose different tumor types. By combining electron microscopy with optical imaging,

multimodal imaging techniques are driving tumor research forward. These techniques provide a crucial scientific basis for understanding tumor biological characteristics, evolution processes, disease diagnosis, and treatment monitoring. A typical example of multimodal imaging is PET/CT imaging, which combines functional information obtained from PET with anatomical information from CT. This approach enhances disease recognition sensitivity [92]. Compared to PET/CT, PET/MRI provides better soft tissue contrast, lower radiation dose, higher spatial resolution, and the ability to use novel PET agents based on different compound magnetic properties [93]. However, commonly used gadolinium (Gd)-based MRI contrast agents may cause allergic reactions and toxicity due to long-term tissue accumulation, and they are not recommended for patients with renal dysfunction. To address these limitations, researchers are developing new contrast agents, such as targeted functionalized magnetic nanoparticles (MNPs). CT imaging relies on X-ray absorption by tissues with high atomic number elements (such as calcifications and bones), while MRI is more suitable for imaging soft tissues. By combining the advantages of both techniques, MRI/CT imaging contrast agents have attracted increasing interest in clinical and research. Studies have demonstrated that nanoparticles (NPs) can serve as excellent MRI contrast agents, as they have superior relaxation properties compared to Gd chelates and longer plasma half-lives [94]. In addition, optical imaging probes, such as fluorescent probes, surface-enhanced Raman scattering (SERS), polymer dots, and functional QDs, are being developed as intraoperative imaging tools to complement traditional imaging platforms (such as CT, MRI, PET, etc.) and facilitate precise tumor localization. The use of MRI/optical imaging dual-modalities has shown promise in improving the accuracy of cancer diagnosis [95]. Mulder et al. [96] prepared polyethylene glycol-coated paramagnetic QDs (pQDs) as molecular imaging probes for fluorescence microscopy and MRI. Targeting ligands can be conjugated to these pQDs using maleimide or other functional groups. After conjugation with cyclic RGD peptide, successful targeting to human umbilical vein endothelial cells *in vitro* was achieved. The micelle coating contains approximately 150 units of Gd-DTPA-bis(stearylamide), which gives this bimodal contrast agent high relaxivity and potential applications in tumor angiogenesis detection. Additionally, Prasad et al. [97] developed a multifunctional liposome-based nano-therapeutic agent called NFGL. The core design of NFGL includes: (i) surface functionalization with folate for targeting, (ii) loading of Au NPs and emitting GQDs for dual-modal imaging, and (iii) loading of the anticancer drug doxorubicin hydrochloride for photo-triggered chemotherapy. When exposed to near-infrared light (750 nm) irradiation, NFGL exhibited significant ROS scavenging ability and better tumor reduction effects, with site-selective tumor reduction due to the synergistic effect of chemotherapy-photothermal therapy (chemo-PTT). Furthermore, the biocompatibility of NFGL was validated. Therefore, a diagnosis and treatment system based on NFGL could potentially provide a safe multi-modal tumor diagnosis and treatment platform. In summary, multimodal imaging can integrate various imaging paradigms such as optical, electrical, magnetic, and nuclear, allowing for comprehensive dynamic depiction of life activities at different scales. This provides researchers with valuable tools and methods for biomedical research and disease molecular diagnosis.

5.2 QDs based molecular biomarker detection

Tumor biomarkers are features or substances found in blood, tissues, or other biological samples that can indicate the presence, development, treatment response, or prognosis of tumors. Their discovery and application are of great significance for tumor risk assessment, early diagnosis, selection of treatment regimens, disease monitoring, and prognosis evaluation. Tumor biomarkers encompass various forms, including protein biomarkers (like prostate specific antigen (PSA), cancer antigen 125 (CA125), and carcinoembryonic antigen (CEA)), nucleic acid biomarkers (such as specific gene mutations, ctDNA, and miRNAs), cytological biomarkers (which involve changes in cell morphology, surface markers, or quantity), and imaging biomarkers (like CT, MRI, and PET scans, which can display tumor size, location, and distribution). Molecular biomarkers, which occur at the molecular level, are typically more useful in the early stages of the disease [98]. Assessing tumor risk and diagnosing early based on changes in molecular biomarkers can significantly improve therapeutic interventions and patient survival rates. There are two main objectives in tumor molecular biomarker research: (i) to explore new biomarkers or combinations of biomarkers that can indicate tumor occurrence, development, treatment response, or prognosis evaluation, thereby improving the accuracy of early diagnosis and helping doctors create personalized treatment plans, and (ii) to develop sensitive, reliable, cost-effective, and powerful strategies to detect tumor biomarkers. However, detecting tumor biomarkers comes with numerous challenges. Tumors themselves have complex biological characteristics and heterogeneity, and biomarkers can vary between different types of tumors or even within the same type of tumor, making biomarker detection more complex. In the early stages of tumor development, the amount of biomarkers in biological samples like blood or tissues is very low, even far below the detection limit of standard methods. Additionally, biomarker detection is prone to interference from other components in complex biological samples, making accurate detection and quantification difficult. Furthermore, the analysis of nucleic acids faces challenges such as ctDNA fragmentation and miRNA instability. Overcoming these challenges is vital for early tumor detection.

Currently, the construction of detection strategies for specific molecular biomarkers typically comprises three crucial components: signal recognition, signal amplification, and signal transduction and reporting. Signal recognition entails the precise identification and capture of target molecules using specific biological recognition molecules such as antibodies, aptamers, peptides, or DNA/PNA probes. Signal amplification refers to enhancing or amplifying the signals of the target molecules to facilitate their detection and quantification, especially for low abundance targets. Common methods of signal amplification include nucleic acid amplification (such as polymerase chain reaction (PCR), catalytic hairpin assembly (CHA), hybridization chain reaction (HCR)), enzyme labeling (such as horseradish peroxidase commonly used in immunoassays), fluorescent labeling, isotope labeling (such as 32P or 35S labeling commonly used in blotting assays), and gene chip technology. Signal transduction and reporting involve converting biomarker signals into easily quantifiable optoelectronic signals through optical, electrical, magnetic, and mass changes, such as visual visualization, fluorescence, electrochemistry, surface plasmon resonance (SPR), and SERS. QDs-based biomarker detection methods offer multiplexing ability due to their strong and stable fluorescence over a long period, narrow emission spectrum in the near-infrared

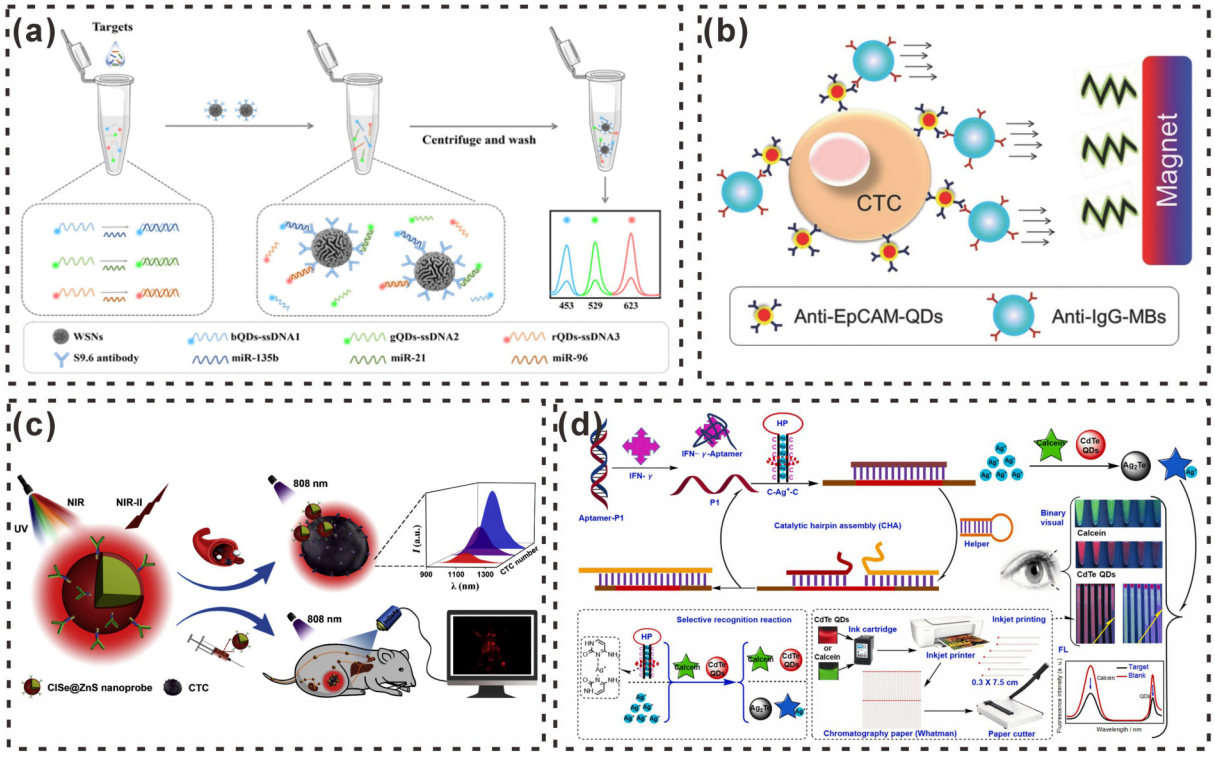

Figure 5 QDs as fluorescent probe. (a) Schematic of the principle of simultaneous determination of target miRNAs using QDs-ssDNA probe. Reproduced with permission from Ref. [100], © American Chemical Society 2024. (b) Schematic representation of CTC capturing using anti-EpCAM-QDs and anti-IgG-MBs. Reproduced with permission from Ref. [101], © WILEY-VCH Verlag GmbH & Co. KGaA, Weinheim 2015. (c) Schematic illustration showing the proposed broadband excitable CISe@ZnS NIR-II luminescent nanoprobes for CTCs bioassay and tumor-targeted bioimaging. Reproduced with permission from Ref. [102], © Elsevier Ltd. All rights reserved 2020. (d) Schematic presentation of nanoscale signal reporter based on the fluorescence quenching properties of QDs caused by metal ions such as Cu^{2+}, Cu^{+} and Ag^{+}. Reproduced with permission from Ref. [104], © Elsevier B.V. All rights reserved 2022.

region, large specific surface area, and the ability to combine with multiple molecules to design multifunctional nanostructures. This enables the simultaneous high sensitivity detection of multiple biomarkers in biological media, thereby promoting cancer diagnosis and prognosis [41, 99]. How exactly are QDs applied in the detection of cancer biomarkers? Common strategies are summarized below.

5.2.1 *QDs as fluorescent probe*

In the history of developing molecular marker detection technology, fluorescence detection stands out for its high sensitivity, low cost, and ease of operation. QDs have excellent fluorescence properties and can be easily modified, making them superior to organic fluorescent dyes in fluorescence detection schemes. The most common approach for designing nanofluorescent probes is to directly use QDs (Fig. 5). For instance, Wang et al. utilized the classic carbodiimide reaction to couple amino-modified ssDNA onto carboxyl-modified QDs as miRNA recognition-reporting probes [100]. When miRNA is present, it captures the QDs-ssDNA probe to form QDs-ssDNA/miRNA complexes. These complexes are then recognized and captured by anti-double-stranded antibodies that are modified on wrinkled silica nanoparticles (WSNs). Ultimately, the QDs' fluorescence signal on the WSNs indicates the results of miRNA detection. By using QDs with different emission wavelengths and specific ssDNA sequences, it is possible to simultaneously analyze different miRNAs. This study successfully demonstrates the sensitive detection of triple miRNAs in bladder cancer using QDs-ssDNA probes. Circulating tumor cells (CTCs), which are popular markers for "liquid biopsy", can be used to monitor the condition of cancer patients and the effectiveness of drugs. However, CTCs are present in extremely low numbers in the bloodstream, and developing simple and efficient strategies for their enrichment and detection remains a major challenge. Min et al. [101] developed a simple strategy for capturing and detecting CTCs using a combination of QDs and magnetic beads. The strategy involves coupling EpCAM antibodies to the surface of 630QDs (anti-EpCAM-QDs) to specifically identify CTCs. The CTCs are then separated using anti-mouse IgG-modified magnetic beads (anti-IgG-MBs). Finally, cell imaging is used to directly quantify the captured CTCs using the fluorescence signals from the QDs. In a similar study, Lian et al. encapsulated $CuInSe_2$ (CISe) QDs with ZnS to create a new CISe@ZnS nanoprobe that exhibits strong NIR-II emission for CTC detection. These CISe@ZnS QDs produce strong near-infrared fluorescence when excited at 808 nm. By modifying the surface of the CISe@ZnS QDs with EpCAM antibodies, they can specifically recognize CTCs both *in vivo* and *in vitro*. The *in vivo* application of this nanoprobe was confirmed in live mice. When the antibody-modified CISe@ZnS nanoprobe was injected into the mouse tail vein, its distribution, targeted accumulation, and clearance were monitored in real time using NIR-II imaging. The probe demonstrated good biocompatibility *in vivo* and could be metabolized and excreted by the liver and kidneys. This nanoprobe holds promise for cancer diagnosis and guided imaging in microsurgery [102]. To further enhance signal amplification, Wu et al. devised a method using a DNA concatamer and the biotin-streptavidin interaction to load a large number of QDs into the DNA concatamer. This DNA concatamer was then employed as a signal reporter for detecting

oral squamous cell carcinoma (OSCC) salivary exosomes. The QD-containing DNA concatamer binds to magnetic microspheres that are modified with exosomal protein (CD63) aptamers through base complementary pairing. This interaction leads to the formation of magnetic and fluorescent bio-probes (MFBPs). When exosomes are present, the DNA concatamer with QDs is released, and the fluorescent signal of the released QDs can be detected through magnetic separation, thanks to the recognition of the exosomes. This system allows for the amplification effect of "one magnetic microsphere-multiple exosomes" and "one exosome-multiple QDs". MFBPs can be added directly to the sample being tested after preparation, which significantly simplifies the operational steps [103]. In addition, Chen et al. directly employed QDs as nanoscale signal reporters to avoid the complexities associated with surface modification. They developed a sensitive and versatile marker detection scheme by exploiting the quenching properties of QDs fluorescence caused by metal ions such as Cu^{2+}, Cu^{+}, and Ag^{+} [104]. In this scheme, the target recognition signal is converted into a concentration change of specific ions in the system, resulting in a corresponding change in QDs fluorescence signal that serves as the final readout.

5.2.2 *QDs for FRET-based fluorescence detection*

FRET is a process in which fluorescence energy is transferred from a donor molecule to an acceptor molecule when they are within a distance less than the Förster radius [105]. FRET-based strategies are commonly used to detect cancer biomarkers such as EVs [106], alpha-fetoprotein (AFP) [107], CEA, PSA [108], and circRNAs [109]. These strategies typically operate in two modes: "turn on" and "turn off". In the presence of the target, "turn on" refers to the recovery of fluorescence, while "turn off" refers to the quenching of fluorescence. QDs are frequently used as donors in FRET systems due to their size-tunable photoluminescence, which allows for the construction of systems without spectral overlap and crosstalk (Fig. 6). QDs also offer higher sensitivity and stability compared to traditional dye-dye pairs. Some reported acceptors of QDs include Au NPs, gold nanorods, graphene oxide, ZnO nanowires, Cy3 dye, Cy5 dye, Ru complex, organic dye, BHQ2 dye, A647 dye, AF660 dye, and doxorubicin (DB). Electrospun nanofibrous films (ENFFs) are materials with a network structure, large specific surface area, and easy functionalization. They are widely used for the development of solid-phase sensing platforms. Yang et al. assembled CdTe QDs, CDs, and ENFFs to create a dual-emission fluorescent film called r-CdTe QDs/g-CDs/CA ENFFs. The FRET between CDs and QDs results in red fluorescence [107]. When the target protein is present, a sandwich structure consisting of an antibody-protein-CuO NPs labeled antibody is formed on the surface of r-CdTe QDs/g-CDs/CA ENFFs through antigen-antibody recognition. Under acidic conditions, CuO NPs release a large amount of Cu^{2+}, selectively quenching the fluorescence of QDs. The detection results of the target protein are reported using the ratio of fluorescence signals. This system has successfully detected AFP at pg/mL levels. Wu et al. also utilized smaller engineered scaffold proteins called ADAPTs instead of natural antibodies, using the principle of immune response. These ADAPTs self-assemble onto the surface of zwitterionic ligand-coated QDs to form ADAPTs-QDs conjugates [107]. In the presence of HER2, immune sandwich complexes are formed between IgG coupled to terbium (Tb) and ADAPTs-QDs conjugates. The smaller size of ADAPTs reduces steric hindrance, enabling FRET between Tb and QDs within an effective distance for direct signal output. In addition to the antigen-antibody

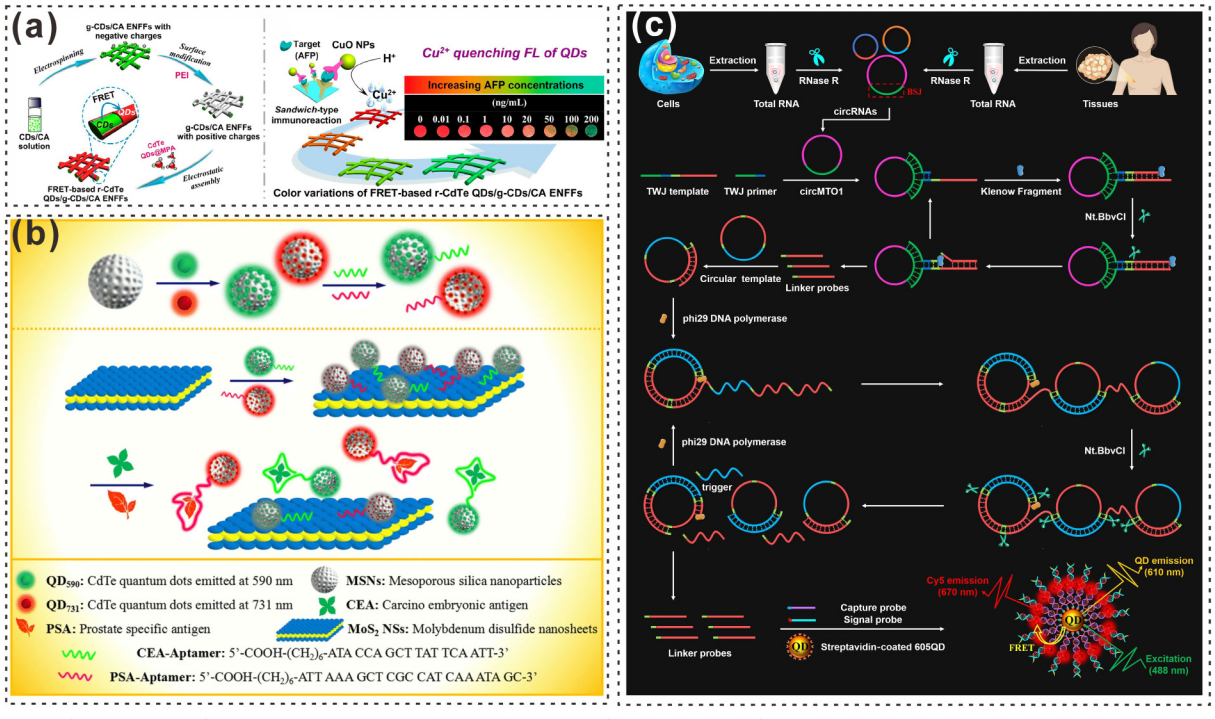

Figure 6 QDs for FRET-based fluorescence detection. (a) Schematic illustration of the preparation of FRET-based r-CdTe QDs/g-CDs/CA ENFFs and application of Cu^{2+}-mediated immunoassay for biomarkers. Reproduced with permission from Ref. [107], © American Chemical Society 2018. (b) Schematic presentation of turn-on fluorescent nanoprobes for simultaneous detection of CEA and PSA. Reproduced with permission from Ref. [108], © Springer-Verlag GmbH Austria, part of Springer Nature 2019. (c) Schematic diagram of a programmable QD nanosensor guided by three-way junction skeleton-mediated cascade signal amplification for sensitive detection of circRNAs. Reproduced with permission from Ref. [109], © Elsevier B.V. All rights reserved 2024.

recognition system, QDs have been applied in aptamers and nucleic acid recognition systems. Sun et al. utilized the porous structure and high specific surface area of mesoporous silica nanoparticles (MSNs) to carry plenty of QDs, resulting in QDs-MSNs with strong fluorescence signals [108]. Aptamer chains are added to QDs-MSNs through covalent attachment to recognize the target being detected. The fluorescence of aptamer-modified QDs-MSNs is quenched by using FRET between QDs and MoS_2 nanosheets (MoS_2 NSs). When the target appears, the binding between the aptamer and the target increases the spatial distance between QDs-MSNs and MoS_2 NSs, causing the QDs fluorescence to be released and resulting in a "turn on" effect. This approach enables the simultaneous analysis of multiple targets using QDs with different emission wavelengths. The study confirms that the use of 590QD and 731QD allows for the simultaneous detection of CEA and PSA dual targets, with a detection limit of fg/mL. In another study, Liu et al. developed a sensitive circRNAs analysis strategy using efficient FRET with 605QD as the donor and Cy5 as the acceptor [109]. In this strategy, the capture probe is immobilized on the surface of 605QD through biotin-avidin interaction. When circRNAs are present in the system, large amounts of ligation probes are generated through nucleic acid cascade amplification. The ligation probe connects the capture probe and the Cy5-labeled reporter probe, reducing the spatial distance between Cy5 and 605QD to enable efficient FRET. Cy5 fluorescence is enhanced upon target appearance, with almost zero background fluorescence, providing signal reporting for the target being detected.

Although numerous studies have explored the use of QDs in FRET-based fluorescence detection, challenges still exist in the design and implementation of this analysis method. One challenge is the modification of QDs' optical properties through surface modification, for which there is no universal solution. Another challenge is steric hindrance, which can affect target recognition and the occurrence of FRET, making the process difficult to control.

5.2.3 QDs for metal-enhanced fluorescence (MEF)-based fluorescence detection

The principle of MEF is based on the interaction between metal and fluorescent substances, known as plasmon resonance. This interaction is characterized by metal colloidal nanoparticles or metal nanostructures enhancing the fluorescence intensity of fluorescent substances when they are located at an optimal distance (3–10 nm) from each other. The occurrence of the MEF effect relies on two important conditions. Firstly, the local surface plasmon resonance (LSPR) band generated by the metal material should significantly overlap with the excitation or emission spectrum of the fluorescent probe. Secondly, the distance between the metal material and the fluorescent probe must be appropriate. If the fluorescent probe is too far away from the metal material (> 10 nm) or too close to it (< 2 nm), no fluorescence enhancement or quenching will be observed [110]. Au NPs are easily coupled to biological molecules such as antibodies, aptamers/nucleic acids, etc., due to their strong affinity with thiol groups. They are widely used in signal recognition and amplification designs. Jia et al. utilized the MEF effect between Au nanorods (Au NRs) and NIR Ag_2S QDs to develop a prostate cancer marker PCA3 detection technology [111]. In this study, DNA was employed to precisely control the distance between Au NRs and QDs, overcoming the limitation of inaccurate control with inorganic spacers. Au NRs and QDs modified with different DNAs were simultaneously captured by the PCA3 sequence through base complementary pairing, resulting in a distance of approximately 8 nm between the two. This approach enabled the enhancement of QDs fluorescence. The proposed method can detect PCA3 at the pM level and has been successfully applied to the analysis of complex biological samples.

5.2.4 QDs-based electrochemical biosensor

Electrochemical biosensing is a widely used method for detecting molecular markers due to its fast reading, simple equipment, and easy miniaturization. These biosensors consist of biorecognition elements (such as antibodies, aptamers, nucleic acids, enzymes, and receptors) and electrochemical converters. They rely on electrolytes that interact with specific conductive materials. By modifying electrodes with nanomaterials that have high specific surface areas, the capture ability of biomarkers can be enhanced, resulting in improved detection sensitivity for trace markers. Over the years, nanomaterials such as carbon nanotubes, graphene, polymer nanoparticles, and QDs have been extensively used in the development of electrochemical biosensors for diagnosing cancer molecular markers. Figure 7 [112] illustrates several strategies of QDs-based electrochemical biosensors. Among various luminophores, GQDs offer several advantages, including a large specific surface area, high electron transfer ability, strong chemical stability, low toxicity, low cost, and good biocompatibility. GQDs can be designed as electrochemiluminescence (ECL) probes with an extremely low starting potential (close to 0 V), which allows for more stable ECL signals. The nanocomposite material poly(5-formylindole)/reduced graphene oxide (P5FIn/erGO) improves conductivity and provides a large surface area for immobilizing biomolecules, making it an excellent choice for modifying electrode materials in potential ECL sensors. Nie et al. developed a sandwich ECL immunosensor using P5FIn/erGO and Au NPs-modified GQDs (GQDs@AuNPs) for ultrasensitive detection of CEA [113]. P5FIn/erGO plays a dual role in promoting ion transport in the reaction and providing a larger surface area for immobilizing CEA-specific antibodies. GQDs@AuNPs, acting as the ECL probe, modify CEA-specific antibodies while maintaining a stable electrochemical signal. Through antigen-antibody specific recognition, the sensor simultaneously binds to the CEA target with the P5FIn/erGO-modified antibody, forming a "sandwich" structure. This ECL immunosensor exhibits excellent selectivity, sensitivity, and stability, with a detection limit as low as the fg/mL level.

MXene-derived QDs (MQDs) are commonly used in ECL sensing as emitters and carriers. However, they are prone to oxidation due to the large number of exposed metal atoms on their surface. This oxidation causes instability, which limits their applications. To address this issue, Li et al. coated MXene-derived QDs with glutathione (GSH), resulting in GSH-MQDs. These GSH-MQDs exhibited excellent conductivity and electrochemical activity, effectively reducing the nanostructure defects of MQDs and improving their antioxidant properties [114]. The maximum ECL peak of GSH-MQDs was observed at 578 nm. In this study, GSH-MQDs were used as stable luminophores for ECL sensing. They were combined with hairpin recognition probe-modified magnetic biomimetic vesicles, which consisted of an internal magnetic core Fe_3O_4@SiO_2 and an outer lipid bilayer. This combination served as the signal recognition and amplifier system for the ECL biosensing of miRNAs. The process involved the

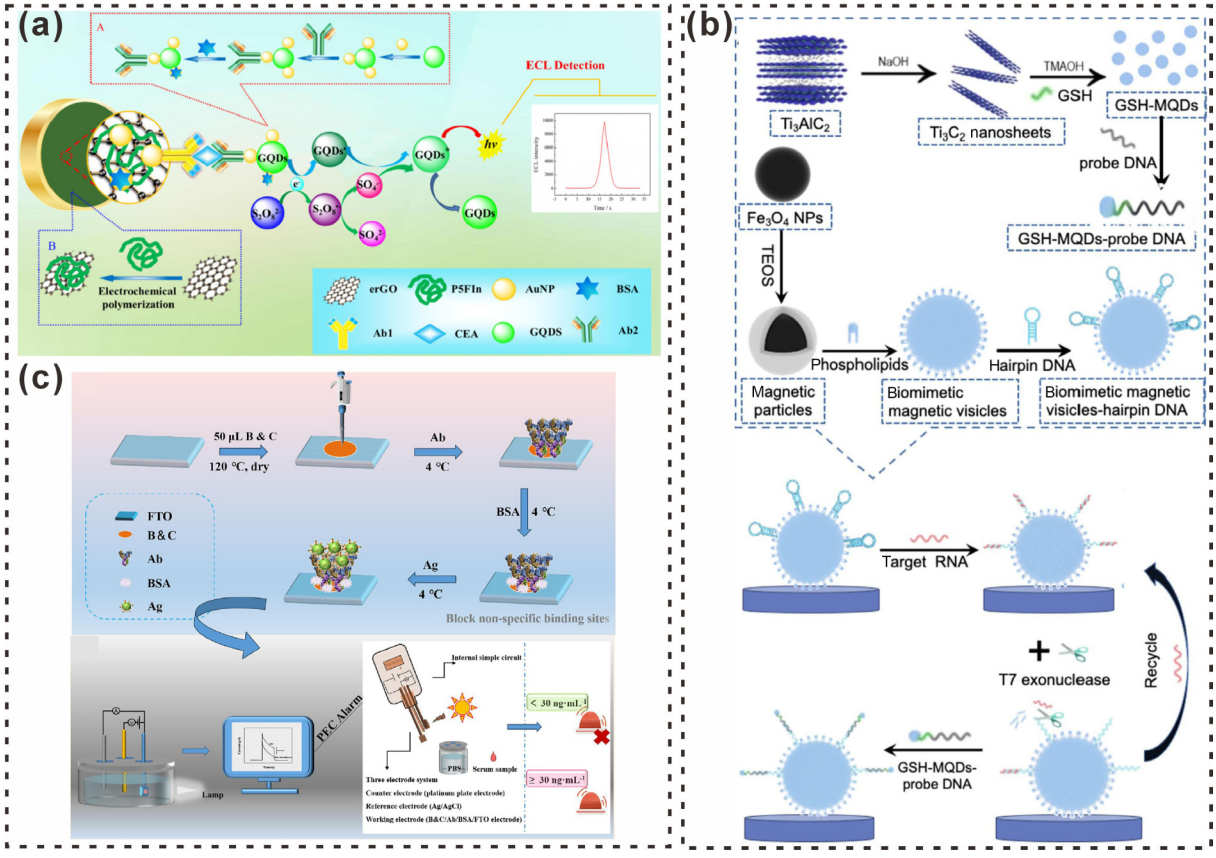

Figure 7 QDs-based electrochemical biosensor. (a) The fabrication progress of GQDs based ECL immunosensor based on P5FIn/erGO nanocomposite. Reproduced with permission from Ref. [113], © Elsevier B.V. All rights reserved 2017. (b) Illustration of the ECL sensing system based on GSH-MQDs and biomimic magnetic vesicles. Reproduced with permission from Ref. [114], © Elsevier B.V. All rights reserved 2022. (c) Illustration of PEC immunosensor based on Bi-MOF & CdS-QDs (B&C) for CYFRA21-1 detection and the construction of PEC alarm. Reproduced with permission from Ref. [116], © Elsevier B.V. All rights reserved 2024.

specific recognition of target miRNA by the hairpin probe on the magnetic biomimetic vesicle, resulting in the formation of double-stranded modified vesicles. These vesicles were then separated by magnetism, and the T7 exonuclease was employed to cut the double-stranded structure, releasing the miRNA for the next round of amplification. The probe on the vesicle bound to the DNA-modified GSH-MQDs through base complementary pairing. Finally, the miRNA detection signal was converted into the ECL signal of GSH-MQDs through a "recognition-cutting-recognition" process.

Photoelectrochemical (PEC) refers to the conversion of light energy, electrical energy, and chemical energy. It involves the absorption of light energy by photoelectrochemically active materials, which leads to photoelectric conversion in the electrode. This unique photoelectric conversion characteristic makes PEC biosensors advantageous in terms of low background signal and high sensitivity. PEC analysis can be classified into two types based on electron transport: photocathode (p-type semiconductor material) and photoanode (n-type semiconductor material). The photocathode utilizes the photoelectric effect to convert incident photons into outgoing electrons. For sensitization, Pei et al. combined BiOI, which has strong visible light absorption ability, with NiO to form a NiO/BiOI heterojunction with photocathode characteristics. The BiOI surface was further modified with Au NPs to enhance conductivity and the SPR effect. These Au NPs can then be used to attach capture DNA probes through Au-S bonds. The DNA probes contain aptamer sequences specific to the EpCAM protein and complementary sequences of CdSe QDs-modified DNA. The introduction of CdSe QDs significantly enhances the photocurrent intensity in the system. When breast cancer-related exosomes are present in the system, a dual desensitization effect occurs. Firstly, the EpCAM protein specifically binds to the aptamer in the capture probe, releasing CdSe QDs and thereby reducing the photocurrent intensity. Secondly, the presence of exosomes on the electrode hinders the electron transfer between the electrode and the electrolyte, further reducing the photocurrent signal. It has been demonstrated that this PEC biosensor is suitable for complex biological environments and exhibits excellent performance [115].

CYFRA21-1 is a serum tumor marker that plays a significant role in lung cancer. In their research, Mao et al. used CdS QDs, which have strong visible light absorption, and a porous material called Bi-MOF to create a photoactive material named B&C. This material exhibited a strong capability to respond to signals and sustained photocurrent. They then developed a highly sensitive material based on Bi-MOF with CdS QDs (B&C), which served as a PEC biosensor for the detection of CYFRA21-1 [116]. By sensitizing B&C, the photocurrent intensity significantly increased. Consequently, the B&C-modified Fluorine-doped tin oxide (FTO) electrode provided the photoanode signal. After further modification with CYFRA21-1-specific antibodies, the captured CYFRA21-1 weakened the photocurrent signal due to the insulating properties of the macromolecule. This system has a simple composition and operates in an alarm reporting mode. When the concentration of CYFRA21-1 reaches the clinical

monitoring threshold, the alarm is automatically triggered, providing a feasible solution for miniaturized PEC immunosensors. Similarly, Zhang et al. used antigen-antibody recognition in their study. They simultaneously used CdS QDs, $CuInS_2$ QDs, and CQDs to construct a PEC biosensor for PSA analysis [117]. CuInS2 QDs were loaded onto the surface of CdS QDs, and the energy level matching between the two contributed to the generation of photocurrent. Further modification with CQDs enhanced the material's light absorption and increased the photocurrent signal by more than ten times. Once the specific antibodies on the surface of $CdS/CuInS_2$/CQDs captured PSA, the photocurrent signal was attenuated, ultimately allowing for the quantification of PSA through the change in photocurrent signal.

5.3 QDs for point-of-care testing (POCT)

QDs linked with appropriate biomolecules have been successfully developed for accurate and personalized real-time remote biomarker monitoring [118, 119]. The remarkable photostability, high quantum yield, and size-tunable emission properties of QDs, as discussed in the preceding sections, render them particularly well-suited for the development of POCT devices. POCT applications demand robust and reliable indicators of biological or chemical events, often in challenging environmental conditions. The inherent attributes of QDs align perfectly with these requirements. The photostability of QDs ensures that they can maintain consistent performance over the lifespan of a POCT device, even when exposed to varying light conditions or continuous use. Their high quantum yield translates into strong and easily detectable signals, which is critical for accurate and rapid diagnosis. Furthermore, the ability to tune the emission properties of QDs allows for the development of multiplexed assays within a single POCT platform, enabling the simultaneous detection of multiple targets. The

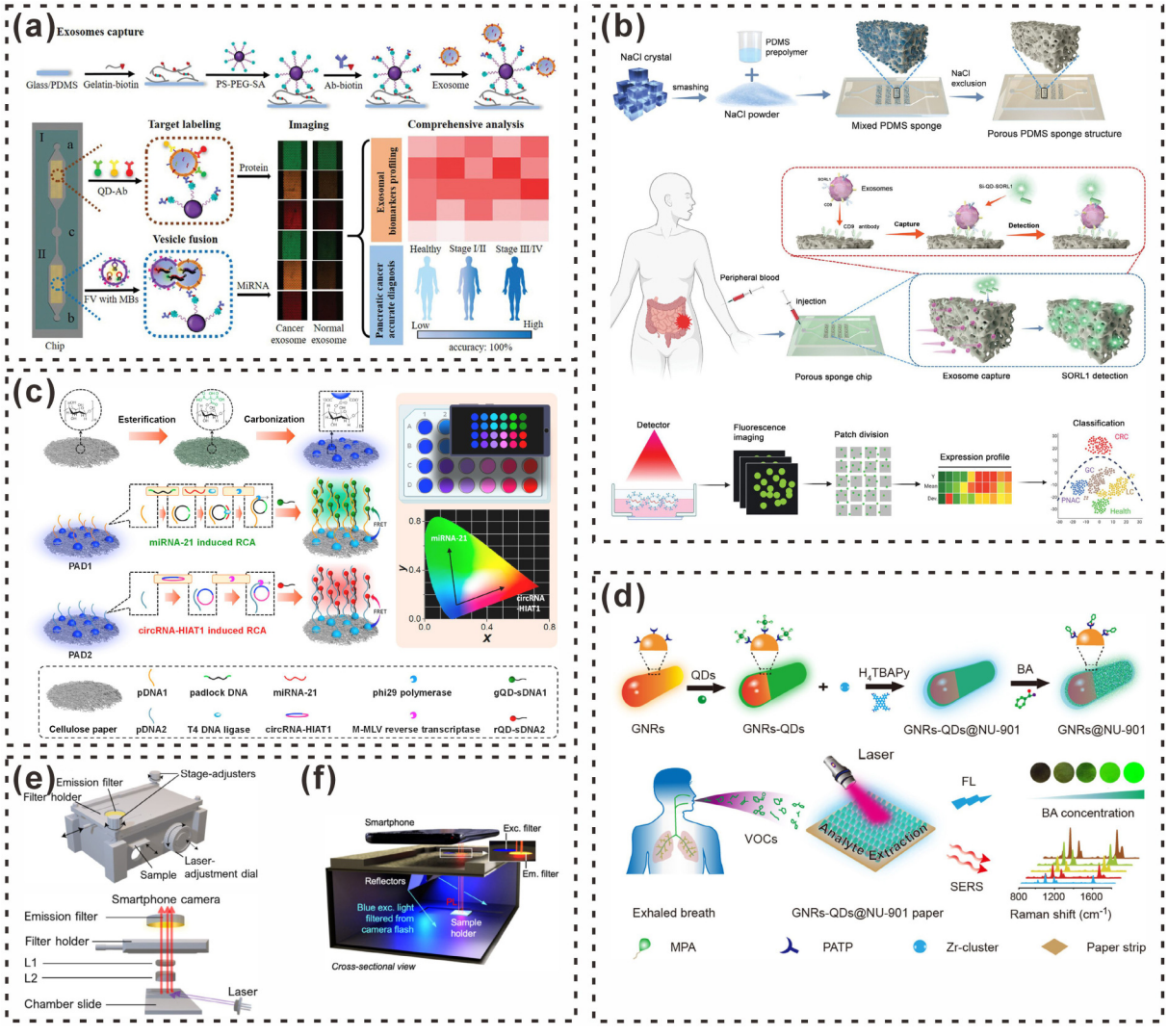

Figure 8 QDs for point-of-care testing. (a) Schematic of the integrated dual-channel 3D microfluidic device for *in situ* multiplex detection of exosomal proteins and miRNAs. Reproduced with permission from Ref. [123], © Wiley-VCH GmbH 2020. (b) Construction of 3D porous sponge chips and analysis of exosomes. Reproduced with permission from Ref. [124], © Wiley-VCH GmbH 2023. (c) Illustration of fluorescent paper-based analytical devices construction and color-analysis of dual-type RNA. Reproduced with permission from Ref. [130], © Elsevier B.V. All rights reserved 2021. (d) Schematic illustrations of synthesizing GNRs-QDs@NU-901 core–shell structures and its dual-modal sensing of volatile BA in human exhalation. Reproduced with permission from Ref. [131], © American Chemical Society 2021. (e) Rendering of the smartphone-based fluorescent cell imaging platform and optical design for imaging. Reproduced with permission from Ref. [136], © American Chemical Society 2019. (f) Cross-sectional view for the design of a smartphone-based platform for imaging with SiO_2@QDs. Reproduced with permission from Ref. [137], © American Chemical Society 2020.

theoretical underpinnings of QDs, rooted in quantum confinement effects and surface chemistry, provide a foundation for tailoring their properties to enhance their performance in POCT applications. By manipulating the size and surface ligands of QDs, researchers can optimize their brightness, stability, and biocompatibility, which are essential for effective integration into POCT devices. In the following sections, we will explore the specific applications of QDs in POCT, highlighting recent advancements and discussing the potential challenges and future directions for this promising area of research (Fig. 8) [120, 121].

5.3.1 *Microfluidic chip-based systems*

Microfluidic chips, as microreactors, have the capability to precisely control the volume, flow direction, pressure, and temperature of fluids. The process of producing and using these chips involves utilizing micro-nano processing technologies such as photolithography, laser etching, 3D printing, micro-milling, and micro-molding. These technologies are used to construct various functional components on materials like silicon, quartz, glass, and elastomer materials such as polydimethylsiloxane (PDMS), as well as thermoplastics like polymethyl methacrylate (PMMA), polycarbonate (PC), polystyrene (PS), polyethylene terephthalate (PET), and polyvinyl chloride (PVC). This integration enables sample pretreatment, enrichment, amplification reactions, and signal reporting, ultimately facilitating input and output of results. The microfluidic detection platform offers numerous advantages, including high integration, minimal sample volumes, compact and portable equipment, effective prevention of cross-contamination, biosafety assurance, high throughput, automation, and low costs. Consequently, microfluidic chips are considered an ideal platform for POCT.

Bai et al. [122] developed a microfluidic chip for efficient capture and detection of exosomes. The chip uses antigen-antibody hybridization, along with QDs and microbeads modified with CD9 antibody, which serves as an exosome marker. The chip is composed of a PDMS plate bonded to a glass sheet, with a microarray of 604 microcolumns on the PDMS to ensure a uniform arrangement of antibody-modified microbeads. Once the microbeads capture the exosomes on the chip, they combine with the antibody-modified QDs to form a double antibody sandwich. The detection of exosomes is then determined by the fluorescence emitted by the QDs. The dispersed arrangement of microbeads helps reduce optical interference, allowing for the collection of fluorescence from individual microbeads and improving the accuracy of detection. Unlike size-based microfluidic separation, this method offers greater specificity, and multiple detections can be achieved by using different QDs labels. Moreover, the study demonstrated that the microfluidic immunoassay system showed promising diagnostic ability both at the cellular level and in clinical plasma samples. However, further evaluation with a larger sample size is necessary to determine the clinical applicability of this chip system.

To enhance the capture rate of exosomes, reduce steric hindrance, and enable a comprehensive analysis of various exosome types, Zhou et al. [123] developed a dual-channel 3D microfluidic device that integrates QDs tags and virus-like structural vesicles. This device allows for *in situ* multiplex detection of exosomal proteins and miRNAs. The solution proposed by Zhou et al. offers several key features to improve exosome capture efficiency. Firstly, the 3D chip incorporates a Y-shaped micropillar array, which increases the contact probability and interaction time between exosomes and immobilized CD63 antibodies. Secondly, the microfluidic control system employs a multi-layer biotinylated gelatin film on the channel, significantly enhancing the channel's biocompatibility. Lastly, PEG-SA linked polystyrene spheres (PS-PEG-SA) are affixed to the biotinylated gelatin film, reducing steric hindrance and providing more sites for exosome capture. The *in situ* detection of multiple exosome proteins is achieved by labeling different QDs with their respective specific antibodies. On the other hand, the detection of multiple exosome miRNAs uses virus-like structural vesicles that can fuse with exosomes and carry specific fluorescent probes. However, one disadvantage of this solution is the complexity of the process and the numerous modification steps, which introduce many uncontrollable factors that may affect the stability of the assay. In a study by Li et al. [124], they constructed an exosome detection platform by combining a 3D porous sponge microfluidic chip with sortilin related receptor 1 (SORL1) antibody labeled with Si-QDs. This platform effectively addresses the complexity of modifications and improves the exosome capture efficiency to approximately 90%. The study also identified SORL1 as a specific exosomal protein marker for early diagnosis of colorectal cancer. To prepare the 3D porous sponge chip with interconnected cavity structures, NaCl is ground into a uniform powder of controllable size using a ball mill. It is then mixed with PDMS prepolymer and curing agent. Subsequently, 30% alcohol is used to remove NaCl, resulting in the desired chip formation. This chip is easy to prepare, versatile in its applications, and offers several functional advantages. The chip's material exhibits good light transmittance, enabling *in-situ* fluorescence detection. The porous structure provides a large specific surface area, allowing for the immobilization of more CD9 antibodies. Additionally, the grooves in the 3D sponge chip induce turbulence, enhancing the binding probability of exosomes and antibodies. The system employs an integrated classification method based on artificial intelligence to analyze the final Si-QDs fluorescence signal. This approach yields an area under the curve as high as 0.99, demonstrating excellent diagnostic performance in early-stage, CEA-negative colorectal cancer patients.

Apart from their role as reporters in microfluidic chips, Wang et al. utilized the biocompatibility of GOQDs to develop microcavity chips for single-cell culture. This innovation enables high-throughput single cell isolation. The researchers combined these chips with antibody barcode chips and machine learning techniques to analyze extensive tumor cell secretion data and classify tumor cells. Therefore, this study demonstrates that microcavities modified with GOQDs maintain long-term hydrophilicity, making them ideal for cell growth and expansion [125].

5.3.2 *Paper-based analytical devices*

As a flexible substrate, paper offers several advantages. It is highly flexible, and its preparation technology is well-established. Paper is readily available from a wide range of raw materials. It can be folded and printed on, and it has a large specific surface area. Furthermore, paper is biodegradable and cost-effective. One of the main benefits of paper is its ability to facilitate capillary action. This means that there is no need for an external power device when constructing microfluidic elements. As a result, paper is widely used in the production of sensor devices [126]. Paper-based sensors are simple to prepare, easy to operate, portable, and disposable. These characteristics make them highly suitable for application in resource-

limited areas. There are various types of paper-based sensors available, which utilize different signal reporting modes. These include color [127], current [128], and fluorescence [129]. Among these, fluorescence reporting is the most widely used. There are two main design principles for fluorescence-based paper sensors. The first involves using the gaps on the paper substrate to immobilize the capture probe. This probe is labeled with a fluorescent dye that reports the presence of the target by recognizing and capturing it. The second design principle involves attaching a single dispersed fluorescent biosensor to the paper substrate. This biosensor reports the signal through ratio fluorescence or an "off-on" mode, using the FRET/bioluminescence resonance energy transfer (BRET) mechanism. Liu et al. [130] have developed a new fluorescent paper-based molecular recognizer based on CDs and QDs. They successfully applied this recognizer to detect dual RNA related to gastric cancer. The focus of their design strategy is as follows: First, they modify the cellulose paper through citric acid, and then they synthesize CDs through *in situ* carbonization. They further modify the target recognition probe. After target recognition, they use it as a template to trigger rolling circle amplification for signal amplification. Finally, nucleic acid probes are labeled with different emission QDs to achieve a ratio fluorescence signal output. The CDs synthesized in this scheme have excellent uniformity and stability. In addition, the sensing platform utilizes the dual functions of QDs' autofluorescence and their ability to quench the blue fluorescence of CDs through the FRET mechanism. This ultimately provides a visual report of RNA at the femtosecond level, with a significant proportional fluorescence change. Such a platform has high potential in POCT. Xia et al. [131] developed a smart vapor generation paper-based thin-film microextraction (VG-PTFM) system based on gold nanorods (GNRs) coated with QDs and NU-901 (GNRs-QDs@NU-901). This system successfully detects volatile benzaldehyde (BA), a respiratory volatile organic compound associated with lung cancer. The GNRs-QDs are assembled using amino-modified GNRs and carboxyl-coated QDs, which effectively quench the fluorescence of the QDs. Gaseous BA interacts with the metals through the "cavity-diffusion" effect. The aldehyde group in BA interacts with the amino group of p-aminothiophenol (PATP) (a modification on GNRs), triggering the Schiff base reaction. This leads to the dissociation of GNRs-QDs, ultimately resulting in an increase in fluorescence and Raman signals in the system. Therefore, the system enables the dual-mode detection of BA.

5.3.3 *Smartphone-based platform*

In recent years, there have been significant advancements in mobile devices, such as smartphones, tablets, and wearable devices, that have been developed for use in medical and public health practices. Smartphones, in particular, have shown great potential for POCT due to advancements in optics, software engineering, and electronic microchip technology. They have become smaller, more powerful, and offer a better user experience. Mobile health platforms based on smartphones have gained popularity due to their portability and low cost. These platforms have a wide range of applications, including home care, community care, and food safety testing. Additionally, the data transmission function of smartphones facilitates remote diagnosis. Currently, smartphone cameras can support various methods such as colorimetric detection and fluorescence detection. They can also be used to analyze a wide range of analytes, including enzymes, hormones, and viruses. It is worth noting that researchers have engineered a "do it yourself" fluorescence reader, which uses simple, readily available, and low-cost paper materials and a mid-range smartphone camera [132]. These homemade systems for the detection of CdSe/ZnS QDs spotted on lateral flow paper strips demonstrate comparable performance to commercially available readers and therefore pave the way for future innovative off-the-shelf designs [2]. Barcodes can be used as reporters for targeting multiple biomarkers and facilitate improved speed, sensitivity, specificity, precision, and accuracy of diagnosis [133]. Size-dependent luminescence of QDs has been utilized for barcode technology, in which QDs with different sizes are embedded into polymeric particles, providing more than a million codes [134]. Ming et al. combined recent advances in QDs barcode technology with smartphones and isothermal amplification to engineer a simple and low-cost chip-based wireless multiplex diagnostic device [135]. The integration of QDs barcoding technology with the smartphone reader provides the capacity for global surveillance of diseases.

Smartphone detection platforms using luminescent QDs have emerged in the field of cancer diagnosis. These platforms typically employ immune-conjugation strategies and are primarily used to separate and detect specific cell types. Tran et al. [136] developed a smartphone-based imaging platform (SIP) that enables specific cell separation, imaging, and counting using magnetic luminescent nanoparticle assemblies (MNP@QD) and immunological principles. QDs are assembled onto dextran-coated magnetic iron oxide nanoparticles through coordination interactions with imidazole groups, and an outer layer of dextran further stabilizes the assembly. Tetrameric antibody complexes (TACs) act as connecting bridges, with one end fixed on MNP@QD via anti-dextran antibodies and the other end attached to cell-specific recognition antibodies. In this study, anti-HER2 antibodies were used to identify HER2-positive breast cancer cells. After incubating the immunoconjugate with the sample, it can be imaged and counted using SIP following magnetic separation, washing, and resuspension. Similarly, Darwish et al. [137] used SiO_2 NPs instead of MNPs to prepare super nanoparticle assemblies (SiO_2@QDs). Through the connection of TACs, the self-assembly of SiO_2@QDs immunoconjugates was achieved, successfully labeling breast cancer cells. SiO_2@QDs exhibited fluorescence that was an order of magnitude higher compared to single QDs and showed enhanced sensitivity in smartphone imaging. SiO_2 NPs have become one of the most commonly used scaffolds for preparing QDs super nanoassemblies due to their compatibility with water, chemical stability, lack of optical background, and ease of chemical modification.

6 QDs assist cancer therapy

QDs have enormous potential in the treatment of tumors and are commonly used as an additional material in various tumor treatment strategies. Their unique physical and chemical properties enable them to play a therapeutic role through unconventional methods, which can help overcome tumor resistance and improve treatment effectiveness. QDs possess excellent photothermal conversion abilities, meaning they can release tumor cell antigens when exposed to laser, thereby improving the tumor immune microenvironment. Additionally, certain QDs can be modified to serve as drug carriers, exerting anti-tumor effects through various mechanisms. The exceptional optical properties of QDs, such as

near-infrared luminescence, can assist in guiding targeted therapy, assessing the patient's immune status, and monitoring treatment efficacy and response.

6.1 QDs for targeted imaging-guided surgery

Surgical resection is the preferred treatment for most solid tumors because it plays a crucial role in improving patient survival and controlling tumor metastasis. However, accurately identifying the tumor tissue boundary during surgery is challenging due to the invasive nature of tumors. This can lead to incomplete resection and an increased risk of recurrence and metastasis. To address this issue, NIR-II fluorescence imaging utilizes the long wavelength region, which has minimal light scattering and autofluorescence, to obtain precise submicroscopic fluorescence images. This technique provides an effective solution for intraoperative navigation. Currently, Indocyanine Green (ICG) has been approved by the Food and Drug Administration (FDA) and successfully used in human liver tumor resection surgery. Various NIR-II fluorescent nanoprobes, including carbon nanotubes, organic dye aggregates, and rare-earth based downshifting nanocrystals, have also been developed [138, 139]. However, these imaging molecules and nanoprobes have limitations such as susceptibility to photobleaching, limited penetration depth, and low quantum yield. Consequently, there is extensive interest in using QDs for NIR-II fluorescence bioimaging research due to their small size, high quantum yield, strong NIR-II fluorescence emission, and excellent photobleaching resistance. Nonetheless, their potential toxicity and rapid renal clearance require modifications to achieve low toxicity, prolonged retention, good biocompatibility, and precise tumor targeting in surgical imaging guidance [140]. Recent studies have demonstrated that multiple hydrophilic coatings on the surface of QDs significantly enhance biosafety. However, this approach inevitably leads to some loss of quantum yield and NIR-II fluorescence, creating a challenge of blurred boundaries during intraoperative navigation [141]. Therefore, a suitable encapsulation strategy for QDs is crucial to achieving higher quantum yield, brighter fluorescence, and enhanced photobleaching resistance in intraoperative navigation.

As shown in Fig. 9, Wang et al. [141] utilized MnO_2-modified QDs and IR1061 to create a versatile NIR-II fluorescent nanoprobe with low physiological toxicity and pH sensitivity. The probe also possesses NIR-II fluorescence imaging capabilities and a photothermal effect, demonstrating its potential in intraoperative navigation and photothermal therapy. In this study, CdS QDs were initially used to encapsulate PbS QDs, resulting in PbS@CdS QDs with improved antioxidant and fluorescence properties (emission at 1670 nm). Subsequently, PbS@CdS QDs were covalently attached to the surface of hollow virus-like mesoporous MnO_2 loaded with IR1061 ($HvMnO_2$@IR1061) to obtain $HvMnO_2$@QDs-IR1061. $HvMnO_2$@QDs-IR1061 is pH-responsive, exhibiting "off" state NIR-II fluorescence in normal tissue (pH 7.4), while the weakly acidic characteristics of the tumor microenvironment (pH 6.5–6.8) trigger the biological activity of $HvMnO_2$. This leads to the release of QDs and IR1061, resulting in a significantly enhanced signal-to-noise ratio NIR-II fluorescence, even at the tumor's edge. Additionally, the probe's NIR-II photothermal effect can initiate photothermal therapy. Apart from MnO_2 modification, Li et al. employed poly(ethylene glycol) methyl ether thiol (mPEG-SH, MW: 2000) to coat core-shell structured PbS@CdS QDs, resulting in PbS@CdS@PEG NPs. mPEG-SH is an FDA-approved safe modification material. The coated PbS@CdS@PEG NPs maintain a small size (~ 8 nm) and achieve water solubility while remaining biosafe. With a high quantum yield (~ 30.2%) and anti-bleaching ability, the fluorescence of PbS@CdS@PEG NPs is long-lasting and stable. The application of its aqueous solution in intraoperative navigation of cervical tumors can significantly reduce damage to normal tissue at the edges. This mPEG-SH coating strategy provides new insights into QD modification, further enhancing the potential of QDs in future intraoperative navigation applications [142].

6.2 QDs-assisted tumor radiotherapy, chemotherapy and targeted therapy

Apart from their application in surgical navigation, QDs have also been extensively investigated for their potential use in radiotherapy, chemotherapy, and targeted therapy (Fig. 10). Radiotherapy is an important method for treating cancer, as it utilizes ionizing radiation and oxidative damage to break DNA, effectively killing cancer cells. It also stimulates the release of chemokines and danger signals, attracting antigen-presenting cells that activate cytotoxic T cells within the tumor microenvironment. This process ultimately enhances the body's immune response against tumors [143]. However, radiotherapy faces several challenges, including potential damage to healthy tissues from ionizing radiation, radiation resistance due to hypoxia in the tumor microenvironment, and immunosuppression that limits the effectiveness of radiation. To ensure precise radiotherapy for localized tumors, accurately delineating the tumor site is crucial to minimize side effects on healthy tissues. Simultaneously, alleviating hypoxia within the tumor microenvironment can effectively improve radiation resistance and immunosuppression [144]. Research has shown that nanoparticles can enhance the effectiveness of radiotherapy by facilitating the deposition of radiation energy and decomposing H_2O_2 to produce O_2, thereby alleviating hypoxia within the tumor [145]. Specifically, NIR-IIb QDs containing Pb and Ag possess potential radiosensitization capabilities and can be used for deep tissue imaging. This enables *in vivo* tracking, aiding in determining the extent and timing of radiotherapy. Li et al. [144] have reported the development of a tumor diagnosis and treatment nanoprobe (QD-Cat-RGD) based on PbS/CdS QDs. This nanoprobe is designed for high-resolution imaging of tumor sites and to enhance the sensitivity of radiotherapy. The probe is made up of PbS/CdS QDs that have been modified with PEG, catalase (Cat), and arginine-glycine-aspartic acid (RGD) peptides. It functions as a radiosensitizer, which means it helps directly kill of cancer cells. Additionally, it enhances the immunogenicity of cancer cells by inducing immunogenic cell death (ICD). This process stimulates anti-tumor immune responses and prevents tumor metastasis. The RGD peptide guides the probe to accumulate at the tumor site, while Cat facilitates the rapid decomposition of H_2O_2, relieving the hypoxic state within the tumor. As a result, this not only improves radiosensitivity but also reduces immunosuppression.

In addition to low pH and hypoxia, the tumor microenvironment also contains high concentrations of GSH and expresses specific enzymes. GSH is a crucial component of the antioxidant system and plays a role in clearing intracellular ROS. However, the clearance of intracellular ROS can lead to resistance to radiotherapy and chemotherapy, reducing their therapeutic effectiveness [146]. Therefore, reducing intracellular GSH levels can enhance the therapeutic sensitivity of various cancer treatment

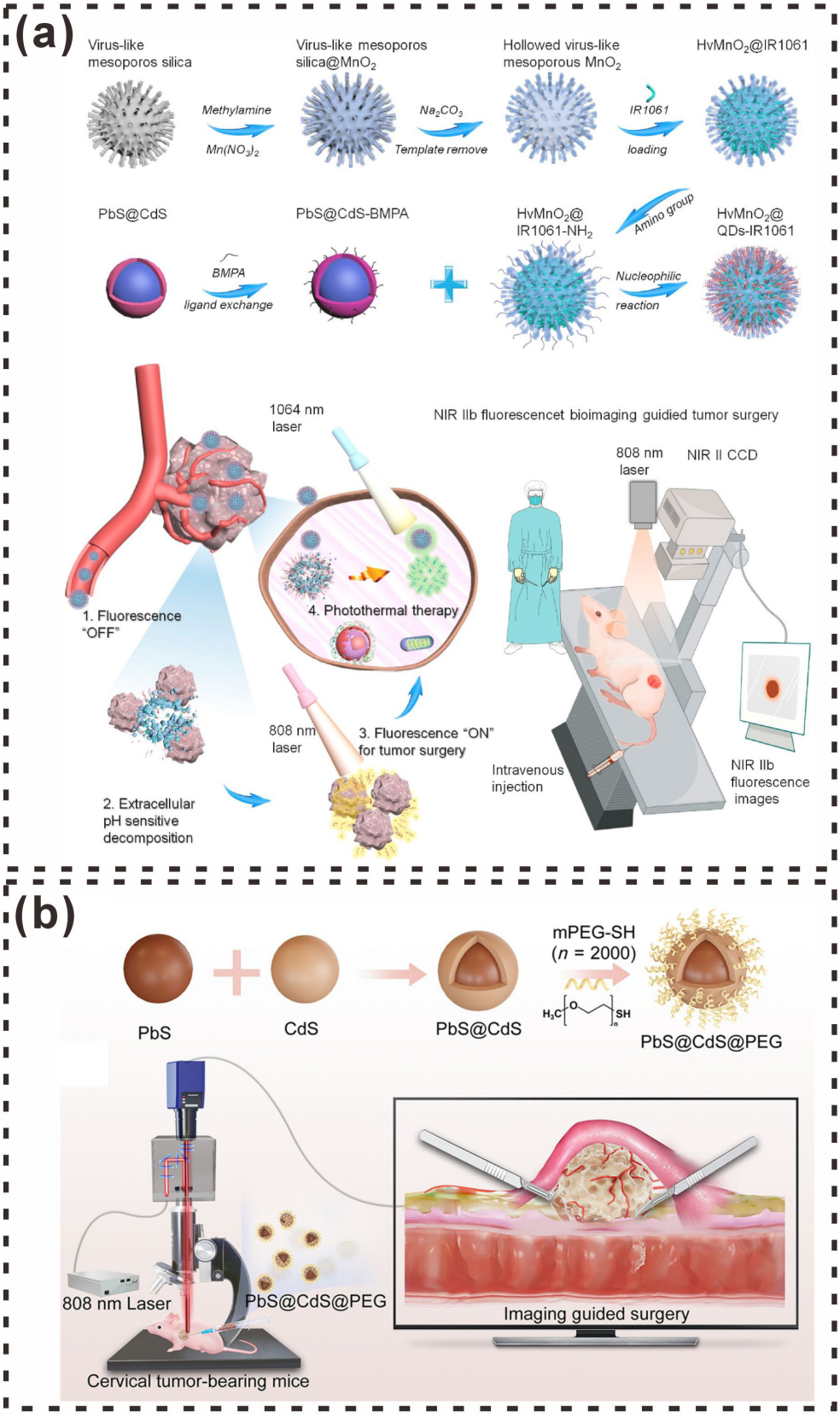

Figure 9 QDs for targeted imaging-guided surgery. (a) NIR-IIb quantum dots anchored and IR1061 loaded hollow virus-bionic MnO_2 for pH sensitive NIR-IIb fluorescent imaging guided solid tumor precise resection and NIR-II photothermal therapy. Reproduced with permission from Ref. [141], © Elsevier Ltd. All rights reserved 2022. (b) Schematic illustration of the synthesis route of PbS@CdS@PEG NPs and fluorescence-guided tumor resection under the NIR-IIb fluorescence microscopic imaging system. Reproduced with permission from Ref. [142], © American Chemical Society 2024.

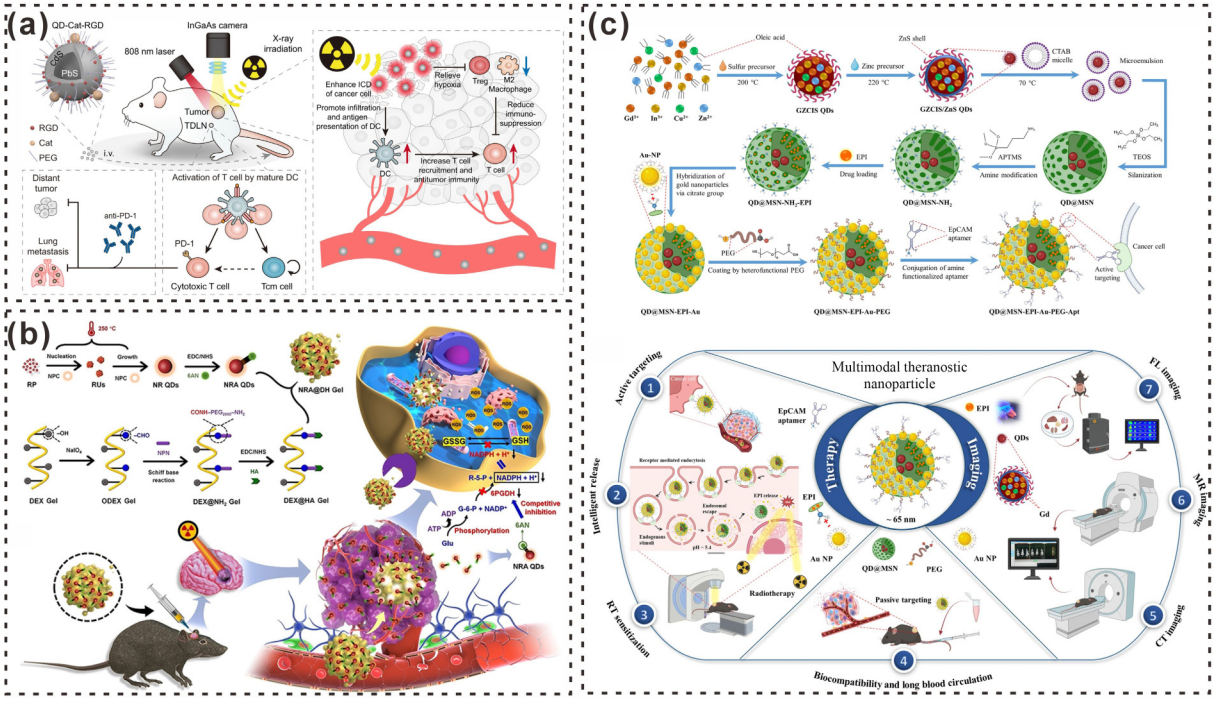

Figure 10 QDs-assisted tumor radiotherapy, chemotherapy and targeted therapy. (a) Schematic showing the mechanism by which QD-Cat-RGD nanoprobe-based RT boosts the antitumor immune response and abscopal effect to inhibit cancer metastases. Reproduced with permission from Ref. [144], © H. Li, et al. 2021. (b) Schematic illustration showing the synthesis of multifunctional NRA@DH Gel, and the *in vivo* mechanisms underlying synergistic therapy with NRA@DH Gel including accumulation in tumor tissues, deep penetration, and sustained ROS generation. Reproduced with permission from Ref. [148], © Y. Wang, et al. 2023. (c) Schematic illustration of QD@MSN-EPI-Au-PEG-Apt nanocarriers' multimodal capabilities in theranostic applications. Reproduced with permission from Ref. [150], © A. Abrishami, et al. 2024.

regimens. Glutathione disulfide (GSSG) is converted into GSH intracellularly through the action of nicotinamide adenine dinucleotide phosphate (NADPH). As an inhibitor, 6-aminonicotinamide (6-AN) can hinder the pentose phosphate pathway (PPP), decreasing NADPH production, which in turn reduces intracellular GSH and causes ROS accumulation [147]. Wang et al. prepared the anti-tumor drug realgar as nano-realgar QDs to improve biocompatibility and anti-tumor activity. They further modified the 6-AN molecule to obtain NRA QDs with both pharmacological and fluorescent properties. Subsequently, the NRA QDs were coated with a pH-sensitive dextran hydrogel with a hyaluronic acid coating (DEX-HA gel) to create a multifunctional nano-realgar hydrogel (NRA@DH Gel) that allows for controlled release of NRA QDs at the tumor site. NRA@DH Gel has the dual function of enhancing radiotherapy and chemotherapy, making it highly promising for various applications. It can serve as an anti-tumor drug, producing a chemotherapeutic effect, while also acting as a "persistent ROS generator" to enhance the efficacy of radiotherapy by inhibiting the PPP and reducing NADPH and GSH production [148].

There is no perfect single treatment for cancer. Combined multimodal therapy is an important approach to improve the effectiveness of treatment and patient survival. Currently, numerous NPs-based multimodal therapeutic agents have been developed. These agents are combined with chemotherapeutic drugs, radioisotopes, and various compounds that can perform electromagnetic radiation in the form of PTT and PDT to achieve combined therapy [149]. Abrishami et al. [150] synthesized multimodal therapeutic nanoprobes for intelligent targeted drug delivery of colorectal cancer using QDs, MSNs, and Au NPs. The system first synthesized gadolinium-doped zinc copper-indium-sulfur (GZCIS)/ZnS QDs using Gd^{3+}, Zn^{2+}, Cu^{2+}, In^{3+}, sulfur precursor, and zinc precursor as raw materials. After forming a microemulsion with cetyltrimethylammonium bromide (CTAB) micelles, QDs were further encapsulated in MSNs by silanization to improve biosafety (QD@MSN). MSNs are biocompatible, easily modifiable, porous, and stable, making them ideal drug delivery carriers with high load capacity [151]. In this study, the chemotherapeutic drug epirubicin (EPI) was loaded into the pores of MSNs and capped with Au NPs (QD@MSN-EPI-Au). The gating effect of Au NPs allows the encapsulated chemotherapeutic drug to be released in the low-pH tumor microenvironment and lysosomes. Additionally, Au NPs possess multiple properties such as easy modification, radiosensitization, and CT traceability [152]. Finally, the surface of QD@MSN-EPI-Au was modified by adding FDA-approved PEG. This modification serves to further enhance the carrier's half-life, toxicity profile, and immunogenicity. Additionally, the epithelial cell adhesion molecule (EpCAM) aptamer was incorporated to actively target colorectal cancer cells, resulting in the creation of QD@MSN-EPI-Au-PEG-Apt. In summary, QD@MSN-EPI-Au-PEG-Apt offers a multimodal approach to cancer treatment. It combines various features such as biocompatibility, active targeting, intelligent drug release, enhanced chemoradiotherapy, CT imaging, magnetic resonance imaging, and fluorescence imaging capabilities.

6.3 QDs-assisted tumor immunotherapy

Immunotherapy has revolutionized tumor treatment and is a crucial focus in clinical cancer research. It works by regulating the host's immune system, reactivating the body's immune response against tumor cells, and suppressing and killing tumors. The

established strategies for tumor immunotherapy include immune checkpoint inhibitors (ICIs), therapeutic vaccines, and adoptive T cell transfer, such as chimeric antigen receptor (CAR) engineering and T cell receptor (TCR) engineering T cell therapy [153]. However, despite the impressive results of immunotherapies, there are challenges in their practical clinical application. Currently, only

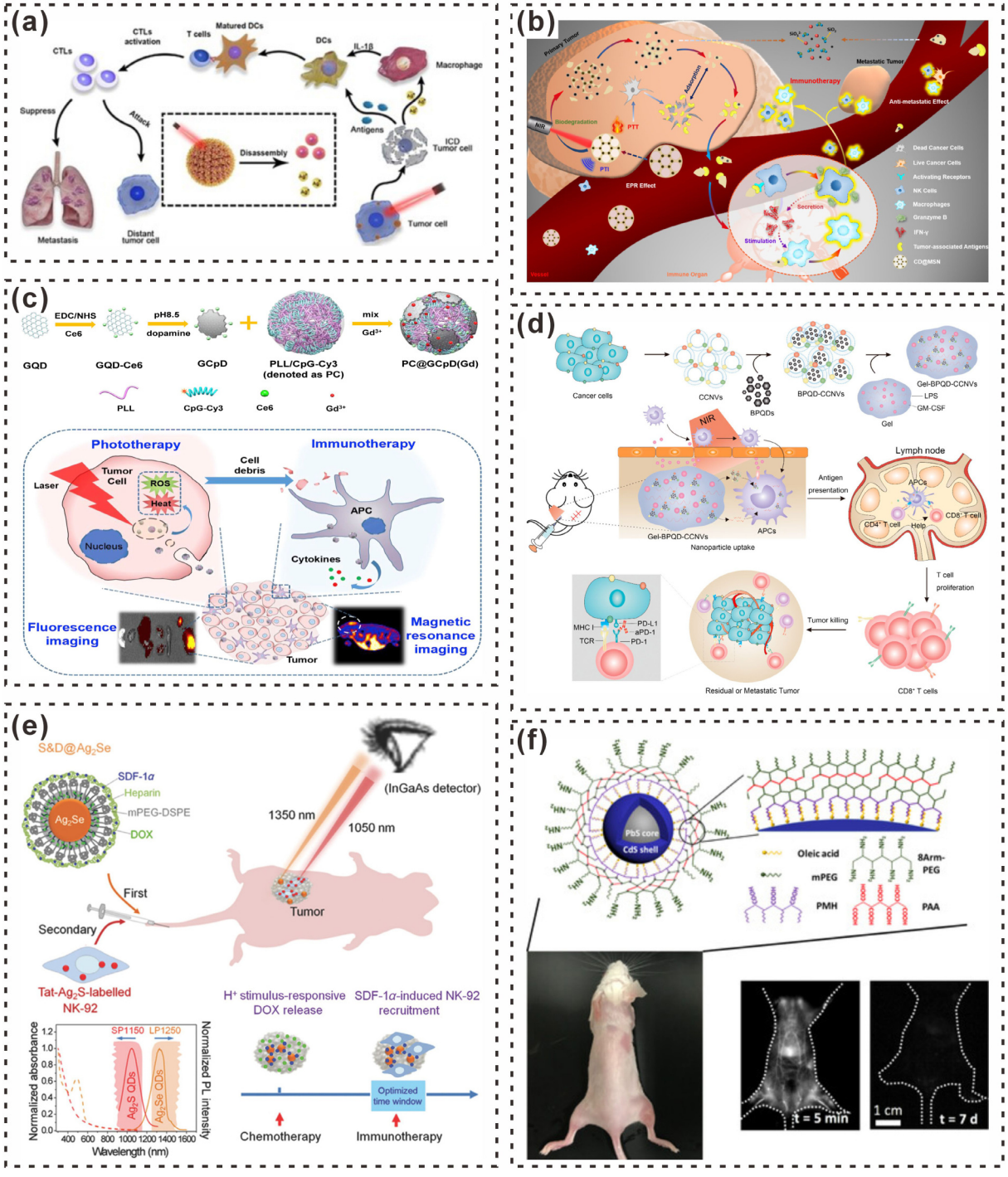

Figure 11 QDs-assisted tumor immunotherapy. (a) Illustration of the synthesis and properties of BP Ve-Ag$^+$. Reproduced with permission from Ref. [164], © Wiley-VCH GmbH 2020. (b) Schematic diagram of *in vivo* delivery process of framework swelling-triggered biodegradable CD@MSN and its application for photothermal imaging-guided tumor-targeted PTT cooperated with debris-mediated immunotherapy against tumor metastasis. Reproduced with permission from Ref. [167], © American Chemical Society 2019. (c) Schematic presentation of MRI/FI bimodal imaging-guided photo-immunotherapy mediated by PC@GCpD (Gd). Reproduced with permission from Ref. [170], © Elsevier Ltd. All rights reserved 2019. (d) Schematic illustration and characterization of black phosphorus quantum dot nanovesicles (BPQD-CCNVs) combined with PD-1 antibody for postsurgical cancer immunotherapy. Reproduced with permission from Ref. [184], © American Chemical Society 2019. (e) Schematic illustration of multiplexed NIR-II fluorescence imaging strategy to program the chemotherapy and immunotherapy against breast cancer. Under the guidance of the NIR-II fluorescence of Ag_2Se and Ag_2S QDs. Reproduced with permission from Ref. [195], © WILEY-VCH Verlag GmbH & Co. KGaA, Weinheim 2018. (f) Functionalized nanoparticles with a cross-linked surface coating (branched PEG-linear PAA-branched PEG, P3) enable rapid excretion of nanomaterials from the body, establishing a foundation for the clinical translation of the nanomedicine-based theranostics. Reproduced with permission from Ref. [199], © Wiley-VCH GmbH 2020.

a small percentage of tumors respond to immunotherapy due to the tumor's ability to evade the immune system and its adaptive and acquired resistance mechanisms [154]. To overcome these challenges, many studies have explored the use of nanotherapeutics to enhance the effectiveness of tumor immunotherapy. One promising direction in nano-immunotherapy is the use of QDs to improve the efficacy of immunotherapy and induce effective anti-tumor immune responses [155–157]. Current research on the application of QDs in tumor immunotherapy mainly focuses on two strategies: (i) Using QD-based PTT or PDT to induce ICD of cancer cells, thereby promoting innate and adaptive immunity; (ii) utilizing the excellent luminescence properties of QDs for real-time tracking of immunotherapy in the body, monitoring treatment effects, and revealing the treatment mechanism. Furthermore, in some tumor treatment approaches, CDs and GQDs with porous structures are used as carriers for immunotherapy drugs. By taking advantage of the small size and fluorescent tracing capabilities of QDs, drugs can be delivered inside cells, even reaching the nucleus, to exert a more potent therapeutic effect. Additionally, real-time monitoring of the drug's *in vivo* distribution and immunotherapy response is possible (Fig. 11) [158, 159].

6.3.1 *Enhanced immunotherapy by QDs PTT/PDT induced ICD*

PTT and PDT are two types of photo-stimulation therapies that use photosensitizers to exert therapeutic effects. PTT works by generating high temperatures in a localized area to kill tumors, while PDT inhibits tumors through specific chemical reactions. In PTT, photothermal agents absorb energy and increase the temperature of cells and tissues in a specific area when exposed to light of a particular wavelength. When the tissue temperature exceeds 60 °C, tumor cells rapidly die due to protein denaturation and destruction of the plasma membrane. In contrast, PDT induces cytotoxicity by generating ROS through photosensitizers when exposed to light [60]. Recently, various nanomaterials, such as organic nanomaterials, metal nanomaterials, carbon-based nanomaterials, and QDs, have been used as photosensitizers in PTT or PDT. QDs, known for their high photoluminescence efficiency, good photostability, and high photothermal conversion efficiency, are widely employed in tumor PTT or PDT. The flexible synthesis method and excellent modification potential of QDs further enhance the targeting of PTT and PDT. They can effectively accumulate around tumors, accurately indicate tumor location, and yield better therapeutic effects while minimizing undesired side effects [160].

Whether it is thermal injury (PTT) or chemical injury (PDT), both treatments can induce ICD, which promotes the release of tumor antigens and activates the body's immune response to tumor cells while ablating or destroying them. ICD refers to the process in which tumor cells transition from non-immunogenic to immunogenic when exposed to external stimulation and die. This process triggers the production of anti-tumor immune responses in the body. Unlike some cancer treatments that primarily cause tumor cell apoptosis, ICD is characterized by the explosive necrosis of tumor cells, leading to the release of damage-associated molecular patterns (DAMPs) such as calreticulin, high mobility group protein 1 (HMGB1), ATP molecules, and heat shock proteins (HSP70, HSP90). These DAMPs can bind to pattern recognition receptors (PRRs) on the surface of dendritic cells (DC), initiating a series of inflammatory responses, attracting immune cells, and ultimately activating both innate and adaptive immune responses [161, 162]. ICD can regulate the tumor immune microenvironment (TIME), mobilize antigen presentation through chemokines, and transform the immunosuppressive "cold" tumor microenvironment (TME) into an immune-activated "hot" TME. Thermal stimulation can increase the expression and release of cytokines such as interleukin-6 (IL-6) and interferon-γ (IFN-γ), promoting the maturation of various types of adaptive immune cells (regulatory T cells (Treg) and $CD8^+$ T cells) and innate immune cells (natural killer (NK) cells, macrophages, and neutrophils). These reactions significantly enhance the tumor's response to immunotherapy, reverse drug resistance mechanisms, and improve therapeutic effects. Additionally, ICD trains the body's immune system to enhance the clearance of residual tumor cells, inhibiting tumor metastasis and recurrence [163].

Using QD-based PTT and PDT strategies to induce ICD and activate the host anti-tumor immune response is an important approach in QD immunotherapy. Li et al. developed a self-assembled vesicle using BP QDs activated by NIR light, along with Ag^+ and ROS-sensitive polypropylene sulfide (PPS). This vesicle, called BP Ve, is used for PDT while delivering Ag^+. The hydrophobic PPS shell protects Ag^+ and allows its enrichment at the tumor site. During PDT, the vesicles rupture, causing tumor cell membrane rupture and mitochondrial damage, which, along with BP QDs-mediated PDT, promotes ICD. The released Ag^+ is taken up by macrophages, leading to increased release of pro-inflammatory factors and induction of inflammatory responses. This, along with the occurrence of ICD, promotes the maturation of dendritic cells (DCs) and the enrichment of $CD8^+/CD4^+$ T cells, ultimately resulting in effective anti-tumor and inhibitory effects [164]. Some studies have focused on the impact of PTT or PDT strategies based on QDs on immune cells in the TME. Zhao et al. investigated the effect of the photothermal effect induced by Ag2S QDs on macrophages in the TME. They combined bifidobacteria with hypoxia-targeting ability and Ag_2S QDs to create a hybrid bacterium for tumor-targeted therapy. The hybrid bacteria, with their strong penetrating ability and hypoxic targeting, effectively aggregate nanomaterials at tumors and enable precise PTT. Bifidobacteria, as an immunomodulator, induces the polarization of macrophages from M2 to M1 after being phagocytosed in the TME, leading to tumor cell killing. This process, in combination with the Ag_2S photothermal effect, promotes ICD, increases the release of tumor antigens, and facilitates the infiltration of immune cells, thereby reversing the suppressive immune microenvironment [165]. M1 macrophages, as important innate immune cells that suppress tumors, play a crucial role in tumor treatment by exerting phagocytosis and enhancing anti-tumor inflammatory responses. On the contrary, M2 macrophages promote tumor development through immune suppression, neovascularization, and matrix activation and remodeling. Therefore, it is essential to induce the polarization of macrophages in the TME towards the M1 type in order to effectively improve the efficacy of immunotherapy. NK cells, which are vital components of the innate immune system, also play a significant role in anti-tumor responses [166]. Qian et al. conducted a study using MSNs as carriers for CDs. By harnessing the photothermal effect of CDs, they stimulated the proliferation and activation of NK cells and macrophages, resulting in anti-tumor effects. However, the addition of CDs to MSNs causes material expansion and structural weakening, leading to the undesirable accumulation and degradation of nanomaterials within the body. Importantly, the degraded nanomaterial fragments can bind to tumor-associated antigens (TAAs) released by tumor cells

destroyed by PTT and transport these antigens to lymph nodes to promote immune activation. This process can increase the expression of NK cell activation receptors and promote M1 macrophage polarization, while also increasing the secretion of granzyme B and IFN-γ. These activated immune components then enter the TME to further exert their inhibitory effects [167]. In the work of Yang et al., iron-doped CDs were synthesized to take advantage of the preferential iron uptake characteristics of tumor-associated macrophages. This approach successfully formed iron-loaded macrophages, which synergistically inhibited IL-10 and promoted M1-type polarization [168]. Gu's team used human serum albumin-encapsulated BP QDs (BPQDs@HSA) as an immune sensitizer to enhance the activity of NK cells against tumor cells. This was done in coordination with PDT to exert anti-tumor effects. BPQDs@HSA activates NK cells through interactions with Toll-like receptors while also maintaining the cell viability and immune function of NK cells by reprogramming cellular glycolytic metabolism. With the assistance of X-rays, BPQDs@HSA can produce more singlet oxygen ($^1O_2$), further enhancing the anti-tumor effect [169].

QD-induced PTT or PDT combined with additional tumor treatment drugs can enhance the effects of immunotherapy. Wu et al. developed a tumor nanotherapeutic strategy by combining functionalized photoactive GQD nanocomposites with CpG oligodeoxynucleotide (CpG OND) immune adjuvants. This strategy triggers a cascade immune response, where PTT and PDT induce ICD and promote the maturation of DCs while killing tumor cells. Once the nanoparticles are phagocytosed by macrophages, CpG OND is released within lysosomes and interacts with Toll-like receptor 9 (TLR9). This process stimulates the secretion of IL-6 and tumor necrosis factor-α (TNF-α), further promoting DC maturation and T cell infiltration [170]. In another study, Fang et al. wrapped BP QDs and the CDK4/6 inhibitor abemaciclib with macrophage membranes to construct a biomimetic nanoparticle that inhibits breast cancer cells through multiple mechanisms. Abemaciclib specifically inhibits the phosphorylation of retinoblastoma protein (RB), arresting the cell cycle in the G1 phase and inhibiting tumor cell proliferation. Additionally, abemaciclib down-regulates DNA methyltransferase (DNMT) to suppress the proliferation of immunosuppressive regulatory Tregs and regulate the immunosuppressive microenvironment. NIR laser-induced PTT and PDT from BP QDs complement this mechanism to reverse the immunosuppressive microenvironment and achieve the combined anti-cancer effects of phototherapy, chemotherapy, and immunotherapy [171]. In the work by Hou et al., self-assembled hydrogels were used to encapsulate Ag_2S QDs, the chemotherapy drug doxorubicin (DOX), and the immune adjuvant bestatin to combat breast cancer. These gel-like nanomedicines can be injected and administered in situ. The photothermal effect of QDs allows for efficient and controlled drug release, which enhances the tumor-killing function of DOX and the immune activation function of bestatin. The combined effect of ICD and bestatin-induced immune enhancement effectively improves the TIME and promotes the maturation of lymph node DCs [172].

ICIs are a revolutionary approach to tumor immunotherapy. They work by blocking natural immune checkpoints like programmed death receptor 1/programmed cell death ligand 1 (PD-1/PD-L1) and cytolytic T lymphocyte-associated antigen-4 (CTLA-4), offering new hope to patients with advanced cancers [173]. However, it's important to note that not all tumors respond to ICIs, and there is a risk of treatment resistance and disease progression [154, 174]. To enhance the therapeutic efficacy and patient sensitivity of ICIs, additional adjuvant strategies are necessary. One such strategy involves utilizing the photothermal effect of QDs to induce the occurrence of ICD. This effectively stimulates the maturation and accumulation of immune cells in tumors and reprograms TEM, Increasing the sensitivity of tumor cells to ICIs and helping them respond to different tumor immunosuppressive mechanisms. Currently, the combination of QDs-mediated PTT with nanodrug carriers, such as biomimetic nanomaterials, has shown enhanced efficacy of ICIs in various tumors [175, 176]. Hypoxia is a significant factor that leads to resistance to tumor ICIs treatment and immune evasion. Hypoxia can activate hypoxia-inducible factor 1α (HIF-1α), hinder tumor antigen presentation and T cell-mediated cytotoxicity, and activate immunosuppressive cells such as Tregs and M2 macrophages [177]. To address this, Li et al. employed PbS/CdS QDs as radiophotosensitizers and combined them with catalase to construct a TIME modulator. This modulator enhances the therapeutic effect of ICIs by reversing TME hypoxia. By leveraging the NIR-IIb luminescence properties of QDs and the tumor accumulation of nanoparticles, radiotherapy (RT) treatment can be accurately targeted and the appropriate treatment timing can be determined. QDs constructed with high atomic number elements effectively induce the occurrence of ICD as radiosensitizers and activate catalase to decompose H_2O_2 and release O_2, improving the hypoxic environment of tumors. Reversing hypoxia simultaneously improves tumor sensitivity to RT and ICIs. When combined with PD-1 antibody treatment, this strategy effectively inhibits tumor metastasis and prolongs survival [144]. Another approach involves creating a nitric oxide (NO) delivery system using tert-butyl nitrite and Ag_2S QDs, which helps alleviate the immunosuppression caused by the hypoxic TME [178]. Under NIR laser irradiation, QDs precisely generate and release NO at the tumor site. As radiosensitizers, NO enhances the tumor-killing activity of NIR and Ag_2S QDs by inducing DNA damage. NO also normalizes tumor vasculature and activates anti-tumor immune cells in the tumor microenvironment by regulating angiogenesis [179, 180]. NIR and Ag_2S QDs achieve sustained release of NO in TEM, continuously improving the immunosuppressive microenvironment and working in cooperation with QDs-mediated ICD to enhance tumor sensitivity to anti-PD-L1 treatment.

QD-mediated PTT or PDT has been shown to enhance the effectiveness of therapeutic tumor vaccines by modulating the TIME and activating anti-tumor immunity. The development of therapeutic tumor vaccines has been driven by the identification of TAAs and advancements in antigen delivery technologies. These vaccines can induce host immunity, leading to tumor regression, eradication of minimal residual disease, and long-lasting anti-tumor memory, while minimizing non-specific or adverse reactions [181]. In the digital era, new analytical technologies have enabled the identification of patient-specific tumor mutations and antigens, further advancing the personalization of therapeutic tumor vaccines [182]. However, most current therapeutic tumor vaccines rely on non-mutated tumor antigens that are shared among patients, often resulting in ineffective anti-tumor immune responses. Therefore, the addition of vaccine "adjuvants" is crucial for enhancing the efficacy of tumor vaccines. Inducing ICD can also promote the maturation of DCs and attract the infiltration of adaptive immune cells by releasing tumor antigens endogenously, thus mimicking the effects of therapeutic tumor vaccines. Combining QDs-mediated

PTT or PDT with therapeutic tumor vaccines can simultaneously stimulate endogenous and exogenous tumor antigens, leading to potent anti-tumor immune responses. Liu et al. demonstrated that heat-treated tumor serum exosomes can express TAAs at higher levels and possess strong immunomodulatory capabilities for promoting DCs differentiation and maturation. Consequently, they encapsulated BP QDs into heat-treated tumor exosomes to construct a tumor vaccine. By leveraging the homing effect of tumors, these exosomes can effectively accumulate at tumor sites, activate the immune system, and synergize with precise PTT to combat tumors [183]. Similarly, Ye et al. directly utilized BP QDs coated with the membrane of surgically excised tumor cells to create a tumor vaccine. These QDs were then loaded into a thermosensitive hydrogel containing granulocyte-macrophage colony-stimulating factor (GM-CSF) and lipopolysaccharide (LPS). Following NIR laser irradiation, the hydrogels implanted in tumors could sustainably release tumor vaccines and adjuvant components, thereby inducing long-term immune responses [184].

6.3.2 *QDs enable immunotherapy tracking*

As numerous clinical studies and practices continue to demonstrate the remarkable effects of immunotherapy in treating various tumors, it is crucial to develop technology that can promptly and accurately assess the impact of immunotherapy and provide an intuitive display of the patient's immune status. Traditional tumor treatment evaluation indicators are inadequate for meeting this need. Therefore, some studies are now focused on tracking drugs and related immune system components during immunotherapy through *in vivo* imaging, in order to better guide the development of immunotherapy drugs and patient care. This approach allows for real-time assessment of changes in tumors and their microenvironment caused by immunotherapy [185]. The utilization of QDs with their exceptional optical properties has emerged as a critical research avenue in QD-assisted tumor immunotherapy. QDs have the potential to construct detection probes, visualize immunotherapy responses, and trace immune components *in vivo*. This has significant implications for tumor diagnosis, uncovering disease mechanisms, and monitoring the patient's immune system status in real-time to evaluate treatment effectiveness [186, 187]. Furthermore, in addition to the luminescence effect of QDs themselves, their photothermal effect can enhance cell membrane permeability, facilitate the entry of fluorescent labels into cells, and aid in cell imaging. This process, known as photoporation, involves the formation of vapor nanobubbles (VNBs) through localized heating induced by QDs. The VNBs then mechanically puncture the cell membrane, enabling the diffusion of the external fluorescent label into the cytoplasm. Luminescent materials such as AuNPs, GQDs, and polydopamine NPs have demonstrated efficient photoporation and are currently used for optical microscopy imaging [188–190].

For the post-treatment monitoring of the immune system, Dai and colleagues combined anti-CD8 monoclonal antibodies with PbS QDs to target $CD8^+$ cytotoxic T cells (CTL) for *in vivo* imaging. PbS QDs can be fluorescently imaged in the NIR-IIb window, effectively penetrate tissues, and provide clear visualization of CTL distribution *in vivo*. They have also been successfully used to detect changes in CTL after PD-L1 antibody treatment [191]. Myeloid-derived suppressor cells (MDSCs) are crucial immunosuppressive cells in the TME and contribute to the failure of immunotherapy, such as ICIs. Yu et al. used PbS QDs and CdS QDs as fluorophores and labeled two specific antibodies for MDSCs. They constructed a pair of fluorescent nanoprobes for dual-color fluorescent molecular imaging of MDSCs *in vivo*. By utilizing the tunable emission wavelength characteristics of QDs, this multi-color fluorescent probe enables non-overlapping fluorescence imaging in the NIR-IIa and NIR-IIb windows, which correspond to specific surface markers of MDSCs (CD11b and granzyme-1 (Gr-1)). With dual fluorescent labeling and NIR-II imaging, this technology allows for non-invasive high-resolution imaging of MDSCs in various organs and tissues. It can also evaluate anti-tumor immunity by monitoring changes in MDSC numbers in the TME before and after drug treatment [192]. In addition to immune cells and immunosuppressive cells, immune-related molecules can serve as treatment response markers for efficacy monitoring. Zhang and colleagues developed a multifunctional nanoprobe capable of simultaneous immunotherapy using ICIs and detecting granzyme B (GrB). They used a new ICI drug that specifically targets leukocyte immunoglobulin-like receptor B4 on the surface of leukemia cells and assembled it on the surface of natural dopamine (PDA) nanoparticles. This ICI induces granulocytes to secrete GrB, promoting tumor cell apoptosis. Therefore, real-time monitoring of GrB secretion is crucial for assessing efficacy. To achieve this, they constructed a sensor based on fluorescence quenching on the surface of PDA. They bound a GQD labeled with a cleavable peptide to PDA through π-π interactions and used FRET to quench the GQD's fluorescence. When the ICI promotes the release of GrB, GrB cleaves its recognition peptide and releases a fluorescent signal, allowing for real-time visualization of GrB levels in the body [193]. Adoptive cell therapy is a personalized cancer treatment approach that involves training immune cells outside the body and then injecting them into the patient's body for effective immunotherapy. One type of adoptive cell therapy, known as chimeric antigen receptor T cells (CAR-T), is particularly effective in recognizing and killing tumor cells by targeting specific antigens on their surface. CAR-T therapy has had remarkable success in treating various types of tumors, especially hematological malignancies [194]. Monitoring the presence and evaluating the therapeutic effects of infused immune cells in the patient's body is crucial for the success of adoptive cell therapy. To address this, Wang and his team used Ag_2S QDs to label NK-92 cells for tumor cell therapy. They employed the fluorescence of Ag_2S QDs at NIR-II to monitor the distribution and therapeutic effect of the cells in the body. Additionally, to ensure the specific accumulation of NK-92 cells at the tumor site, they injected Ag_2Se QDs loaded with stromal cell-derived factor-1α (SDF-1α) and the chemotherapy drug DOX into the body six hours before treatment. Through the EPR effect, Ag_2Se QDs accumulate in the tumor and release SDF-1α and the drug, attracting NK-92 cells through the chemotaxis of SDF-1α and leading to a synergistic anti-tumor response [195]. Another study by Li et al. focused on accurately locating the tumor site to guide subsequent treatment. They achieved this by designing a fluorescence signal switch using QDs. They embedded Au/PDA NPs (gold/polydopamine nanoparticles) and Ag_2S QDs containing horseradish peroxidase (HRP) on the CAR-T cell membrane. The fluorescence of Ag_2S QDs is quenched by Au/PDA NPs. When macrophages engulf the Ag_2S QDs, the two nanoparticles separate, and the original fluorescence signal is restored. This indicates the infiltration of CAR-T cells in the tumor and provides guidance for follow-up treatments, such as radiotherapy and PTT [196].

Using a similar principle, QDs are sometimes employed as

fluorescent labels in tumor vaccines to visualize their movement in the body over time and space. In a study conducted by Sun et al., immune adjuvants and tumor antigens were attached to the surface of QDs to create tumor vaccines. The researchers then utilized the dynamics of QDs in the NIR window to monitor the trajectory of these vaccines in living organisms. This visual tracking system effectively reveals how the vaccine activates anti-tumor immunity within the body, including successful antigen delivery to DCs, localization within lysosomes, accumulation in lymph nodes, and sustained activation of immune cells [197]. This technology, which offers insights into the circulation of vaccines within the body, is crucial for vaccine development, as the immune response is closely connected to factors such as vaccine formulation, kinetics and biodistribution of vaccine exposure, and plays a significant role in the effective activation of immunity.

However, a current issue with *in vivo* imaging nanoparticles is their slow metabolism in the body. This can lead to their retention in the reticuloendothelial system (RES) for an extended period, ranging from months to years. While many studies have demonstrated the short-term biosafety of nanoparticles, the long-term retention in the body may introduce unforeseen risks and place an additional burden on the body [198]. To address this issue, Dai et al. developed a method to functionalize QDs with a cross-linked coating called P3, which is based on amphiphilic polymers. This coating enhances the biocompatibility of the nanoparticles and facilitates their rapid excretion from the body. The polymer coating protects the QDs, keeping them stable in aqueous environments and preventing aggregation. As a result, the nanoparticles can be quickly excreted through the biliary tract. Within two weeks of intravenous injection, over 90% of P3-functionalized QDs were found to be cleared from the body via the biliary tract. Furthermore, by covalently attaching a PEG layer to the coating surface, the interaction between the QDs and proteins or tissues in the body can be avoided. This allows the nanoparticles to evade *in vivo* clearance mechanisms like macrophage phagocytosis, consequently enabling rapid metabolism [199].

7 Comparison of QDs and other fluorescent materials

Compared to other fluorescent materials, such as organic dyes and fluorescent proteins, QDs offer several advantages in constructing fluorescent nanosensors due to their unique optical properties. First, QDs can achieve multicolor luminescence, providing flexibility for designing multiple biosensors with different colors and enabling multicolor fluorescent imaging. These are referred to as fluorescent QD barcodes, which are also cost-effective [200]. The ability to produce multicolor luminescence can be precisely controlled by adjusting the size of the QDs. Changes in size affect the energy difference between the highest valence band and the lowest valence band; a larger size requires more energy for excitation, resulting in greater energy release. Therefore, by adjusting the size of QDs, their fluorescence can span from the ultraviolet spectrum to the infrared spectrum [201, 202]. Secondly, QDs exhibit ultra-high fluorescence brightness, approximately 100 times greater than that of organic fluorescent dyes, due to their higher quantum yield. This enhanced fluorescence intensity improves the sensitivity and signal-to-noise ratio of biosensors and bioimaging, thereby reducing complex signal conversion steps and increasing the efficiency of biological monitoring. High fluorescence signals enable biosensors to detect or observe smaller biological substances, such as virus particles and small biomolecules, facilitating continuous imaging and tracking. This capability is crucial for exploring biological mechanisms and detecting markers [203]. Additionally, this high fluorescence signal is not only reliable but also stable. The molar extinction coefficient of QDs is 10 to 50 times higher than that of conventional organic fluorescent dyes. QDs demonstrate stronger resistance to photobleaching, maintaining their fluorescence intensity for extended periods, sometimes up to several months. Besides their resistance to photobleaching, QDs also exhibit excellent adaptability to environmental factors such as temperature, pH, and ion concentration. This adaptability enables biosensors based on QDs to function effectively in more complex clinical detection scenarios, making them promising candidates for various detection strategies [204]. It is worth noting that the fluorescence peak position of fluorescent QDs can be flexibly and precisely controlled by adjusting their size. QDs typically exhibit a wide excitation spectrum and a narrow emission spectrum. The wide excitation spectrum allows different QDs to be excited by a single beam of excitation light, resulting in the release of fluorescence at various wavelengths. This simplifies and reduces the cost of multicolor fluorescence detection or imaging, such as the simultaneous imaging of intracellular proteins and cytoskeletal components, as it eliminates the need to select different excitation lights for various fluorescent dyes. Moreover, selecting a more suitable excitation wavelength from the wide excitation spectrum of QDs can minimize the spontaneous fluorescence of biological samples, thereby improving resolution and sensitivity. The narrow emission spectrum effectively reduces spectral overlap and minimizes mutual interference between different fluorescence emissions, significantly enhancing the potential signal [205]. Beyond their optical properties, the flexible synthesis pathways of QDs and their extensive surface modification capabilities provide a range of physical and chemical properties, as well as functionalization strategies. This versatility broadens their biological application prospects compared to traditional one-step organic fluorescent dyes and fluorescent proteins. QDs can adjust their properties through processes such as alloying, doping, encapsulation, dendrite formation, and intercalation. Their outer shells enable the coupling of ligands with various functions via surface receptors or chemical groups, serving diverse biological purposes [206]. However, the presence of heavy metals, such as cadmium, in the elements used to synthesize QDs raises safety concerns. To address this, amphiphilic polymers or hydrophilic ligands can be added to encapsulate the QD core, improving biocompatibility while maintaining high fluorescence and stability. Using ZnS to encapsulate CdSe QDs also reduces toxicity, and their photostability is 100 to 1000 times greater than that of organic fluorophores [39, 207]. In summary, fluorescent QDs possess characteristics such as size-controlled tunable emission, a wide excitation spectrum, a narrow emission spectrum, high quantum yield, long-term photostability, and resistance to photobleaching. These features distinguish QDs from other fluorescent materials, making them powerful candidates for constructing multicolor fluorescent nanosensors and ultra-high-resolution fluorescent imaging technologies.

8 Conclusions and perspectives

This article focuses on the current status and advancements of QDs

in cancer research. Their tunable optical properties and high quantum yields offer unique advantages over traditional fluorescent markers, making them suitable for various applications in cancer diagnosis, therapy, and prevention research. In terms of cancer diagnosis, QDs have powerful fluorescent properties that make them effective tools for biomarker labeling, imaging, and detecting molecular markers as signal reporters. They can be used for high-resolution imaging of tumor tissues and sensitive analysis of tumor-specific markers, potentially improving the accuracy of early cancer detection. For cancer therapy, QDs have extensive potential applications. They can be used for intraoperative navigation, as drug carriers for precise drug delivery and controlled release when combined with various biomolecules. QDs can also play a role in PTT or PDT, where they kill tumor cells by generating localized hyperthermia or ROS. Their FRET effect compensates for the optical weaknesses of traditional phototherapy agents. Additionally, studies suggest the potential value of QDs in cancer immunotherapy, which may lead to novel strategies for cancer treatment in the future. Among these applications, tumor vaccines serve as a strategy for cancer immunotherapy and prevention. Some clinical trials have shown the potential of tumor vaccines, such as mutation-specific vaccines that target malignant brain tumors. In these studies, QDs have been used as immunological adjuvants. Tumor antigens are conjugated on the surface of QDs to prepare tumor vaccines, which enhance the presentation of antigens by DCs and stimulate a stronger specific anti-tumor immune response. Furthermore, the imaging capability of QDs in the NIR window allows for dynamic tracking of the fate of vaccines within the body. This offers new perspectives and methods for vaccine research. With continuous technological advancements and innovation, QDs are expected to play an increasingly important role in future cancer research.

However, the clinical application of QDs still faces challenges.

Firstly, the biosafety and potential toxicity of QDs are key challenges that must be addressed before their clinical application. While QDs offer a multitude of advantages in various applications, it is essential to acknowledge and discuss their inherent limitations. One of the primary concerns associated with QDs is their potential cytotoxicity, which can impact their safety for biological applications. Cytotoxicity refers to the ability of a substance to be toxic to cells, potentially leading to cell death or other adverse effects. QDs, particularly those synthesized with heavy metal components such as cadmium, have been reported to exhibit cytotoxic effects. The toxicity can arise from the release of heavy metal ions, which can disrupt cellular processes and lead to oxidative stress. Additionally, the surface chemistry of QDs, including the type of surface ligands or capping agents, can influence their biocompatibility and potential toxicity. To mitigate the cytotoxic effects of QDs, researchers have been exploring various strategies: (i) Surface modification. By modifying the surface of QDs with biocompatible ligands, such as PEG or biomolecules, their interaction with biological systems can be made less harmful. This approach has shown promise in reducing the cytotoxicity of QDs. (ii) Core/shell structures. Encapsulating the QD core with a less toxic shell material can help to confine the heavy metal ions within the core, thereby reducing their release and associated toxicity. (iii) Size and shape control. Smaller QDs with specific shapes may have lower toxicity due to reduced surface area and potential for interaction with cellular components. (iv) Alternative materials. Research is ongoing to develop QDs made from less toxic materials or to create entirely new types of nanomaterials that can mimic the properties of QDs without the associated risks. The use of QDs in biological and medical applications necessitates rigorous safety assessments and adherence to regulatory guidelines.

Secondly, the long-term stability, biodistribution, and clearance mechanisms of QDs within the body are not yet fully understood and require further research. Ensuring the safety of QDs involves not only addressing their cytotoxicity but also considering their long-term effects, potential for bioaccumulation, and environmental impact.

Looking ahead, several key areas warrant further investigation: (i) Biosafety and toxicity. Continued research is needed to understand and mitigate the cytotoxic effects of QDs, especially those containing heavy metals. Strategies such as surface modification and the development of heavy-metal-free QDs are promising avenues. (ii) Biodistribution and clearance. Elucidating the long-term biodistribution and clearance mechanisms of QDs is crucial for ensuring their safety in clinical applications. This will require comprehensive *in vivo* studies and translational research. (iii) Cost-effective production. Scaling up QDs production for clinical use must be balanced with cost-effectiveness. Exploring alternative, environmentally friendly synthesis methods is an important consideration. (iv) Interdisciplinary collaboration. The successful translation of QDs research into clinical practice will require the combined expertise of materials scientists, nanotechnologists, biologists, oncologists, and clinicians. Collaborative efforts will be essential to address the multifaceted challenges associated with QDs-based theranostics.

In summary, while QDs offer exciting possibilities for cancer diagnosis, therapy, and prevention, their clinical application necessitates a concerted focus on biosafety, biocompatibility, and translational research. With ongoing innovation and interdisciplinary collaboration, QDs are poised to play an increasingly important role in advancing cancer research and patient care.

Data availability

Not applicable.

Acknowledgements

This work was funded by the Science and Technology Program of Sichuan Province, China (Nos. 2024NSFSC1922, 2022YFS0095, and 2022YFS0083); Post-Doctor Research Project, West China Hospital, Sichuan University (No. 2021HXBH009); Sichuan University Postdoctoral Interdisciplinary Innovation Fund; the Liaoning Revitalization Talents Program (No. XLYC2203019) and Shenyang Young and Middle-aged Scientific and Technological Innovation Talents Project (No. RC220478).

Declaration of competing interest

All the contributing authors report no conflict of interests in this work.

Author contribution statement

M. L.: Designed, wrote, and revised the manuscript. Y. H.: Designed, wrote, and revised the manuscript. C. S.: Designed,

wrote, and revised the manuscript. Y. Q. W.: Participated in revising the manuscript. Y. A. L.: Participated in revising the manuscript. Z. J. W.: Managed the project, designed, and revised the manuscript. N. C.: Managed the project, designed, and revised the manuscript. Y. L.: Managed the project, designed, and revised the manuscript. All the authors have approved the final manuscript.

Informed consent

Not applicable.

Ethics statement

Not applicable.

Use of AI statement

None.

References

[1] Singh, S.; Raina, D.; Rishipathak, D.; Babu, K. R.; Khurana, R.; Gupta, Y.; Garg, K.; Rehan, F.; Gupta, S. M. Quantum dots in the biomedical world: A smart advanced nanocarrier for multiple venues application. *Arch Pharm* **2022**, *355*, 2200299.

[2] Soldado, A.; Barrio, L. C.; Díaz-Gonzalez, M.; de la Escosura-Muñiz, A.; Costa-Fernandez, J. M. Advances in quantum dots as diagnostic tools. *Adv. Clin. Chem.* **2022**, *107*, 1–40.

[3] Ekimov, A. I.; Efros, A. L.; Onushchenko, A. A. Quantum size effect in semiconductor microcrystals. *Solid State Commun.* **1985**, *56*, 921–924.

[4] Onoshima, D.; Yukawa, H.; Baba, Y. Multifunctional quantum dots-based cancer diagnostics and stem cell therapeutics for regenerative medicine. *Adv. Drug Deliv. Rev.* **2015**, *95*, 2–14.

[5] Gill, R.; Zayats, M.; Willner, I. Semiconductor quantum dots for bioanalysis. *Angew. Chem., Int. Ed.* **2008**, *47*, 7602–7625.

[6] Jin, Z. W.; Hildebrandt, N. Semiconductor quantum dots for *in vitro* diagnostics and cellular imaging. *Trends Biotechnol.* **2012**, *30*, 394–403.

[7] Suárez, P. L.; García-Cortés, M.; Fernández-Argüelles, M. T.; Encinar, J. R.; Valledor, M.; Ferrero, F. J.; Campo, J. C.; Costa-Fernández, J. M. Functionalized phosphorescent nanoparticles in (bio)chemical sensing and imaging - a review. *Anal. Chim. Acta* **2019**, *1046*, 16–31.

[8] Zhang, C. Y.; Yeh, H. C.; Kuroki, M. T.; Wang, T. H. Single-quantum-dot-based DNA nanosensor. *Nat Mater* **2005**, *4*, 826–831.

[9] Chu, T. C.; Shieh, F.; Lavery, L. A.; Levy, M.; Richards-Kortum, R.; Korgel, B. A.; Ellington, A. D. Labeling tumor cells with fluorescent nanocrystal-aptamer bioconjugates. *Biosens Bioelectron.* **2006**, *21*, 1859–1866.

[10] Abdellatif, A. A. H.; Younis, M. A.; Alsharidah, M.; Al Rugaie, O.; Tawfeek, H. M. Biomedical applications of quantum dots: Overview, challenges, and clinical potential. *Int. J. Nanomed.* **2022**, *17*, 1951–1970.

[11] Hildebrandt, N. Biofunctional quantum dots: Controlled conjugation for multiplexed biosensors. *ACS Nano* **2011**, *5*, 5286–5290.

[12] Sanderson, K.; Castelvecchi, D. Tiny 'quantum dot' particles win chemistry Nobel. *Nature* **2023**, *622*, 227–228.

[13] Rossetti, R.; Nakahara, S.; Brus, L. E. Quantum size effects in the redox potentials, resonance Raman spectra, and electronic spectra of CdS crystallites in aqueous solution. *J. Chem. Phys.* **1983**, *79*, 1086–1088.

[14] Murray, C. B.; Norris, D. J.; Bawendi, M. G. Synthesis and characterization of nearly monodisperse CdE (E = sulfur, selenium, tellurium) semiconductor nanocrystallites. *J. Am. Chem. Soc.* **1993**, *115*, 8706–8715.

[15] Bruchez, M. Jr. ; Moronne, M.; Gin, P.; Weiss, S.; Alivisatos, A. P. Semiconductor nanocrystals as fluorescent biological labels. *Science* **1998**, *281*, 2013–2016.

[16] Chan, W. C. W.; Nie, S. M. Quantum dot bioconjugates for ultrasensitive nonisotopic detection. *Science* **1998**, *281*, 2016–2018.

[17] Peng, Z. A.; Peng, X. G. Formation of high-quality CdTe, CdSe, and CdS nanocrystals using CdO as precursor. *J. Am. Chem. Soc.* **2001**, *123*, 183–184.

[18] Han, M. Y.; Gao, X. H.; Su, J. Z.; Nie, S. M. Quantum-dot-tagged microbeads for multiplexed optical coding of biomolecules. *Nat. Biotechnol.* **2001**, *19*, 631–635.

[19] Gaponik, N.; Talapin, D. V.; Rogach, A. L.; Hoppe, K.; Shevchenko, E. V.; Kornowski, A.; Eychmüller, A.; Weller, H. Thiol-capping of CdTe nanocrystals: An alternative to organometallic synthetic routes. *J. Phys. Chem. B* **2002**, *106*, 7177–7185.

[20] Larson, D. R.; Zipfel, W. R.; Williams, R. M.; Clark, S. W.; Bruchez, M. P.; Wise, F. W.; Webb, W. W. Water-soluble quantum dots for multiphoton fluorescence imaging *in vivo*. *Science* **2003**, *300*, 1434–1436.

[21] Gao, X. H.; Cui, Y. Y.; Levenson, R. M.; Chung, L. W. K.; Nie, S. M. *In vivo* cancer targeting and imaging with semiconductor quantum dots. *Nat. Biotechnol.* **2004**, *22*, 969–976.

[22] Derfus, A. M.; Chan, W. C. W.; Bhatia, S. N. Probing the cytotoxicity of semiconductor quantum dots. *Nano Lett.* **2004**, *4*, 11–18.

[23] Utzat, H.; Sun, W. W.; Kaplan, A. E. K.; Krieg, F.; Ginterseder, M.; Spokoyny, B.; Klein, N. D.; Shulenberger, K. E.; Perkinson, C. F.; Kovalenko, M. V. et al. Coherent single-photon emission from colloidal lead halide perovskite quantum dots. *Science* **2019**, *363*, 1068–1072.

[24] Medintz, I. L.; Uyeda, H. T.; Goldman, E. R.; Mattoussi, H. Quantum dot bioconjugates for imaging, labelling and sensing. *Nat. Mater.* **2005**, *4*, 435–446.

[25] Michalet, X.; Pinaud, F. F.; Bentolila, L. A.; Tsay, J. M.; Doose, S.; Li, J. J.; Sundaresan, G.; Wu, A. M.; Gambhir, S. S.; Weiss, S. Quantum dots for live cells, *in vivo* imaging, and diagnostics. *Science* **2005**, *307*, 538–544.

[26] Yang, Y.; Lian, T. Q. Multiple exciton dissociation and hot electron extraction by ultrafast interfacial electron transfer from PbS QDs. *Coord. Chem. Rev.* **2014**, *263-264*, 229–238.

[27] Bhaskar, S.; Patra, R.; Kowshik, N. C. S. S.; Ganesh, K. M.; Srinivasan, V.; Chandran, S. P.; Ramamurthy, S. S. Nanostructure effect on quenching and dequenching of quantum emitters on surface plasmon-coupled interface: A comparative analysis using gold nanospheres and nanostars. *Phys. E: Low-Dimension. Syst. Nanostruct.* **2020**, *124*, 114276.

[28] Kwak, D. H.; Ramasamy, P.; Lee, Y. S.; Jeong, M. H.; Lee, J. S. High-performance hybrid InP QDs/black phosphorus photodetector. *ACS Appl. Mater. Interfaces* **2019**, *11*, 29041–29046.

[29] Yuan, S.; Chen, D. Q.; Li, X. Y.; Zhong, J. S.; Xu, X. H. *In situ* crystallization synthesis of $CsPbBr_3$ perovskite quantum dot-embedded glasses with improved stability for solid-state lighting and random upconverted lasing. *ACS Appl. Mater. Interfaces* **2018**, *10*, 18918–18926.

[30] Chi, W. G.; Banerjee, S. K. Application of perovskite quantum dots as an absorber in perovskite solar cells. *Angew. Chem., Int. Ed.* **2022**, *61*, e202112412.

[31] Erwin, S. C.; Efros, A. L. Electronic transport in quantum-dot-in-perovskite solids. *Nanoscale* **2022**, *14*, 17725–17734.

[32] Zhou, Q. X.; Yue, Z. K.; Li, Q. Z.; Zhou, R. R.; Liu, L. Exposure to PbSe nanoparticles and male reproductive damage in a rat model. *Environ. Sci. Technol.* **2019**, *53*, 13408–13416.

[33] Okamura, Y.; Shimizu, R.; Tominaga, Y.; Maki, S.; Aki, T.; Matsumura, Y.; Nakashimada, Y. Characterization of biogenic PbS quantum dots. *Int. J. Mol. Sci.* **2023**, *24*, 14149.

[34] Gao, L. F.; Wang, L. D.; Kuklin, A. V.; Gao, J.; Yin, S. C.; Ågren, H.; Zhang, H. A facile approach for elemental-doped carbon quantum dots and their application for efficient photodetectors. *Small* **2021**, *17*, 2105683.

[35] Li, Z.; Zhao, C. Y.; Fu, Q. R.; Ye, J. M.; Su, L. C.; Ge, X. G.; Chen, L. L.; Song, J. B.; Yang, H. H. Neodymium (3+)-coordinated black phosphorus quantum dots with retrievable NIR/X-ray optoelectronic switching effect for anti-glioblastoma. *Small* **2022**, *18*, 2105160.
[36] Majumdar, S.; Gogoi, D.; Boruah, P. K.; Thakur, A.; Sarmah, P.; Gogoi, P.; Sarkar, S.; Pachani, P.; Manna, P.; Saikia, R. et al. Hexagonal boron nitride quantum dots embedded on layer-by-layer films for peroxidase-assisted colorimetric detection of β-galactosidase producing pathogens. *ACS Appl. Mater. Interfaces* **2024**, *16*, 26870–26885.
[37] Wang, H.; Pu, G. Q.; Devaramani, S.; Wang, Y. F.; Yang, Z. F.; Li, L. F.; Ma, X. F.; Lu, X. Q. Bimodal electrochemiluminescence of G-CNQDs in the presence of double coreactants for ascorbic acid detection. *Anal. Chem.* **2018**, *90*, 4871–4877.
[38] Perini, G.; Palmieri, V.; Ciasca, G.; De Spirito, M.; Papi, M. Unravelling the potential of graphene quantum dots in biomedicine and neuroscience. *Int. J. Mol. Sci.* **2020**, *21*, 3712.
[39] Sobhanan, J.; Rival, J. V.; Anas, A.; Sidharth Shibu, E.; Takano, Y.; Biju, V. Luminescent quantum dots: Synthesis, optical properties, bioimaging and toxicity. *Adv. Drug Delivery Rev.* **2023**, *197*, 114830.
[40] Ding, X. G.; Peng, F.; Zhou, J.; Gong, W. B.; Slaven, G.; Loh, K. P.; Lim, C. T.; Leong, D. T. Defect engineered bioactive transition metals dichalcogenides quantum dots. *Nat. Commun.* **2019**, *10*, 41.
[41] Das, P.; Sedighi, A.; Krull, U. J. Cancer biomarker determination by resonance energy transfer using functional fluorescent nanoprobes. *Anal. Chim. Acta* **2018**, *1041*, 1–24.
[42] Zhou, J.; Yang, Y.; Zhang, C. Y. Toward biocompatible semiconductor quantum dots: From biosynthesis and bioconjugation to biomedical application. *Chem. Rev.* **2015**, *115*, 11669–11717.
[43] Uyeda, H. T.; Medintz, I. L.; Jaiswal, J. K.; Simon, S. M.; Mattoussi, H. Synthesis of compact multidentate ligands to prepare stable hydrophilic quantum dot fluorophores. *J. Am. Chem. Soc.* **2005**, *127*, 3870–3878.
[44] Bharali, D. J.; Lucey, D. W.; Jayakumar, H.; Pudavar, H. E.; Prasad, P. N. Folate-receptor-mediated delivery of InP quantum dots for bioimaging using confocal and two-photon microscopy. *J. Am. Chem. Soc.* **2005**, *127*, 11364–11371.
[45] Boeneman, K.; Mei, B. C.; Dennis, A. M.; Bao, G.; Deschamps, J. R.; Mattoussi, H.; Medintz, I. L. Sensing caspase 3 activity with quantum dot-fluorescent protein assemblies. *J. Am. Chem. Soc.* **2009**, *131*, 3828–3829.
[46] Goldman, E. R.; Balighian, E. D.; Mattoussi, H.; Kuno, M. K.; Mauro, J. M.; Tran, P. T.; Anderson, G. P. Avidin: A natural bridge for quantum dot-antibody conjugates. *J. Am. Chem. Soc.* **2002**, *124*, 6378–6382.
[47] Ostermann, J.; Merkl, J. P.; Flessau, S.; Wolter, C.; Kornowksi, A.; Schmidtke, C.; Pietsch, A.; Kloust, H.; Feld, A.; Weller, H. Controlling the physical and biological properties of highly fluorescent aqueous quantum dots using block copolymers of different size and shape. *ACS Nano* **2013**, *7*, 9156–9167.
[48] Bernardin, A.; Cazet, A.; Guyon, L.; Delannoy, P.; Vinet, F.; Bonnaffé, D.; Texier, I. Copper-free click chemistry for highly luminescent quantum dot conjugates: Application to *in vivo* metabolic imaging. *Bioconjugate Chem.* **2010**, *21*, 583–588.
[49] Li, F.; Wang, Q. B. Fabrication of nanoarchitectures templated by virus-based nanoparticles: Strategies and applications. *Small* **2014**, *10*, 230–245.
[50] Siegel, R. L.; Miller, K. D.; Wagle, N. S.; Jemal, A. Cancer statistics, 2023. *CA: Cancer J. Clinicians* **2023**, *73*, 17–48.
[51] Siegel, R. L.; Miller, K. D.; Fedewa, S. A.; Ahnen, D. J.; Meester, R. G. S.; Barzi, A.; Jemal, A. Colorectal cancer statistics, 2017. *CA: Cancer J. Clin.* **2017**, *67*, 177–193.
[52] Hosny, A.; Parmar, C.; Quackenbush, J.; Schwartz, L. H.; Aerts, H. J. W. L. Artificial intelligence in radiology. *Nat. Rev. Cancer* **2018**, *18*, 500–510.
[53] Kauczor, H. U.; Baird, A. M.; Blum, T. G.; Bonomo, L.; Bostantzoglou, C.; Burghuber, O.; Čepická, B.; Comanescu, A.; Couraud, S.; Devaraj, A. et al. ESR/ERS statement paper on lung cancer screening. *Eur. Radiol.* **2020**, *30*, 3277–3294.
[54] Burggraaf, J.; Kamerling, I. M. C.; Gordon, P. B.; Schrier, L.; de Kam, M. L.; Kales, A. J.; Bendiksen, R.; Indrevoll, B.; Bjerke, R. M.; Moestue, S. A. et al. Detection of colorectal polyps in humans using an intravenously administered fluorescent peptide targeted against c-Met. *Nat. Med.* **2015**, *21*, 955–961.
[55] Bera, K.; Schalper, K. A.; Rimm, D. L.; Velcheti, V.; Madabhushi, A. Artificial intelligence in digital pathology-new tools for diagnosis and precision oncology. *Nat. Rev. Clin. Oncol.* **2019**, *16*, 703–715.
[56] Calderaro, J.; Ziol, M.; Paradis, V.; Zucman-Rossi, J. Molecular and histological correlations in liver cancer. *J. Hepatol.* **2019**, *71*, 616–630.
[57] Lehrich, B. M.; Zhang, J.; Monga, S. P.; Dhanasekaran, R. Battle of the biopsies: Role of tissue and liquid biopsy in hepatocellular carcinoma. *J. Hepatol.* **2024**, *80*, 515–530.
[58] Huang, A.; Zhao, X.; Yang, X. R.; Li, F. Q.; Zhou, X. L.; Wu, K.; Zhang, X.; Sun, Q. M.; Cao, Y.; Zhu, H. M. et al. Corrigendum to "Circumventing intratumoral heterogeneity to identify potential therapeutic targets in hepatocellular carcinoma" [J Hepatol 67 (2017) 293–301]. *J. Hepatol.* **2017**, *67*, 1123.
[59] Wang, Y. A.; Yan, Q. J.; Fan, C. M.; Mo, Y. Z.; Wang, Y. M.; Li, X. Y.; Liao, Q. J.; Guo, C.; Li, G. Y.; Zeng, Z. Y. et al. Overview and countermeasures of cancer burden in China. *Sci. China Life Sci.* **2023**, *66*, 2515–2526.
[60] Li, X. S.; Lovell, J. F.; Yoon, J.; Chen, X. Y. Clinical development and potential of photothermal and photodynamic therapies for cancer. *Nat. Rev. Clin. Oncol.* **2020**, *17*, 657–674.
[61] Luo, D. D.; Carter, K. A.; Miranda, D.; Lovell, J. F. Chemophototherapy: An emerging treatment option for solid tumors. *Adv. Sci.* **2017**, *4*, 1600106.
[62] Chou, S. W.; Shau, Y. H.; Wu, P. C.; Yang, Y. S.; Shieh, D. B.; Chen, C. C. *In vitro* and *in vivo* studies of FePt nanoparticles for dual modal CT/MRI molecular imaging. *J. Am. Chem. Soc.* **2010**, *132*, 13270–13278.
[63] Yong, K. T.; Ding, H.; Roy, I.; Law, W. C.; Bergey, E. J.; Maitra, A.; Prasad, P. N. Imaging pancreatic cancer using bioconjugated InP quantum dots. *ACS Nano* **2009**, *3*, 502–510.
[64] Dash, P.; Piras, A. M.; Dash, M. Cell membrane coated nanocarriers - an efficient biomimetic platform for targeted therapy. *J. Control. Release* **2020**, *327*, 546–570.
[65] Kargozar, S.; Hoseini, S. J.; Milan, P. B.; Hooshmand, S.; Kim, H. W.; Mozafari, M. Quantum dots: A review from concept to clinic. *Biotechnol. J.* **2020**, *15*, 2000117.
[66] Abdelhamid, H. N.; El-Bery, H. M.; Metwally, A. A.; Elshazly, M.; Hathout, R. M. Synthesis of CdS-modified chitosan quantum dots for the drug delivery of Sesamol. *Carbohydr. Polym.* **2019**, *214*, 90–99.
[67] Zhang, J.; Zhang, X. Y.; Bi, S. Two-dimensional quantum dot-based electrochemical biosensors. *Biosensors* **2022**, *12*, 254.
[68] Hildebrandt, N.; Spillmann, C. M.; Algar, W. R.; Pons, T.; Stewart, M. H.; Oh, E.; Susumu, K.; Díaz, S. A.; Delehanty, J. B.; Medintz, I. L. Energy transfer with semiconductor quantum dot bioconjugates: A versatile platform for biosensing, energy harvesting, and other developing applications. *Chem. Rev.* **2017**, *117*, 536–711.
[69] Colino, C. I.; Millán, C. G.; Lanao, J. M. Nanoparticles for signaling in biodiagnosis and treatment of infectious diseases. *Int. J. Mol. Sci.* **2018**, *19*, 1627.
[70] Tawfik, S. M.; Huy, B. T.; Sharipov, M.; Abd-Elaal, A.; Lee, Y. I. Enhanced fluorescence of CdTe quantum dots capped with a novel nonionic alginate for selective optosensing of ibuprofen. *Sens. Actuators B: Chem.* **2018**, *256*, 243–250.
[71] Qian, Z. S.; Shan, X. Y.; Chai, L. J.; Chen, J. R.; Feng, H. A fluorescent nanosensor based on graphene quantum dots-aptamer probe and graphene oxide platform for detection of lead (II) ion. *Biosens. Bioelectron.* **2015**, *68*, 225–231.
[72] Li, C. X.; Yang, Q.; Wang, X. Y.; Arabi, M.; Peng, H. L.; Li, J. H.; Xiong, H.; Chen, L. X. Facile approach to the synthesis of molecularly imprinted ratiometric fluorescence nanosensor for the

visual detection of folic acid. *Food Chem.* **2020**, *319*, 126575.
[73] Fu, X. M.; Tan, X. R.; Yuan, R.; Chen, S. H. A dual-potential electrochemiluminescence ratiometric sensor for sensitive detection of dopamine based on graphene-CdTe quantum dots and self-enhanced Ru(II) complex. *Biosens. Bioelectron.* **2017**, *90*, 61–68.
[74] Hu, J.; Li, Y. Y.; Li, Y.; Tang, B.; Zhang, C. Y. Single quantum dot-based nanosensor for sensitive detection of O–GlcNAc transferase activity. *Anal. Chem.* **2017**, *89*, 12992–12999.
[75] Wang, Y.; Howes, P. D.; Kim, E.; Spicer, C. D.; Thomas, M. R.; Lin, Y. Y.; Crowder, S. W.; Pence, I. J.; Stevens, M. M. Duplex-specific nuclease-amplified detection of MicroRNA using compact quantum dot-DNA conjugates. *ACS Appl. Mater. Interfaces* **2018**, *10*, 28290–28300.
[76] Augustine, R.; Al Mamun, A.; Hasan, A.; Salam, S. A.; Chandrasekaran, R.; Ahmed, R.; Thakor, A. S. Imaging cancer cells with nanostructures: Prospects of nanotechnology driven non-invasive cancer diagnosis. *Adv. Colloid Interface Sci.* **2021**, *294*, 102457.
[77] Campbell, E.; Hasan, M. T.; Gonzalez Rodriguez, R.; Akkaraju, G. R.; Naumov, A. V. Doped graphene quantum dots for intracellular multicolor imaging and cancer detection. *ACS Biomater. Sci. Eng.* **2019**, *5*, 4671–4682.
[78] Ren, X.; Zhang, F.; Guo, B. P.; Gao, N.; Zhang, X. L. Synthesis of N-doped micropore carbon quantum dots with high quantum yield and dual-wavelength photoluminescence emission from biomass for cellular imaging. *Nanomaterials (Basel)* **2019**, *9*, 495.
[79] Feng, S. X.; Li, H. L.; Pan, J. Q.; Li, C. R.; Zheng, Y. Y. Preparation and cell imaging of nitrogen-doped graphene quantum dot conjugated indomethacin. *IOP Conf. Ser.: Earth Environ. Sci.* **2019**, *358*, 032006.
[80] Nifontova, G.; Baryshnikova, M.; Ramos-Gomes, F.; Alves, F.; Nabiev, I.; Sukhanova, A. Engineering of fluorescent biomaging tools for cancer cell targeting based on polyelectrolyte microcapsules encoded with quantum dots. In *Proceedings of the Fourth International Conference on Applications of Optics and Photonics*, Lisbon, Portugal, 2019, pp 516–521.
[81] Liu, B.; Jiang, B.; Zheng, Z. P.; Liu, T. C. Semiconductor quantum dots in tumor research. *J. Lumin.* **2019**, *209*, 61–68.
[82] Wu, X. Y.; Liu, H. J.; Liu, J. Q.; Haley, K. N.; Treadway, J. A.; Larson, J. P.; Ge, N. F.; Peale, F.; Bruchez, M. P. Immunofluorescent labeling of cancer marker Her2 and other cellular targets with semiconductor quantum dots. *Nat. Biotechnol.* **2003**, *21*, 41–46.
[83] Xue, W. T.; Di, Z. H.; Zhao, Y.; Zhang, A. P.; Li, L. L. DNA-mediated coordinative assembly of upconversion hetero-nanostructures for targeted dual-modality imaging of cancer cells. *Chin. Chem. Lett.* **2019**, *30*, 899–902.
[84] Li, Z. M.; Huang, P.; He, R.; Lin, J.; Yang, S.; Zhang, X. J.; Ren, Q. S.; Cui, D. X. Aptamer-conjugated dendrimer-modified quantum dots for cancer cell targeting and imaging. *Mater. Lett.* **2010**, *64*, 375–378.
[85] Mangeolle, T.; Yakavets, I.; Lequeux, N.; Pons, T.; Bezdetnaya, L.; Marchal, F. The targeting ability of fluorescent quantum dots to the folate receptor rich tumors. *Photodiagnosis Photodyn. Ther.* **2019**, *26*, 150–156.
[86] Yang, Y. Q.; Qian, X. P.; Zhang, L. H.; Miao, W. J.; Ming, D. M.; Jiang, L.; Huang, H. Enhanced imaging of glycan expressing cancer cells using poly(glycidyl methacrylate)-grafted silica nanospheres labeled with quantum dots. *Anal. Chim. Acta* **2020**, *1095*, 138–145.
[87] Rana, M.; Jain, A.; Rani, V.; Chowdhury, P. Glutathione capped core/shell CdSeS/ZnS quantum dots as a medical imaging tool for cancer cells. *Inorg. Chem. Commun.* **2020**, *112*, 107723.
[88] Fu, Y.; Jang, M. S.; Wu, T. P.; Lee, J. H.; Li, Y.; Lee, D. S.; Yang, H. Y. Multifunctional hyaluronic acid-mediated quantum dots for targeted intracellular protein delivery and real-time fluorescence imaging. *Carbohydr. Polym.* **2019**, *224*, 115174.
[89] Pons, T.; Bouccara, S.; Loriette, V.; Lequeux, N.; Pezet, S.; Fragola, A. *In vivo* imaging of single tumor cells in fast-flowing bloodstream using near-infrared quantum dots and time-gated imaging. *ACS Nano* **2019**, *13*, 3125–3131.
[90] Duman, F. D.; Akkoc, Y.; Demirci, G.; Bavili, N.; Kiraz, A.; Gozuacik, D.; Acar, H. Y. Bypassing pro-survival and resistance mechanisms of autophagy in EGFR-positive lung cancer cells by targeted delivery of 5FU using theranostic Ag_2S quantum dots. *J. Mater. Chem. B* **2019**, *7*, 7363–7376.
[91] Liang, Z. B.; Yang, Y. Q.; Jia, F. J.; Sai, K.; Ullah, S.; Fidelis, C.; Lin, Z.; Li, F. Intrathecal delivery of folate conjugated near-infrared quantum dots for targeted *in vivo* imaging of gliomas in mice brains. *ACS Appl. Bio Mater.* **2019**, *2*, 1432–1439.
[92] Townsend, D. W.; Carney, J. P. J.; Yap, J. T.; Hall, N. C. PET/CT today and tomorrow. *J. Nucl. Med.* **2004**, *45*, 4S–14S.
[93] Delso, G.; Ziegler, S. PET/MRI system design. *Eur. J. Nucl. Med. Mol. Imaging* **2009**, *36 Suppl 1*, S86–S92.
[94] Sk Md, N.; Kim, H. K.; Park, J. A.; Chang, Y. M.; Kim, T. J. Gold nanoparticles coated with Gd-chelate as a potential CT/MRI bimodal contrast agent. *Bull. Korean Chem. Soc.* **2010**, *31*, 1177–1181.
[95] Guo, K.; Berezin, M. Y.; Zheng, J.; Akers, W.; Lin, F.; Teng, B.; Vasalatiy, O.; Gandjbakhche, A.; Griffiths, G. L.; Achilefu, S. Near infrared-fluorescent and magnetic resonance imaging molecular probe with high T_1 relaxivity for *in vivo* multimodal imaging. *Chem. Commun.* **2010**, *46*, 3705–3707.
[96] Mulder, W. J. M.; Koole, R.; Brandwijk, R. J.; Storm, G.; Chin, P. T. K.; Strijkers, G. J.; de Mello Donegá, C.; Nicolay, K.; Griffioen, A. W. Quantum dots with a paramagnetic coating as a bimodal molecular imaging probe. *Nano Lett.* **2006**, *6*, 1–6.
[97] Prasad, R.; Jain, N. K.; Yadav, A. S.; Chauhan, D. S.; Devrukhkar, J.; Kumawat, M. K.; Shinde, S.; Gorain, M.; Thakor, A. S.; Kundu, G. C. et al. Liposomal nanotheranostics for multimode targeted *in vivo* bioimaging and near-infrared light mediated cancer therapy. *Commun. Biol.* **2020**, *3*, 284.
[98] Wu, L.; Qu, X. G. Cancer biomarker detection: Recent achievements and challenges. *Chem. Soc. Rev.* **2015**, *44*, 2963–2997.
[99] Mathur, D.; Thakur, M.; Díaz, S. A.; Susumu, K.; Stewart, M. H.; Oh, E.; Walper, S. A.; Medintz, I. L. Hybrid nucleic acid-quantum dot assemblies as multiplexed reporter platforms for cell-free transcription translation-based biosensors. *ACS Synth. Biol.* **2022**, *11*, 4089–4102.
[100] Wang, P.; Wei, X. W.; Shen, L. M.; Xu, K. X.; Wen, Z. T.; Gao, N. J.; Fan, T.; Xun, S. M.; Zhu, Q. Y.; Qu, X. J. et al. Amplification-free analysis of bladder cancer MicroRNAs on wrinkled silica nanoparticles with DNA-functionalized quantum dots. *Anal. Chem.* **2024**, *96*, 4860–4867.
[101] Min, H.; Jo, S. M.; Kim, H. S. Efficient capture and simple quantification of circulating tumor cells using quantum dots and magnetic beads. *Small* **2015**, *11*, 2536–2542.
[102] Lian, W.; Tu, D. T.; Hu, P.; Song, X. R.; Gong, Z. L.; Chen, T.; Song, J. B.; Chen, Z.; Chen, X. Y. Broadband excitable NIR-II luminescent nano-bioprobes based on $CuInSe_2$ quantum dots for the detection of circulating tumor cells. *Nano Today* **2020**, *35*, 100943.
[103] Wu, M.; Chen, Z. K.; Xie, Q. H.; Xiao, B. L.; Zhou, G.; Chen, G.; Bian, Z. One-step quantification of salivary exosomes based on combined aptamer recognition and quantum dot signal amplification. *Biosens. Bioelectron.* **2021**, *171*, 112733.
[104] Chen, P. P.; Li, M.; Peng, W.; Liu, T. Y. H.; Huang, J.; Ying, B. W. Multiple signal amplification and selective recognition reactions-assisted homogeneous binary visual aptasensor of tuberculosis interferon γ in clinical samples. *Sens. Actuators B: Chem.* **2023**, *376*, 132997.
[105] Riegler, J.; Nann, T. Application of luminescent nanocrystals as labels for biological molecules. *Anal. Bioanal. Chem.* **2004**, *379*, 913–919.
[106] Xiao, S. T.; Yao, Y.; Liao, S. L.; Xu, B.; Li, X.; Zhang, Y. X.; Zhang, L.; Chen, Q.; Tang, H. N.; Song, Q. B. et al. Accurate and convenient lung cancer diagnosis through detection of extracellular vesicle membrane proteins via förster resonance energy transfer. *Nano Lett.* **2023**, *23*, 8115–8125.
[107] Yang, T.; Li, C. M.; He, J. H.; Chen, B.; Li, Y. F.; Huang, C. Z.

Ratiometrically fluorescent electrospun nanofibrous film as a Cu^{2+}-mediated solid-phase immunoassay platform for biomarkers. *Anal. Chem.* **2018**, *90*, 9966–9974.
[108] Sun, Y. L.; Fan, J. F.; Cui, L. Y.; Ke, W.; Zheng, F. J.; Zhao, Y. Fluorometric nanoprobes for simultaneous aptamer-based detection of carcinoembryonic antigen and prostate specific antigen. *Microchim. Acta* **2019**, *186*, 152.
[109] Liu, W. J.; Song, R.; Yang, D. M.; Zhao, S. L.; Zhang, C. Y. A programmable quantum dot nanosensor guided by three-way junction skeleton-mediated cascade signal amplification for sensitive detection of circRNAs in breast cancer. *Chem. Eng. J.* **2024**, *484*, 149788.
[110] Lee, T.; Jang, J.; Jeong, H.; Rho, J. Plasmonic- and dielectric-based structural coloring: From fundamentals to practical applications. *Nano Converg.* **2018**, *5*, 1.
[111] Jia, P. D.; Ding, C. P.; Sun, Z. W.; Song, L. P.; Zhang, D.; Yan, Z. J.; Zhang, Z. L.; Su, F. M.; Mostafa, A. A.; Huang, Y. J. DNA precisely regulated Au nanorods/Ag_2S quantum dots satellite structure for ultrasensitive detection of prostate cancer biomarker. *Sens. Actuators B: Chem.* **2021**, *347*, 130585.
[112] Tabish, T. A.; Hayat, H.; Abbas, A.; Narayan, R. J. Graphene quantum dot-based electrochemical biosensing for early cancer detection. *Curr. Opin. Electrochem.* **2021**, *30*, 100786.
[113] Nie, G. M.; Wang, Y.; Tang, Y.; Zhao, D.; Guo, Q. F. A graphene quantum dots based electrochemiluminescence immunosensor for carcinoembryonic antigen detection using poly(5-formylindole)/reduced graphene oxide nanocomposite. *Biosens. Bioelectron.* **2018**, *101*, 123–128.
[114] Li, Z. R.; Wang, Z. Z.; Nie, Y. X.; Wang, P. L.; Ma, Q. A novel GSH-capping MXene QD-based ECL biosensor for the detection of miRNA221 in triple-negative breast cancer tumor. *Chem. Eng. J.* **2022**, *448*, 137636.
[115] Pei, Y. J.; Ge, Y. H.; Zhang, X. R.; Li, Y. Cathodic photoelectrochemical aptasensor based on NiO/BiOI/Au NP composite sensitized with CdSe for determination of exosomes. *Microchim. Acta* **2021**, *188*, 51.
[116] Mao, C. L.; Qin, Y.; Zhou, X. Y.; Dai, R. H.; Zhao, L. S. Late-model Bi-MOF&CdS-QDs materials: Excellent properties and performance in PEC sensors for lung cancer markers. *Chem. Eng. J.* **2024**, *490*, 151560.
[117] Zhang, S. H.; Tang, X. M.; Zang, L. H.; Zhao, L. S. Carbon quantum dots(CQDs)-sensitized CdS/$CuInS_2$ heterojunction as a photoelectrochemical biosensing platform for highly sensitive detection of prostate-specific antigen. *Talanta* **2024**, *272*, 125811.
[118] Cayuela, A.; Soriano, M. L.; Carrillo-Carrión, C.; Valcárcel, M. Semiconductor and carbon-based fluorescent nanodots: The need for consistency. *Chem. Commun.* **2016**, *52*, 1311–1326.
[119] Christodouleas, D. C.; Kaur, B.; Chorti, P. From point-of-care testing to eHealth diagnostic devices (eDiagnostics). *ACS Cent. Sci.* **2018**, *4*, 1600–1616.
[120] Kim, C.; Hoffmann, G.; Searson, P. C. Integrated magnetic bead-quantum dot immunoassay for malaria detection. *ACS Sens.* **2017**, *2*, 766–772.
[121] Medina-Sánchez, M.; Miserere, S.; Morales-Narváez, E.; Merkoçi, A. On-chip magneto-immunoassay for Alzheimer's biomarker electrochemical detection by using quantum dots as labels. *Biosens. Bioelectron.* **2014**, *54*, 279–284.
[122] Bai, Y. N.; Lu, Y. X.; Wang, K.; Cheng, Z. L.; Qu, Y. L.; Qiu, S. H.; Zhou, L.; Wu, Z. H.; Liu, H. Y.; Zhao, J. L. et al. Rapid isolation and multiplexed detection of exosome tumor markers via queued beads combined with quantum dots in a microarray. *Nano-Micro Lett.* **2019**, *11*, 59.
[123] Zhou, S. S.; Hu, T.; Han, G. H.; Wu, Y. F.; Hua, X.; Su, J.; Jin, W. W.; Mou, Y. P.; Mou, X. Z.; Li, Q. et al. Accurate cancer diagnosis and stage monitoring enabled by comprehensive profiling of different types of exosomal biomarkers: Surface proteins and miRNAs. *Small* **2020**, *16*, 2004492.
[124] Li, P. L.; Chen, J. C.; Chen, Y. Q.; Song, S. L.; Huang, X. W.; Yang, Y. R.; Li, Y.; Tong, Y.; Xie, Y.; Li, J. et al. Construction of exosome SORL1 detection platform based on 3D porous microfluidic chip and its application in early diagnosis of colorectal cancer. *Small* **2023**, *19*, 2207381.
[125] Wang, C.; Wang, C. H.; Wu, Y.; Gao, J. W.; Han, Y. K.; Chu, Y. J.; Qiang, L.; Qiu, J. Y.; Gao, Y. K.; Wang, Y. H. et al. High-throughput, living single-cell, multiple secreted biomarker profiling using microfluidic chip and machine learning for tumor cell classification. *Adv. Healthc. Mater.* **2022**, *11*, 2102800.
[126] Gong, M. M.; Sinton, D. Turning the page: Advancing paper-based microfluidics for broad diagnostic application. *Chem. Rev.* **2017**, *117*, 8447–8480.
[127] Li, L. P.; Geng, Y. M.; Xiang, Y. H.; Qiang, H.; Wang, Y. X.; Chang, J. Q.; Zhao, H. N.; Zhang, L. Instrument-free enrichment and detection of phosphopeptides using paper-based Phos-PAD. *Anal. Chim. Acta* **2019**, *1062*, 102–109.
[128] Narang, J.; Singhal, C.; Mathur, A.; Sharma, S.; Singla, V.; Pundir, C. S. Portable bioactive paper based genosensor incorporated with Zn–Ag nanoblooms for herpes detection at the point-of-care. *Int. J. Biol. Macromol.* **2018**, *107*, 2559–2565.
[129] Seok, Y.; Batule, B. S.; Kim, M. G. Lab-on-paper for all-in-one molecular diagnostics (LAMDA) of zika, dengue, and chikungunya virus from human serum. *Biosens. Bioelectron.* **2020**, *165*, 112400.
[130] Liu, Y. Q.; Li, R. Y.; Liang, F. Y.; Deng, C.; Seidi, F.; Xiao, H. N. Fluorescent paper-based analytical devices for ultra-sensitive dual-type RNA detections and accurate gastric cancer screening. *Biosens. Bioelectron.* **2022**, *197*, 113781.
[131] Xia, Z. P.; Li, D.; Deng, W. Identification and detection of volatile aldehydes as lung cancer biomarkers by vapor generation combined with paper-based thin-film microextraction. *Anal. Chem.* **2021**, *93*, 4924–4931.
[132] Ireta-Muñoz, L. A.; Morales-Narváez, E. Smartphone and paper-based fluorescence reader: A do it yourself approach. *Biosensors (Basel)* **2020**, *10*, 60.
[133] Yang, M. Z.; Liu, Y.; Jiang, X. Y. Barcoded point-of-care bioassays. *Chem. Soc. Rev.* **2019**, *48*, 850–884.
[134] Kim, J.; Biondi, M. J.; Feld, J. J.; Chan, W. C. W. Clinical validation of quantum dot barcode diagnostic technology. *ACS Nano* **2016**, *10*, 4742–4753.
[135] Ming, K.; Kim, J.; Biondi, M. J.; Syed, A.; Chen, K.; Lam, A.; Ostrowski, M.; Rebbapragada, A.; Feld, J. J.; Chan, W. C. W. Integrated quantum dot barcode smartphone optical device for wireless multiplexed diagnosis of infected patients. *ACS Nano* **2015**, *9*, 3060–3074.
[136] Tran, M. V.; Susumu, K.; Medintz, I. L.; Algar, W. R. Supraparticle assemblies of magnetic nanoparticles and quantum dots for selective cell isolation and counting on a smartphone-based imaging platform. *Anal. Chem.* **2019**, *91*, 11963–11971.
[137] Darwish, G. H.; Asselin, J.; Tran, M. V.; Gupta, R.; Kim, H.; Boudreau, D.; Algar, W. R. Fully self-assembled silica nanoparticle-semiconductor quantum dot supra-nanoparticles and immunoconjugates for enhanced cellular imaging by microscopy and smartphone camera. *ACS Appl. Mater. Interfaces* **2020**, *12*, 33530–33540.
[138] Zhong, Y. T.; Ma, Z. R.; Zhu, S. J.; Yue, J. Y.; Zhang, M. X.; Antaris, A. L.; Yuan, J.; Cui, R.; Wan, H.; Zhou, Y. et al. Boosting the down-shifting luminescence of rare-earth nanocrystals for biological imaging beyond 1500 nm. *Nat. Commun.* **2017**, *8*, 737.
[139] Sun, C. X.; Li, B. H.; Zhao, M. Y.; Wang, S. F.; Lei, Z. H.; Lu, L. F.; Zhang, H. X.; Feng, L. S.; Dou, C. R.; Yin, D. R. et al. *J*-aggregates of cyanine dye for NIR-II *in vivo* dynamic vascular Imaging beyond 1500 nm. *J. Am. Chem. Soc.* **2019**, *141*, 19221–19225.
[140] Wang, X.; Guo, Z.; Zhang, C. Y.; Zhu, S.; Li, L. L.; Gu, Z. J.; Zhao, Y. L. Ultrasmall BiOI quantum dots with efficient renal clearance for enhanced radiotherapy of cancer. *Adv. Sci.* **2020**, *7*, 1902561.
[141] Wang, P. Y.; Li, J. Q.; Wei, M.; Yang, R. Q.; Lou, K. L.; Dang, Y. Y.; Sun, W.; Xue, F. Q.; Liu, X. L. Tumor-microenvironment triggered signal-to-noise boosting nanoprobes for NIR-IIb

fluorescence imaging guided tumor surgery and NIR-II photothermal therapy. *Biomaterials* **2022**, *287*, 121636.
[142] Li, H.; Du, Z.; Zhu, L. J.; Zhang, C.; Xiong, J. B.; Zhou, B. S.; Dong, B.; Zhang, X. L.; Alifu, N. Ultrabright NIR-IIb fluorescence quantum dots for targeted imaging-guided surgery. *ACS Appl. Mater. Interfaces* **2024**, *16*, 32045–32057.
[143] Weichselbaum, R. R.; Liang, H.; Deng, L. F.; Fu, Y. X. Radiotherapy and immunotherapy: A beneficial liaison. *Nat. Rev. Clin. Oncol.* **2017**, *14*, 365–379.
[144] Li, H.; Wang, M.; Huang, B.; Zhu, S. W.; Zhou, J. J.; Chen, D. R.; Cui, R.; Zhang, M. X.; Sun, Z. J. Theranostic near-infrared-IIb emitting nanoprobes for promoting immunogenic radiotherapy and abscopal effects against cancer metastasis. *Nat. Commun.* **2021**, *12*, 7149.
[145] Fan, W. P.; Tang, W.; Lau, J.; Shen, Z. Y.; Xie, J.; Shi, J. L.; Chen, X. Y. Breaking the depth dependence by nanotechnology-enhanced X-ray-excited deep cancer theranostics. *Adv. Mater.* **2019**, *31*, 1806381.
[146] Zhang, J. M.; Chen, Y. X.; Fang, J. G. Targeting thioredoxin reductase by micheliolide contributes to radiosensitizing and inducing apoptosis of HeLa cells. *Free Radic. Biol. Med.* **2022**, *186*, 99–109.
[147] Kaushik, N.; Kaushik, N. K.; Choi, E. H.; Kim, J. H. Blockade of cellular energy metabolism through 6-aminonicotinamide reduces proliferation of non-small lung cancer cells by inducing endoplasmic reticulum stress. *Biology (Basel)* **2021**, *10*, 1088.
[148] Wang, Y. H.; Wei, Y. Z.; Wu, Y. C.; Zong, Y.; Song, Y. Y.; Pu, S. Y.; Wu, W. W.; Zhou, Y.; Xie, J.; Yin, H. T. Multifunctional nano-realgar hydrogel for enhanced glioblastoma synergistic chemotherapy and radiotherapy: A new paradigm of an old drug. *Int. J. Nanomedicine* **2023**, *18*, 743–763.
[149] Liu, M.; Anderson, R. C.; Lan, X. L.; Conti, P. S.; Chen, K. Recent advances in the development of nanoparticles for multimodality imaging and therapy of cancer. *Med. Res. Rev.* **2020**, *40*, 909–930.
[150] Abrishami, A.; Bahrami, A. R.; Nekooei, S.; Sh Saljooghi, A.; Matin, M. M. Hybridized quantum dot, silica, and gold nanoparticles for targeted chemo-radiotherapy in colorectal cancer theranostics. *Commun. Biol.* **2024**, *7*, 393.
[151] Wang, Y.; Gu, H. C. Core-shell-type magnetic mesoporous silica nanocomposites for bioimaging and therapeutic agent delivery. *Adv. Mater.* **2015**, *27*, 576–585.
[152] Chen, Y.; Yang, J.; Fu, S. Z.; Wu, J. B. Gold nanoparticles as radiosensitizers in cancer radiotherapy. *Int. J. Nanomedicine* **2020**, *15*, 9407–9430.
[153] Kubli, S. P.; Berger, T.; Araujo, D. V.; Siu, L. L.; Mak, T. W. Beyond immune checkpoint blockade: Emerging immunological strategies. *Nat. Rev. Drug Discov.* **2021**, *20*, 899–919.
[154] Yang, X. P.; Yang, C.; Zhang, S.; Geng, H. G.; Zhu, A. X.; Bernards, R.; Qin, W. X.; Fan, J.; Wang, C.; Gao, Q. Precision treatment in advanced hepatocellular carcinoma. *Cancer Cell* **2024**, *42*, 180–197.
[155] Goldberg, M. S. Improving cancer immunotherapy through nanotechnology. *Nat. Rev. Cancer* **2019**, *19*, 587–602.
[156] Martin, J. D.; Cabral, H.; Stylianopoulos, T.; Jain, R. K. Improving cancer immunotherapy using nanomedicines: Progress, opportunities and challenges. *Nat. Rev. Clin. Oncol.* **2020**, *17*, 251–266.
[157] Li, J. C.; Cui, D.; Huang, J. G.; He, S. S.; Yang, Z. B.; Zhang, Y.; Luo, Y.; Pu, K. Y. Organic semiconducting pro-nanostimulants for near-infrared photoactivatable cancer immunotherapy. *Angew. Chem., Int. Ed.* **2019**, *58*, 12680–12687.
[158] Zhang, X. L.; Yi, C.; Zhang, L. J.; Zhu, X. Y.; He, Y.; Lu, H. Z.; Li, Y. M.; Tang, Y. Q.; Zhao, W.; Chen, G. S. et al. Size-optimized nuclear-targeting phototherapy enhances the type I interferon response for "cold" tumor immunotherapy. *Acta Biomater.* **2023**, *159*, 338–352.
[159] Hou, L.; Chen, D. D.; Wang, R. T.; Wang, R. B.; Zhang, H. J.; Zhang, Z. Z.; Nie, Z. H.; Lu, S. Y. Transformable honeycomb-like nanoassemblies of carbon dots for regulated multisite delivery and enhanced antitumor chemoimmunotherapy. *Angew. Chem., Int. Ed.* **2021**, *60*, 6581–6592.
[160] Chung, Y. J.; Kim, J.; Park, C. B. Photonic carbon dots as an emerging nanoagent for biomedical and healthcare applications. *ACS Nano* **2020**, *14*, 6470–6497.
[161] Kroemer, G.; Galassi, C.; Zitvogel, L.; Galluzzi, L. Immunogenic cell stress and death. *Nat. Immunol.* **2022**, *23*, 487–500.
[162] Meier, P.; Legrand, A. J.; Adam, D.; Silke, J. Immunogenic cell death in cancer: Targeting necroptosis to induce antitumour immunity. *Nat. Rev. Cancer* **2024**, *24*, 299–315.
[163] Yang, Z.; Gao, D.; Zhao, J.; Yang, G. J.; Guo, M.; Wang, Y.; Ren, X. C.; Kim, J. S.; Jin, L.; Tian, Z. M. et al. Thermal immuno-nanomedicine in cancer. *Nat. Rev. Clin. Oncol.* **2023**, *20*, 116–134.
[164] Li, Z.; Fu, Q. R.; Ye, J. M.; Ge, X. G.; Wang, J.; Song, J. B.; Yang, H. H. Ag^{+}-coupled black phosphorus vesicles with emerging NIR-II photoacoustic imaging performance for cancer immune-dynamic therapy and fast wound healing. *Angew. Chem., Int. Ed.* **2020**, *59*, 22202–22209.
[165] Zhao, J. Y.; Huang, H. B.; Zhao, J. Y.; Xiong, X.; Zheng, S. B.; Wei, X. Q.; Zhou, S. B. A hybrid bacterium with tumor-associated macrophage polarization for enhanced photothermal-immunotherapy. *Acta Pharm. Sin. B* **2022**, *12*, 2683–2694.
[166] Chen, S. Z.; Saeed, A. F. U. H.; Liu, Q.; Jiang, Q.; Xu, H. Z.; Xiao, G. G.; Rao, L.; Duo, Y. Macrophages in immunoregulation and therapeutics. *Sig. Transduct. Target. Ther.* **2023**, *8*, 207.
[167] Qian, M.; Chen, L. L.; Du, Y. L.; Jiang, H. L.; Huo, T. T.; Yang, Y. F.; Guo, W.; Wang, Y.; Huang, R. Q. Biodegradable mesoporous silica achieved via carbon nanodots-incorporated framework swelling for debris-mediated photothermal synergistic immunotherapy. *Nano Lett.* **2019**, *19*, 8409–8417.
[168] Yang, M. X.; Li, H. Q.; Liu, X. C.; Huang, L.; Zhang, B. Y.; Liu, K. X.; Xie, W. N.; Cui, J.; Li, D. W.; Lu, L. J. et al. Fe-doped carbon dots: A novel biocompatible nanoplatform for multi-level cancer therapy. *J. Nanobiotechnol.* **2023**, *21*, 431.
[169] He, L. Z.; Zhao, J. F.; Li, H. J.; Xie, B.; Xu, L. G.; Huang, G. N.; Liu, T.; Gu, Z.; Chen, T. F. Metabolic reprogramming of NK cells by black phosphorus quantum dots potentiates cancer immunotherapy. *Adv. Sci.* **2023**, *10*, 2202519.
[170] Wu, C. H.; Guan, X. T.; Xu, J. M.; Zhang, Y. X.; Liu, Q. Y.; Tian, Y.; Li, S.; Qin, X.; Yang, H.; Liu, Y. Y. Highly efficient cascading synergy of cancer photo-immunotherapy enabled by engineered graphene quantum dots/photosensitizer/CpG oligonucleotides hybrid nanotheranostics. *Biomaterials* **2019**, *205*, 106–119.
[171] Fang, Y. X.; Zhang, Z. P.; Liu, Y.; Gao, T.; Liang, S.; Chu, Q. H.; Guan, L.; Mu, W. W.; Fu, S. L.; Yang, H. Z. et al. Artificial assembled macrophage Co-deliver black phosphorus quantum dot and CDK4/6 inhibitor for colorectal cancer triple-therapy. *ACS Appl. Mater. Interfaces* **2022**, *14*, 20628–20640.
[172] Hou, X. L.; Dai, X.; Yang, J.; Zhang, B.; Zhao, D. H.; Li, C. Q.; Yin, Z. Y.; Zhao, Y. D.; Liu, B. Injectable polypeptide-engineered hydrogel depot for amplifying the anti-tumor immune effect induced by chemo-photothermal therapy. *J. Mater. Chem. B* **2020**, *8*, 8623–8633.
[173] Tison, A.; Garaud, S.; Chiche, L.; Cornec, D.; Kostine, M. Immune-checkpoint inhibitor use in patients with cancer and pre-existing autoimmune diseases. *Nat. Rev. Rheumatol.* **2022**, *18*, 641–656.
[174] Doroshow, D. B.; Bhalla, S.; Beasley, M. B.; Sholl, L. M.; Kerr, K. M.; Gnjatic, S.; Wistuba, I. I.; Rimm, D. L.; Tsao, M. S.; Hirsch, F. R. PD-L1 as a biomarker of response to immune-checkpoint inhibitors. *Nat. Rev. Clin. Oncol.* **2021**, *18*, 345–362.
[175] Liang, X.; Ye, X. Y.; Wang, C.; Xing, C. Y.; Miao, Q. W.; Xie, Z. J.; Chen, X. L.; Zhang, X. D.; Zhang, H.; Mei, L. Photothermal cancer immunotherapy by erythrocyte membrane-coated black phosphorus formulation. *J. Control. Release* **2019**, *296*, 150–161.
[176] Zhao, P. Q.; Xu, Y. L.; Ji, W.; Zhou, S. Y.; Li, L. F.; Qiu, L. H.; Qian, Z. Z.; Wang, X. H.; Zhang, H. L. Biomimetic black phosphorus quantum dots-based photothermal therapy combined with anti-PD-L1 treatment inhibits recurrence and metastasis in triple-negative breast cancer. *J. Nanobiotechnol.* **2021**, *19*, 181.

[177] Yuan, X. Y.; Ruan, W.; Bobrow, B.; Carmeliet, P.; Eltzschig, H. K. Targeting hypoxia-inducible factors: Therapeutic opportunities and challenges. *Nat. Rev. Drug Discovery* **2024**, *23*, 175–200.
[178] Zhou, X. F.; Meng, Z. Q.; She, J. L.; Zhang, Y. J.; Yi, X.; Zhou, H. L.; Zhong, J.; Dong, Z. L.; Han, X.; Chen, M. C. et al. Near-infrared light-responsive nitric oxide delivery platform for enhanced radioimmunotherapy. *Nano-Micro Lett.* **2020**, *12*, 100.
[179] Lundberg, J. O.; Weitzberg, E. Nitric oxide signaling in health and disease. *Cell* **2022**, *185*, 2853–2878.
[180] Wang, Z. X.; Jin, A.; Yang, Z.; Huang, W. Advanced nitric oxide generating nanomedicine for therapeutic applications. *ACS Nano* **2023**, *17*, 8935–8965.
[181] Saxena, M.; van der Burg, S. H.; Melief, C. J. M.; Bhardwaj, N. Therapeutic cancer vaccines. *Nat. Rev. Cancer* **2021**, *21*, 360–378.
[182] Sahin, U.; Türeci, Ö. Personalized vaccines for cancer immunotherapy. *Science* **2018**, *359*, 1355–1360.
[183] Liu, Q.; Fan, T. J.; Zheng, Y. Y.; Yang, S. L.; Yu, Z. Q.; Duo, Y. H.; Zhang, Y. H.; Adah, D.; Shi, L. L.; Sun, Z. et al. Immunogenic exosome-encapsulated black phosphorus nanoparticles as an effective anticancer photo-nanovaccine. *Nanoscale* **2020**, *12*, 19939–19952.
[184] Ye, X. Y.; Liang, X.; Chen, Q.; Miao, Q. W.; Chen, X. L.; Zhang, X. D.; Mei, L. Surgical tumor-derived personalized photothermal vaccine formulation for cancer immunotherapy. *ACS Nano* **2019**, *13*, 2956–2968.
[185] Shankar, L. K.; Schöder, H.; Sharon, E.; Wolchok, J.; Knopp, M. V.; Wahl, R. L.; Ellingson, B. M.; Hall, N. C.; Yaffe, M. J.; Towbin, A. J. et al. Harnessing imaging tools to guide immunotherapy trials: Summary from the National Cancer Institute Cancer Imaging Steering Committee workshop. *Lancet Oncol.* **2023**, *24*, e133–e143.
[186] Zhang, Y. Y.; Wang, T. G.; Tian, Y.; Zhang, C. N.; Ge, K.; Zhang, J. C.; Chang, J.; Wang, H. J. Gold nanorods-mediated efficient synergistic immunotherapy for detection and inhibition of postoperative tumor recurrence. *Acta Pharm. Sin. B* **2021**, *11*, 1978–1992.
[187] Ma, X. B.; Mao, M. C.; He, J. Q.; Liang, C.; Xie, H. Y. Nanoprobe-based molecular imaging for tumor stratification. *Chem. Soc. Rev.* **2023**, *52*, 6447–6496.
[188] Liu, J.; Li, C. N.; Brans, T.; Harizaj, A.; Van de Steene, S.; De Beer, T.; De Smedt, S.; Szunerits, S.; Boukherroub, R.; Xiong, R. H. et al. Surface functionalization with polyethylene glycol and polyethyleneimine improves the performance of graphene-based materials for safe and efficient intracellular delivery by laser-induced photoporation. *Int. J. Mol. Sci.* **2020**, *21*, 1540.
[189] Xiong, R. H.; Sauvage, F.; Fraire, J. C.; Huang, C. B.; De Smedt, S. C.; Braeckmans, K. Photothermal nanomaterial-mediated photoporation. *Acc. Chem. Res.* **2023**, *56*, 631–643.
[190] Liu, J.; Xiong, R. H.; Brans, T.; Lippens, S.; Parthoens, E.; Zanacchi, F. C.; Magrassi, R.; Singh, S. K.; Kurungot, S.; Szunerits, S. et al. Repeated photoporation with graphene quantum dots enables homogeneous labeling of live cells with extrinsic markers for fluorescence microscopy. *Light: Sci. Appl.* **2018**, *7*, 47.
[191] Zhong, Y. T.; Ma, Z. R.; Wang, F. F.; Wang, X.; Yang, Y. J.; Liu, Y. L.; Zhao, X.; Li, J. C.; Du, H. T.; Zhang, M. X. et al. *In vivo* molecular imaging for immunotherapy using ultra-bright near-infrared-IIb rare-earth nanoparticles. *Nat. Biotechnol.* **2019**, *37*, 1322–1331.
[192] Yu, G. T.; Luo, M. Y.; Li, H.; Chen, S.; Huang, B.; Sun, Z. J.; Cui, R.; Zhang, M. X. Molecular targeting nanoprobes with non-overlap emission in the second near-infrared window for *in vivo* two-color colocalization of immune cells. *Acs Nano* **2019**, *13*, 12830–12839.
[193] Zhang, D. G.; Wu, H. L.; Wang, T. C.; Wang, Y. T.; Liu, S. X.; Wen, F. Q.; Oudeng, G.; Yang, M. Self-driven immune checkpoint blockade and spatiotemporal-sensitive immune response monitoring in acute myeloid leukemia using an all-in-one turn-on bionanoprobe. *J. Mater. Chem. B* **2023**, *11*, 10613–10624.
[194] Hong, M. H.; Clubb, J. D.; Chen, Y. Y. Engineering CAR-T cells for next-generation cancer therapy. *Cancer Cell* **2020**, *38*, 473–488.
[195] Hao, X. X.; Li, C. Y.; Zhang, Y. J.; Wang, H. Z.; Chen, G. C.; Wang, M.; Wang, Q. B. Programmable chemotherapy and immunotherapy against breast cancer guided by multiplexed fluorescence imaging in the second near-infrared window. *Adv. Mater.* **2018**, *30*, 1804437.
[196] Li, H. M.; Yang, X. X.; Wang, Z. C.; She, W. Y.; Liu, Y.; Huang, L.; Jiang, P. A near-infrared-II fluorescent nanocatalyst for enhanced CAR T cell therapy against solid tumor by immune reprogramming. *ACS Nano* **2023**, *17*, 11749–11763.
[197] Sun, J. L.; Liu, F.; Yu, W. Q.; Fu, D. D.; Jiang, Q. Y.; Mo, F. Y.; Wang, X. Y.; Shi, T. H.; Wang, F. A.; Pang, D. W. et al. Visualization of vaccine dynamics with quantum dots for immunotherapy. *Angew. Chem.* **2021**, *133*, 24477–24485.
[198] Donahue, N. D.; Acar, H.; Wilhelm, S. Concepts of nanoparticle cellular uptake, intracellular trafficking, and kinetics in nanomedicine. *Adv. Drug Delivery Rev.* **2019**, *143*, 68–96.
[199] Ma, Z. R.; Wang, F. F.; Zhong, Y. T.; Salazar, F.; Li, J. C.; Zhang, M. X.; Ren, F. Q.; Wu, A. M.; Dai, H. J. Cross-link-functionalized nanoparticles for rapid excretion in nanotheranostic applications. *Angew. Chem.* **2020**, *132*, 20733–20741.
[200] Lv, Z. Y.; Wang, Y.; Chen, J. R.; Wang, J. J.; Zhou, Y.; Han, S. T. Semiconductor quantum dots for memories and neuromorphic computing systems. *Chem. Rev.* **2020**, *120*, 3941–4006.
[201] Jia, Z. X.; Shi, C.; Yang, X. T.; Zhang, J. R.; Sun, X.; Guo, Y. M.; Ying, X. G. QD-based fluorescent nanosensors: Production methods, optoelectronic properties, and recent food applications. *Compr. Rev. Food Sci. Food Saf.* **2023**, *22*, 4644–4669.
[202] Li, W.; Kaminski Schierle, G. S.; Lei, B. F.; Liu, Y. L.; Kaminski, C. F. Fluorescent nanoparticles for super-resolution imaging. *Chem. Rev.* **2022**, *122*, 12495–12543.
[203] Pirzada, M.; Altintas, Z. Nanomaterials for virus sensing and tracking. *Chem. Soc. Rev.* **2022**, *51*, 5805–5841.
[204] Ye, J. Z.; Gaur, D.; Mi, C. J.; Chen, Z. J.; Fernández, I. L.; Zhao, H. T.; Dong, Y. T.; Polavarapu, L.; Hoye, R. L. Z. Strongly-confined colloidal lead-halide perovskite quantum dots: From synthesis to applications. *Chem. Soc. Rev.* **2024**, *53*, 8095–8122.
[205] Liu, X. Y.; Wu, W. J.; Cui, D. X.; Chen, X. Y.; Li, W. W. Functional micro-/nanomaterials for multiplexed biodetection. *Adv. Mater.* **2021**, *33*, 2004734.
[206] Liu, H. Y.; Wang, Z. G.; Liu, S. L.; Pang, D. W. Single-virus tracking with quantum dots in live cells. *Nat. Protoc.* **2023**, *18*, 458–489.
[207] Karakoti, A. S.; Shukla, R.; Shanker, R.; Singh, S. Surface functionalization of quantum dots for biological applications. *Adv. Colloid Interface Sci.* **2015**, *215*, 28–45.